Evidence-Based Complementary and Alternative Medicine

New Discovery of Curcumin Combination Therapy and Action Mechanism

Lead Guest Editor: Chongshan Dai
Guest Editors: Xiuying Zhang and Keyu Zhang

New Discovery of Curcumin Combination Therapy and Action Mechanism

Evidence-Based Complementary and Alternative Medicine

New Discovery of Curcumin Combination Therapy and Action Mechanism

Lead Guest Editor: Chongshan Dai
Guest Editors: Xiuying Zhang and Keyu Zhang

Editorial Board

Contents

Hindawi
Evidence-Based Complementary and Alternative Medicine
Volume 2020, Article ID 4793058, 2 pages
https://doi.org/10.1155/2020/4793058

Editorial

New Discovery of Curcumin Combination Therapy and Action Mechanism

Chongshan Dai,[1] **Xiuying Zhang**,[2] **and Keyu Zhang**[3]

[1]*Department of Surgery, University of Texas Southwestern Medical Center, Harry Hines Blvd, Dallas, TX 5323, USA*
[2]*Department of Basic Veterinary Science, College of Veterinary Medicine, Northeast Agricultural University, Harbin, Heilongjiang 150030, China*
[3]*Key Laboratory of Veterinary Chemical Drugs and Pharmaceutics, Ministry of Agriculture, Shanghai Veterinary Research Institute, Chinese Academy of Agricultural Sciences, No. 518 Ziyue Road, Minhang District, Shanghai 200241, China*

Correspondence should be addressed to Chongshan Dai; chongshan.dai@utsouthwestern.edu

Received 24 February 2020; Accepted 24 February 2020; Published 10 March 2020

Curcumin (diferuloylmethane, a yellow pigment in spice turmeric) is a natural product polyphenol extracted from the rhizome of *Curcuma longa*. Curcumin has been shown to elicit a strong antioxidant activity by directly scavenging free radicals, even more effectively than vitamin E. It has been widely used in pharmaceutical and medical applications based on the broad spectrum of biological actions, including antibacterial, antiviral, antifungal, and anti-inflammatory activities. Direct curcumin targets include cyclooxygenase 2 (COX-2), lipoxygenase, nuclear factor erythroid 2-related factor 2, toll-like receptor (TLR) 4, transforming growth factor-beta (TGF-β)/smad signaling pathway, focal adhesion kinase, glutathione, glycogen synthase kinase- (GSK-) 3 β, phosphorylase-3 kinase, xanthine oxidase, pp60 src tyrosine kinase, and ubiquitin isopeptidase, which play important roles in oxidative stress, inflammation, autophagy, ferroptosis, and apoptosis. Therefore, curcumin has been proposed to increase the therapeutic efficiency of some drugs, albeit the potential molecular mechanisms remain unclear. Importantly, available preclinical and phase I/II data suggest that curcumin is well tolerated and has a good safety profile. A classic example is the combination between curcumin and polymyxins whereby in addition to its synergistic antimicrobial activity, curcumin could potentially ameliorate polymyxin-induced unwanted neurotoxicity. With the proposal of concept on precision medicine in the clinic, the underlying molecular mechanism and potential target for the combination therapy are much emphasized.

In this special issue, investigators contribute original research articles and review articles that would facilitate the understanding of the basic mechanisms of curcumin as well as the development of new and promising complementary and alternative strategies for curcumin combination.

Wang et al. reported the neuroprotective effect of curcumin against oxygen-glucose deprivation/reoxygenation (OGD/R) injury in HT22 neuronal cells. They suggested that curcumin can protect OGD/R-induced neuronal apoptotic cell death by inhibiting intracellular ROS accumulation and mitochondria dysfunction. Knockdown of SOD2 by RNA interference (RNAi) attenuated the protective effect of curcumin on OGD/R-induced neuronal cell death, suggesting that SOD2 may be a target of curcumin death.

Wang and Chen reviewed the bidirectional action of curcumin and curcuminoids as well as synthetic curcumin analog on angiogenesis based on the current research findings. They review paper summarized the antiangiogenesis effect of curcumin. Curcumin could regulate multiple factors, including proangiogenesis factor vascular endothelia growth factor (VEGF), matrix metalloproteinase (MMPs), and fibroblast growth factors (FGF), both in vivo and in vitro, and promote angiogenesis under certain circumstances via these factors.

The relationship between gut microbiota and human diseases has been a major topic of interest for many studies. Pan and his colleagues reviewed the effects of gut microbiota in the pharmacological effect of natural products including ginseng, bebeerine, and curcumin. Natural products may cause changes in the composition of intestinal microbiota, microbial metabolites, intestinal tight junction structure, and mucosal immunology. On the contrary, these changes will eventually result in the exertion of the pharmacological effects by treatment with these natural products. This is a new field for the investigation of curcumin's pharmacological effects, and the potential molecular mechanism needs further investigation.

Curcumin has been widely used as a supplementary agent against drug, carbon tetrachloride (CCl_4), and ethanol-induced liver injury. Inhibiting the TGF-β pathway usually was considered as a potential target of curcumin. Zhang et al.'s results implied that a variant of rs17687727 in TGF-β receptor-associated protein 1 (TGFBRAP1) (a member of TGF-β transmembrane receptors) may influence the susceptibility to antituberculosis drug-induced liver injury in first-line antituberculosis combination treatment in the Han Chinese population in a dependent manner. This result provides the information for potential candidate treatment drugs including curcumin.

Natural products are an important source of drug research for the future. A novel application of natural substances is combination therapy, which consists of the administration of two or more substances, such as conventional chemotherapeutics plus a natural compound or multiple natural compounds at a time. Investigation of potential targets is urgent toward the understanding of molecular mechanisms and the development of key new formulations.

Gong et al. reported an ancient herbal mixture, named Danggui Buxue Tang (DBT_{1155}), which comprises four herbs (e.g., *Angelicae Sinensis Radix*, *Astragali Radix, Jujuba Fructus*, and *Zingiberis Rhizoma Recens* in a weight ratio of 36 : 30 : 15 : 20), on the effects of preventing obesity in an in vitro model by using mouse 3T3-L1 fibroblast cells. Their results showed that DBT_{1155} could actuate brown fat-specific gene activations, such as peroxisome proliferator-activated receptor (PPARγ), mitochondrial uncoupling protein 1 (UCP1), and peroxisome proliferator-activated receptor γ coactivator 1 (PCG1α). Meanwhile, DBT1155 could decrease lipid accumulation by triggering AMPK signaling.

Tian et al. reported *Cynomorium songaricum* extract exhibited potential therapeutic effect on neuroprotection of ovariectomized rats, and its effect was possibly exerted by p-cAMP-response element binding protein (CREB)/brain-derived neurotrophic factor- (BDNF-) mediated down-regulation of extracellular regulated protein kinases (ERK)/p38 mitogen-activated protein kinase (p38MAPK).

We hope that this special issue can be really special for scientists studying the pharmacological effects of curcumin and discoveries of curcumin combination therapy.

Conflicts of Interest

The editors declare that they have no conflicts of interest.

Acknowledgments

The editors thank the academic editors Mario Ledda and Jamal A. Mahajna's editorial contribution in the process of peer-review. The editors express their gratitude to all authors who made this special issue possible. We hope this collection of articles will be useful to the scientific community.

Chongshan Dai
Xiuying Zhang
Keyu Zhang

Hindawi
Evidence-Based Complementary and Alternative Medicine
Volume 2019, Article ID 2160642, 14 pages
https://doi.org/10.1155/2019/2160642

Research Article

SOD2 Mediates Curcumin-Induced Protection against Oxygen-Glucose Deprivation/Reoxygenation Injury in HT22 Cells

Yuqing Wang,[1] Yuanyuan Zhang,[2] Liang Yang,[3] Jin Yuan,[4] Ji Jia,[5] and Shuai Yang[6]

[1]*Department of Rehabilitation, General Hospital of Southern Theatre Command of PLA, Guangzhou 510010, China*
[2]*Department of 1st Geriatrics, General Hospital of Southern Theatre Command of PLA, Guangzhou 510010, China*
[3]*Department of Cardiology, General Hospital of Southern Theatre Command of PLA, Guangzhou 510010, China*
[4]*Department of Pharmacology, General Hospital of Southern Theatre Command of PLA, Guangzhou 510010, China*
[5]*Department of Anesthesiology, General Hospital of Southern Theatre Command of PLA, Guangzhou 510010, China*
[6]*Department of Neurosurgery, The First Affiliated Hospital of Sun Yat-sen University, Guangzhou 510080, China*

Correspondence should be addressed to Ji Jia; jiaji1981@126.com and Shuai Yang; ysh_gzh@126.com

Received 15 June 2019; Revised 24 August 2019; Accepted 10 September 2019; Published 29 September 2019

Guest Editor: Chongshan Dai

Curcumin (Cur) induces neuroprotection against brain ischemic injury; however, the mechanism is still obscure. The aim of this study is to explore the potential neuroprotective mechanism of curcumin against oxygen-glucose deprivation/reoxygenation (OGD/R) injury in HT22 cells and investigate whether type-2 superoxide dismutase (SOD2) is involved in the curcumin-induced protection. In the present study, HT22 neuronal cells were treated with 3 h OGD plus 24 h reoxygenation to mimic ischemia/reperfusion injury. Compared with the normal cultured control group, OGD/R treatment reduced cell viability and SOD2 expression, decreased mitochondrial membrane potential (MMP) and mitochondrial complex I activity, damaged cell morphology, and increased lactic dehydrogenase (LDH) release, cell apoptosis, intracellular reactive oxygen species (ROS), and mitochondrial superoxide ($P < 0.05$). Meanwhile, coadministration of 100 ng/ml curcumin reduced the cell injury and apoptosis, inhibited intracellular ROS and mitochondrial superoxide accumulation, and ameliorated intracellular SOD2, cell morphology, MMP, and mitochondrial complex I activity. Downregulating the SOD2 expression by using siRNA, however, significantly reversed the curcumin-induced cytoprotection ($P < 0.05$). These findings indicated that curcumin induces protection against OGD/R injury in HT22 cells, and SOD2 protein may mediate the protection.

1. Introduction

Stroke is one of the leading causes of disability and death in China and worldwide [1]. In 2015, the number of new patients with stroke was more than 13 million, leading to a cost of 11.3 billion USD, which brought about great economic burden to the patients and the country [2]. However, at present, the effective neuroprotective drug against brain ischemic injury is very limited. Recombinant tissue plasminogen activator (rTPA) is the only neuroprotectant used in clinic; the limited therapeutic time window (within 4.5 h after the onset of stroke) reduces its utilization rate, leading to the result that only 3% to 8.5% of stroke patients can receive rTPA treatment [3, 4]. Therefore, exploring novel neuroprotective medicine against brain ischemic injury is very urgent and important.

Curcumin is derived from seasoning curry and herbal *Carcuma longa* Linn (turmeric), and some latest investigations showed that curcumin protects neuronal cells against brain ischemic injury both in vivo and in vitro [5, 6]. The curcumin-induced protection against ischemic injury, however, is still not clear. Type-2 superoxide dismutase (SOD2) is an antioxidative protein, which is expressed in mitochondria of cells, and the upregulation of SOD2 in cells induces neuroprotective effects [7, 8]. And some latest investigations indicated that neuronal oxidative injury and

mitochondrial dysfunction are involved in the pathophysiological process of brain ischemic injury [9–11]. In addition, one of our studies showed that SOD2 protein mediates curcumin-induced protection against β-amyloid (Aβ) in neuronal cells [12].

Therefore, in the present study, we used oxygen-glucose deprivation plus reoxygenation (OGD/R) in HT22 neuronal cells to mimic neuronal ischemia/reperfusion (I/R) injury [13] and investigated whether SOD2 mediates curcumin-induced protection against OGD/R.

2. Materials and Methods

2.1. Materials. HT22 cells were obtained from the Xuzhou Medical University. Curcumin, Dulbecco's Modified Eagle Medium (DMEM), fetal bovine serum (FBS), dimethyl sulfoxide (DMSO), and methylthiazolyldiphenyl-tetrazolium bromide (MTT) were purchased from Sigma-Aldrich (St. Louis, MO, USA). Lactic dehydrogenase (LDH) reagent kit was obtained from Nanjing Jiancheng Bioengineering Institute (Nanjing, China). SOD2 activity assay kit was obtained from Trevigen (Gaithersburg, USA). The DAPI staining solution and ROS reagent kit were purchased from Beyotime Technology (Nantong, China). MitoSOX staining kits were purchased from Invitrogen Molecular Probes (San Diego, CA). The primary antibodies of anti-SOD2, anti-cleaved caspase-3, and anti-β-actin were purchased from Abcam (Cambridge, UK).

2.2. Cell Culture and OGD Treatment. The HT22 cells were cultured in the medium, containing 90% DMEM medium, 10% FBS, 100 U/ml penicillin, and 100 μg/ml streptomycin. The air of the incubator contained 95% O_2 and 5% CO_2, and the temperature of the incubator was 37°C. The medium was changed every 2 to 3 days, and the cells were passaged 3 times/week with a 1:4 split ratio. We followed the methods of Du et al. [12].

For the OGD treatment, the medium of the cells was changed with DMEM medium without glucose and FBS, and then the cells were cultured in a sealed container; the air of the container contained 95% N_2 and 5% CO_2, and the temperature of the container was 37°C. After 3 h OGD treatment, the medium of the cells was changed with normal medium, and the cells were returned to the normal incubator to mimic reperfusion.

2.3. Experimental Protocols. To explore a suitable curcumin concentration, the cells were divided into 5 groups, including the normal cultured control group, 3 h OGD plus 24 h reoxygenation (OGD/R) treatment group, 10 ng/ml curcumin treatment group (10 ng/ml Cur + OGD/R), 100 ng/ml curcumin treatment group (100 ng/ml Cur + OGD/R), and 500 ng/ml curcumin treatment group (500 ng/ml Cur + OGD/R). After treatments (Figure 1(a)), cell viability and LDH release were assessed. Then, to observe curcumin-induced effect on SOD2 expression in normal cultured cells (Figure 1(b)), the cells were divided into 4 groups, including control and 3 concentrations of curcumin treatment groups (10, 100, and 500 ng/ml curcumin); after 3 h treatment, SOD2 expression was assessed. Next, to evaluate the SOD2-siRNA-induced effects on SOD2 expression and cytotoxicity, the cells were divided into 3 groups, including the normal cultured control group, SOD2-siRNA treatment group, and scrambled-siRNA (SC-siRNA) treatment group; after 6 h incubation, western blot and MTT assay were taken to evaluate SOD2 expression and cell injury level (Figure 1(c)).

To determine whether SOD2 mediates curcumin-induced protection against OGD/R in HT22 cells, the cells were divided into 5 groups, including control group, OGD/R treatment group, 100 ng/ml curcumin treatment group (Cur + OGD/R), SOD2-siRNA treatment group (SOD2-siRNA + Cur + OGD/R), and SC-siRNA treatment group (SC-siRNA + Cur + OGD/R). After the treatments (Figure 1(d)), cell injury, apoptosis, SOD2 expression, cell morphology, mitochondrial functions, intracellular ROS, and mitochondrial superoxide were assessed.

2.4. Cell Viability. The HT22 cells were seeded into a 96-well cell culture plate at a density of 1×10^5 cells per well. After the treatments, 20 μl MTT solution (5 μg/ml) was added into each well; after 4 h incubation at 37°C, the medium of the cell culture plate was removed. Then, 150 μl DMSO was added into each well. After 15 min shaking, as the formazan was dissolved completely, the absorbance of each well was measured by using a spectrophotometer (TECAN, CH).

2.5. LDH Release. The cells were seeded into a 24-well cell culture plate at a density of 5×10^5 cells/well. After the treatments, the supernatants of the plate were collected to measure the LDH activity of each well, as previously described [14].

2.6. Western Blot Analysis. The cells were seeded into a 6-well cell culture plate at a density of 1×10^6 cells/well. After the treatments, the medium was removed, and the cells were collected. Then, the total protein of the treated cells was evaluated by using the Bradford method as described previously [14]. The primary anti-SOD2 (1 : 1000 in dilution), anticleaved caspase-3 (1 : 50 in dilution), and anti-β-actin (1 : 1000 in dilution) antibodies were used. The antigens were assessed by using the chemiluminescence technique (Amersham Pharmacia Biotech Piscataway, USA). Image analysis was evaluated with the computerized analysis software (Bio-Rad, Hercules, CH). We followed the methods of Du et al. [12].

2.7. siRNA Interfering. SOD2-siRNA and SC-siRNA were obtained from Qiangen (Germany). The siRNA oligomers, including SOD2-siRNA and SC-siRNA, were diluted in serum-free DMEM medium, and then the medium was incubated in room temperature for 5 min. The incubated oligomers were combined with diluted Lipofectamine 2000 and incubated for another 20 min. The cell culture medium was then removed from the plate, and the cells were washed

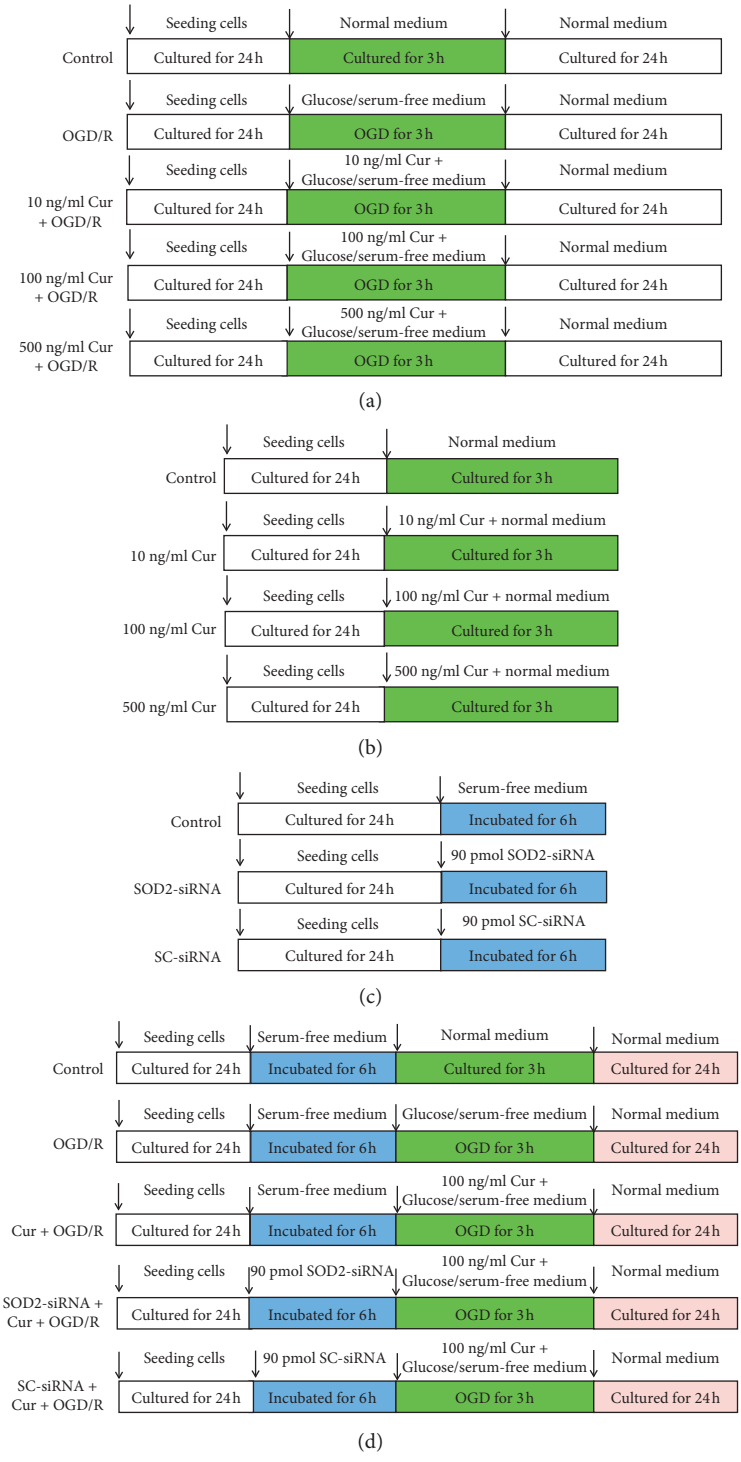

Figure 1: Experimental protocol diagram. (a) Searching a suitable curcumin concentration. The cells were divided into 5 groups, including the normal cultured control group, oxygen glucose 3 h OGD plus 24 reoxygenation treatment group (OGD/R), and 3 concentrations of curcumin treatment groups. After the treatments, cell viability and LDH release were assessed. (b) Observing curcumin-induced effect on SOD2 protein expression. The cells were divided into 4 groups, including normal cultured control group and 3 concentrations of curcumin treatment groups; after 3 h treatment, SOD2 expression was assessed by using western blot analysis. (c) Evaluating interfering effect of SOD2-siRNA. The cells were divided into 3 groups, including control group, SOD2-siRNA treatment group, and scrambled (SC)-siRNA treatment group. After the treatments, SOD2 protein expression was evaluated by using western blot analysis. (d) Exploring the role of SOD2 in curcumin-induced protection in HT22 cells. The cells were divided into 5 groups, including control, OGD/R treatment group, Cur + OGD/R group, SOD2-siRNA + Cur + OGD/R group, and SC-siRNA + Cur + OGD/R group; after the treatments, cell injury, apoptosis, SOD2 expression, cell morphology, intracellular ROS, mitochondrial functions, and superoxide were assessed.

twice with phosphate-buffered saline (PBS) at 37°C. Then, the complexes of 90 pmol siRNA and Lipofectamine were added into the cell culture plate, and the cells were incubated for 6 h in the incubator at 37°C. Then, the cells were washed with PBS at 37°C. The SOD2 expression was measured using western blot analysis.

2.8. SOD2 Activity Evaluation. HT22 cells were seeded into a 6-well cell culture plate at a density of 1×10^6 cells/well. After the treatments, as previously described in detail [15], SOD2 activities in U/mg protein were calculated.

2.9. Cell Apoptosis Evaluation. The cell apoptosis level was measured by using a flow cytometry (BD, USA). The cells were planted into a 6-well cell culture plate at a density of 5×10^5 cells/well. After the treatments, the cells were harvested by centrifugation at 1000 rpm for 10 min. Then, the supernatants of the cells were removed, and the cells were washed twice by ice-cold PBS. After the washing, the apoptotic rates of the cells were evaluated as previously described [12, 14].

2.10. Mitochondrial Function Evaluation. The mitochondria of the treated cells were isolated by using a mitochondrial isolation kit according to the manufacturer's instructions (Qiagen, Hilden, Germany). And the mitochondrial complex I activity was measured at 30°C as previously described by Han et al. [16]. In brief, the mitochondrial complex I activity of HT22 cells was measured by following rotenone-sensitive oxidation of NADH initiated by ubiquinone-1 (Q1). An appropriate amount of cell lysate was added into 0.5 ml assay mixture, containing 20 mM potassium phosphate buffer, 2 mM NaN_3, 0.15 mg/ml phospholipid, 0.1 mM Q1, and 0.15 mM NADH, and the pH value was 8.0. Mitochondrial complex I activity was evaluated by assessing the decrease in absorbance (340 nm) and confirmed by inhibition with 40 μM rotenone. And the activity level (nmol NADH oxidized·min^{-1} mg·protein^{-1}) was calculated with a molar extinction coefficient of 6.22 mM^{-1} cm^{-1}.

Mitochondrial membrane potential (MMP) of the treated HT22 cells was assessed by using the JC-1 (Sigma-Aldrich, St. Louis, MO, USA). According to the manufacturer's instruction, mitochondrial samples were exposed to JC-1 staining buffer. At the end of the experiments, valinomycin was used as the negative control. And the fluorescence intensity of the cells was measured by using a fluorescence spectrophotometer (TECAN, CH), and the measurement temperature was 37°C. The ratio of aggregates to monomer was calculated as the MMP indicator, and the wavelengths testing the aggregates and monomer were 590 nm (red) and 525 nm (green), respectively. We followed the methods of Du et al. [12].

2.11. Cell Morphology Observation. The cells were planted into a 6-well cell culture plate at a density of 5×10^5 cells/well. After the treatments, the cells were observed by using a phase-contrast microscope, and the photos of the cells were taken randomly.

2.12. Intracellular Reactive Oxygen Species. HT22 cells were seeded into a confocal microscopy special dish at a density of 2×10^5 cells/well. After the treatments, a reactive oxygen species (ROS) assay kit (Beyotime Technology, Nantong, China) was taken to evaluate the intracellular ROS level. In brief, the DMEM medium without FBS was added into each well, containing 100 μM DCF-DA (nonfluorescent and colorless). After 20 min incubation at 37°C, the DCF-DA was oxidized into the fluorescent 2′,7′-dichlorofluorescein (DCF) by intracellular ROS. The dish was washed three times with PBS, and then the photos were taken by using a confocal microscope (excitation = 480 nm; emission = 535 nm). Finally, the fluorescence intensities of the photos were evaluated by using Image-Pro Plus software.

2.13. Mitochondrial Superoxide Assay. MitoSOX reagent was used to measure mitochondrial superoxide level. In brief, the cells were seeded into a confocal microscopy special dish at a density of 1×10^5 cells/well. After the treatments, the HT22 cells were treated with 5 μM MitoSOX reagent for 20 min at 37°C; at the end of the treatments, 100 μl DAPI staining solution was added into the dish to mark the cell nuclei. After being washed three times with PBS, a confocal microscope was used to observe and take fluorescence photos of the cells, including mitochondrial superoxide (red, excitation = 510 nm; emission = 580 nm) and nuclei (blue, excitation = 340 nm; emission = 488 nm). Then, the fluorescence intensity of the mitochondrial superoxide was calculated by using Pro-plus software (IPP 6.0, Media Cybernetics, Silver Spring, MD, USA).

2.14. Statistical Analysis. The data of this study were analyzed by using SPSS 13.0 software (SPSS Inc., Chicago, USA). The values of all the experiments were expressed as means ± standard deviation (SD), and one-way ANOVA was used to assess the data. Tukey's multiple comparison was taken to compare the differences between the groups. $P < 0.05$ indicated statistical significance.

3. Results

3.1. Curcumin Reduced Cell Injury in OGD/R-Treated HT22 Cells and Upregulated SOD2 Expression. To find a suitable curcumin (Cur) treatment concentration, the HT22 cells were divided into 5 groups, including control, OGD/R, and 3 concentrations of curcumin treatment groups (10, 100, and 500 ng/ml curcumin plus OGD/R respectively). After 3 h OGD and 24 h reoxygenation treatment, compared with the control, OGD/R treatment reduced cell viability (Figure 2(a)) and increased LDH activity (Figure 2(b)) in the medium significantly ($P < 0.05$), and 100 and 500 ng/ml curcumin treatment restored cell viability and decreased LDH activity obviously ($P < 0.05$). Then, the cells were divided into 4 groups (Figure 2(c)), including control and 3

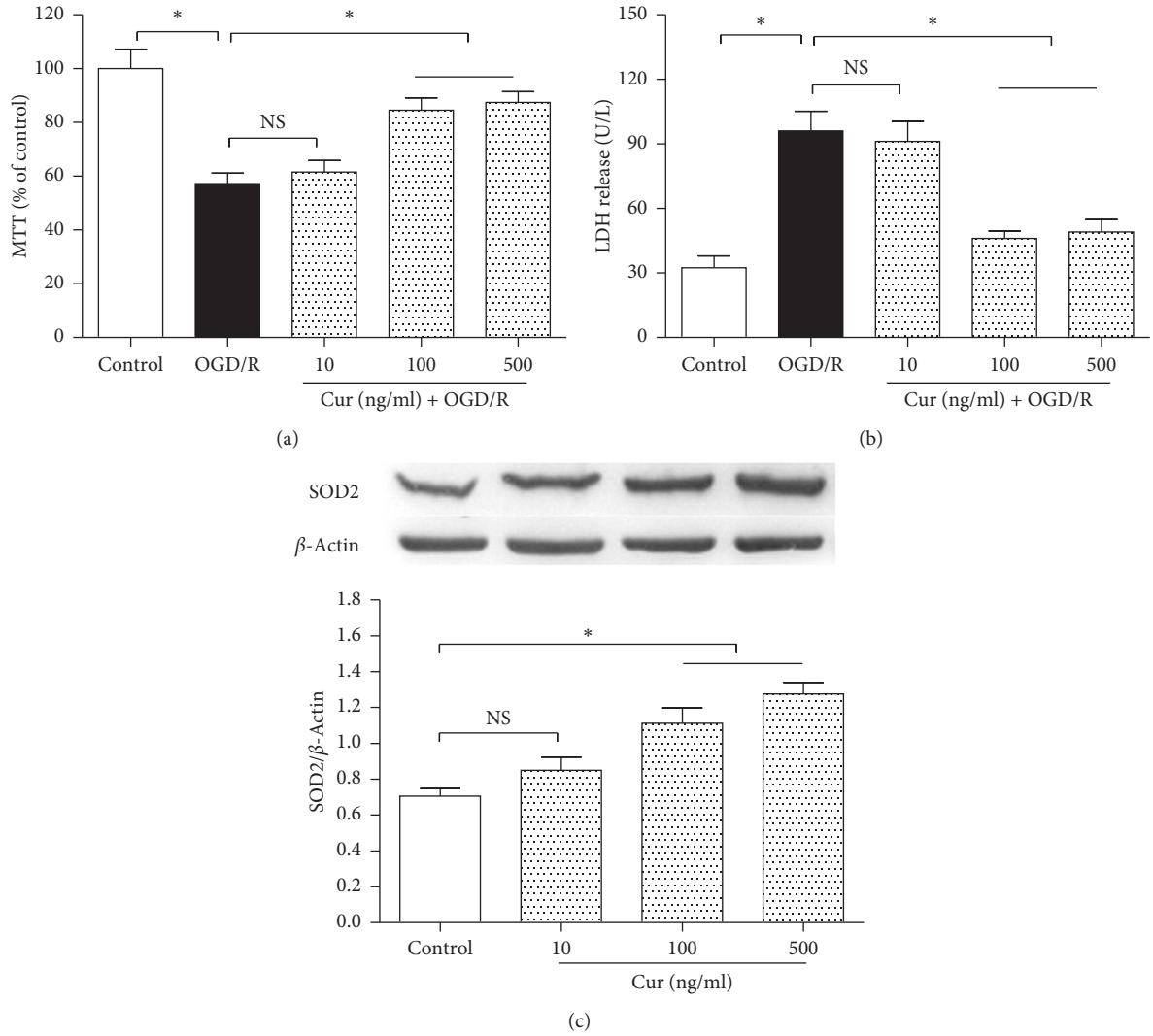

Figure 2: Curcumin decreased cell injury in HT22 cells exposed to OGD/R and upregulated SOD2 expression in normal condition. The HT22 cells were divided into 5 groups, including control, OGD/R, and 3 concentrations (10 ng/ml, 100 ng/ml, and 500 ng/ml) of curcumin plus OGD/R groups. After the treatments, cell viability and LDH release were measured by using the MTT method and reagent kit, respectively. Then, the cells were divided into 4 groups, including control and 3 concentrations (10 ng/ml, 100 ng/ml, and 500 ng/ml) of curcumin treatment groups; after 3 h exposure, western blot was performed to assess SOD2 expression. (a) Curcumin restored cell viability ($n = 8$). (b) Curcumin reduced LDH release ($n = 8$). (c) Curcumin increased SOD2 expression ($n = 4$). Results are expressed as means ± SD. $^*P < 0.05$; NS: no significance.

doses of curcumin treatment groups (10, 100 and 500 ng/ml curcumin). After 3 h treatment, compared with the control group, 100 and 500 ng/ml curcumin groups showed significantly increased SOD2 expression ($P < 0.05$). The curcumin concentration of 100 ng/ml was used in the subsequent experiments.

3.2. Downregulation of SOD2 Expression Reversed Curcumin-Induced Effects on Cell Injury, SOD2 Expression, and Activity. To explore the role of SOD2 in curcumin-induced protection against OGD/R in HT22 cells, SOD2-siRNA was taken to downregulate SOD2 protein expression (Figure 3(a)). The SOD2-siRNA used in this study reduced SOD2 expression significantly (0.31 ± 0.04 vs. 0.82 ± 0.03; $P < 0.05$), but the scrambled siRNA (SC-siRNA) did not reduce SOD2 expression (0.81 ± 0.03 vs. 0.82 ± 0.03; $P > 0.05$). Meanwhile, compared with the normal cultured control (Figure 3(b)), either the SOD2-siRNA or the SC-siRNA induced no obvious cytotoxicity ($P > 0.05$).

Then, the cells were divided into 5 groups, including control, OGD/R, Cur + OGD/R, SOD2-siRNA + Cur + OGD/R, and SC-siRNA + Cur + OGD/R. Compared with the control, 3 h OGD plus 24 h reoxygenation treatment (OGD/R) decreased SOD2 protein expression, SOD2 activity and cell viability, and increased LDH activity in the medium; concurrently, coadministration with 100 ng/ml curcumin restored SOD2 expression, SOD2 activity, and cell viability and reduced LDH release (Figures 3(c)–3(e)). However, the SOD2-siRNA, but not the SC-siRNA

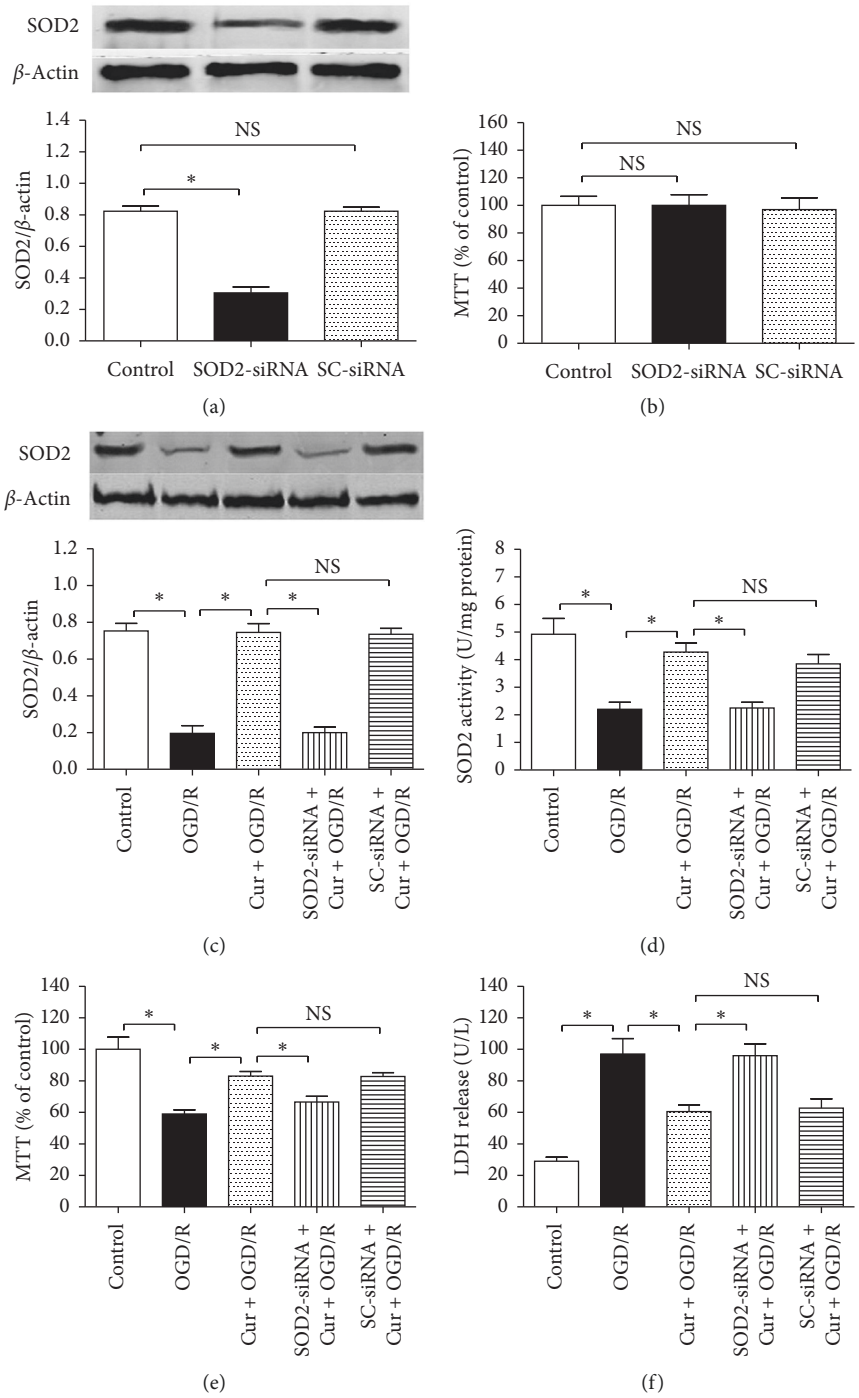

Figure 3: SOD2-siRNA reversed curcumin-induced cytoprotection and SOD2 upregulation in HT22 cells exposed to OGD/R. The cells were divided into 3 groups, including control, SOD2-siRNA, and scrambled (SC)-siRNA; after 6 h incubation, western blot and MTT assay were taken to assess SOD2 expression and cell viability, respectively. Then, the cells were divided into 5 groups, including control, OGD/R, Cur + OGD/R, SOD2-siRNA + Cur + OGD/R, and SC-siRNA + Cur + OGD/R; after 3 h OGD plus 24 h reoxygenation, SOD2 expression and activity, cell viability, and lactic dehydrogenase (LDH) were assessed. (a) SOD2-siRNA inhibited SOD2 protein expression ($n = 4$). (b) Either SOD2-siRNA or SC-siRNA induced no obvious cytotoxicity ($n = 8$). (c, d) SOD2-siRNA reversed curcumin-induced effects on SOD2 expression ($n = 4$) and activity ($n = 8$). (e) SOD2-siRNA reversed curcumin-induced cell viability restoration ($n = 8$). (f) SOD2-siRNA reversed curcumin-induced LDH release decrease ($n = 8$). Results are expressed as means ± SD. $^*P < 0.05$; NS: no significance.

($P > 0.05$), abolished the curcumin-induced cytoprotective effects against OGD/R injury significantly ($P < 0.05$). These findings showed that SOD2 mediates curcumin-induced protective effects against OGD/R in HT22 cells.

3.3. Downregulation of SOD2 Expression Reversed Curcumin-Induced Inhibitions of Cell Apoptosis and Cleaved Caspase-3 Expression. To investigate the curcumin-induced anti-apoptosis in HT22 cells exposed to OGD/R, flow cytometry and western blot were used to evaluate cell apoptotic rate and apoptosis-associated protein cleaved caspase-3 expression (Figures 4(a)–4(c)). Compared with the control, the OGD/R treatment increased cell apoptosis and cleaved caspase-3 expression ($P < 0.05$), and 100 ng/ml curcumin reduced cell apoptosis and cleaved caspase-3 expression level ($P < 0.05$); similarly, SOD2-siRNA, but not the SC-siRNA ($P > 0.05$), markedly abolished the curcumin-induced antiapoptotic effects above ($P < 0.05$). These results indicated that SOD2 protein mediates curcumin-induced anti-apoptosis in HT22 cells treated with OGD/R.

3.4. Downregulation of SOD2 Expression Abolished Curcumin-Induced Ameliorations of Cell Morphology and Mitochondrial Functions. To further observe the curcumin-induced effects on cell morphology and mitochondrial functions in HT22 cells exposed to OGD/R, phase-contrast microscope and reagent kits were taken to assess cell morphology and cellular mitochondrial functions. The cells were divided into 5 groups as shown in the Figure 5. Compared with the control, 3 h OGD plus 24 h reoxygenation (OGD/R) treatment damaged the cellular morphology (Figure 5(a)) and reduced mitochondrial membrane potential (MMP) and mitochondrial complex I activity ($P < 0.05$), which are associated with the mitochondrial functions (Figures 5(b) and 5(c)); 100 ng/ml curcumin maintained cell integrity and restored MMP and mitochondrial complex I activity ($P < 0.05$). However, the SOD2-siRNA, but not the SC-siRNA ($P > 0.05$), reversed the curcumin-induced protection in cell morphology and mitochondrial functions ($P < 0.05$). These findings showed that SOD2 mediates curcumin-induced protection in cell morphology and mitochondrial functions against OGD/R in HT22 cells.

3.5. Downregulation of SOD2 Expression Inhibited Curcumin-Induced Ameliorations on Intracellular ROS and Mitochondrial Superoxide. High level of intracellular ROS and mitochondrial superoxide can damage cell and mitochondria. Compared with the control group, 3 h OGD plus 24 reoxygenation (OGD/R) treatment increased ROS (Figures 6(a) and 6(b)) and mitochondrial superoxide levels (Figures 6(c) and 6(d)), and coadministration with 100 ng/ml curcumin reduced the ROS and mitochondrial superoxide levels obviously ($P < 0.05$); similarly, SOD2-siRNA, but not the SC-siRNA ($P > 0.05$), reversed the curcumin-induced downregulation on intracellular ROS and mitochondrial superoxide ($P < 0.05$). These observations showed that SOD2 mediates curcumin-induced antioxidation effects against OGD/R in HT22 cells.

4. Discussion

In the present study, the HT22 neuronal cells were exposed to OGD for 3 h and then cultured in normal medium for 24 h to imitate the neuronal I/R injury, and 100 ng/ml curcumin was coadministered to reduce the OGD/R-induced cell injury. Compared with the control, OGD/R increased the cell injury, apoptosis, intracellular ROS, and mitochondrial superoxide, reduced mitochondrial functions and intracellular SOD2, and damaged cell morphology; meanwhile, the presence of curcumin reduced cell injury, apoptosis, intracellular ROS, and mitochondrial superoxide, restored mitochondrial functions and SOD2, and maintained cell integrity. However, SOD2-siRNA, but not the SC-siRNA, significantly reversed the curcumin-induced protections above. These findings indicated that curcumin alleviates OGD/R-induced injury in HT22 cells, and SOD2 may mediate the curcumin-induced protection (Figure 7).

Stroke is one of the leading causes of disability and death in the worldwide [17]. Unfortunately, however, effective medicine or therapy in treating the disease is extremely limited. The limited therapeutic time window of rTPA decreases its use greatly. For this reason, exploring medicine or therapy for stroke is of great importance. According to the findings of some latest investigations, oxidative injury and mitochondrial dysfunction participate in the pathophysiological process of stroke [9–11]. Oxidative injury can consume intracellular antioxidants, including glutathione (GSH), catalase (CAT), and SOD, and also damage the neuronal membrane [18, 19]. Meanwhile, especially after reperfusion of stroke, too much ROS could be generated [20], which may injure mitochondria and consume SOD2 [21]. Therefore, ameliorating mitochondrial functions and increasing SOD2 level are regarded to be effective in treating stroke. As stroke causes ischemic injury and reperfusion injury to brain tissue, and reperfusion injury may be more serious than ischemic injury [22]. In this study, the HT22 cells were treated with 3 h OGD injury and then cultured in normal medium for 24 h to mimic the I/R injury of stroke. Apoptosis is an important cell death pattern after I/R injury, and to assess the cell apoptosis degree, we took flow cytometry and western blot to measure cell apoptosis rate and cleaved caspase-3 expression, which is an apoptosis-associated protein, and its expression level is closely related to the apoptosis of cells [23]. In this study, curcumin reduced cleaved caspase-3 expression in the OGD/R-treated HT22 cells, and SOD2-siRNA reversed the antiapoptosis effects of curcumin, indicating that the curcumin-induced anti-apoptosis in neuronal cells exposed to OGD might be via SOD2 protein.

Curcumin is an extract from seasoning curry and herbal *Carcuma longa* Linn. Some recent investigations reported that curcumin can induce antioxidation, anticerebral infarction, anti-inflammation, and neuroprotection [24–26]. In addition, some other studies showed that curcumin can

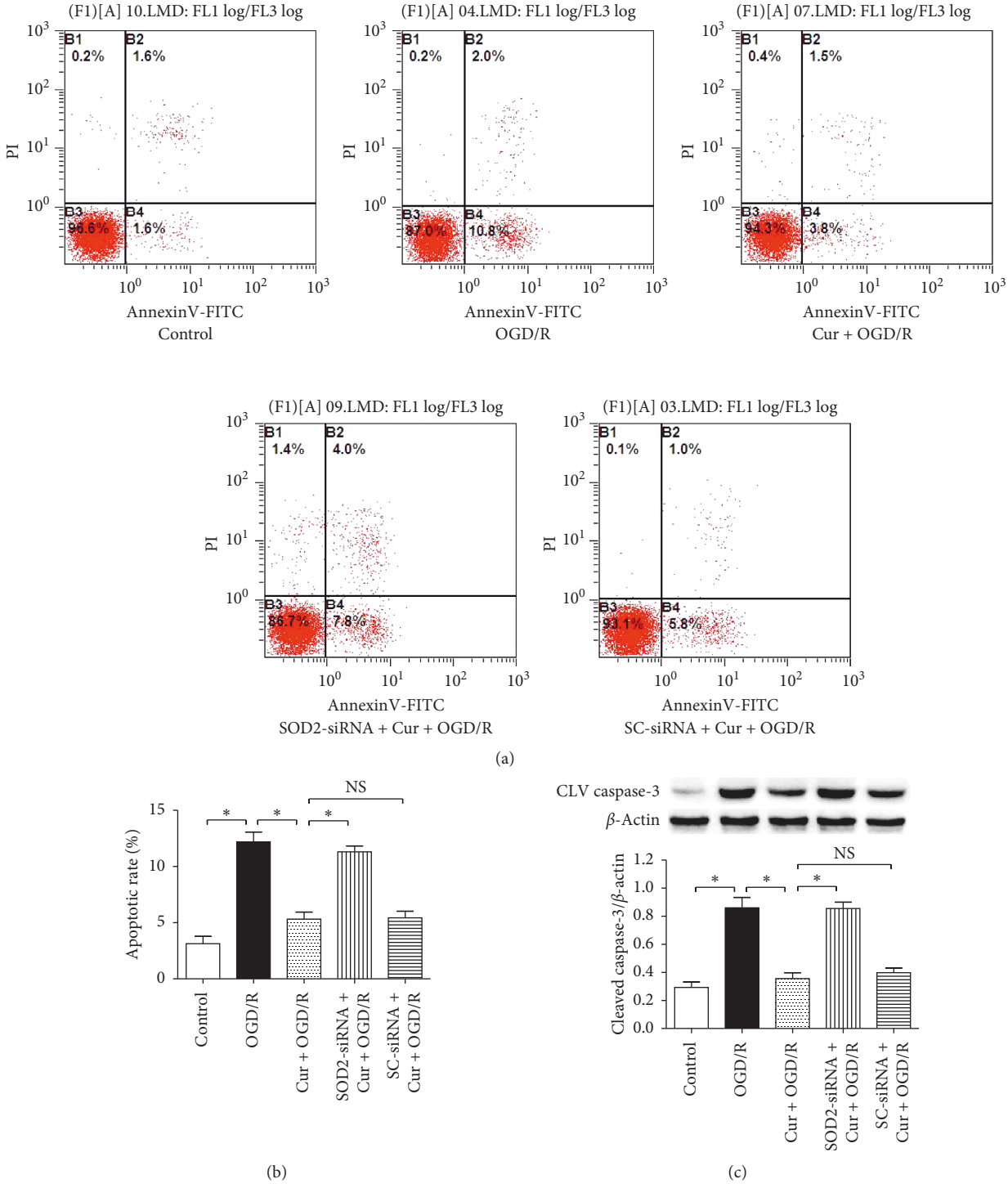

Figure 4: SOD2-siRNA reversed curcumin-induced antiapoptotic effects in HT22 cells exposed to OGD/R. The cells were divided into 5 groups, including control, OGD/R, Cur + OGD/R, SOD2-siRNA + Cur + OGD/R, and SC-siRNA + Cur + OGD/R; after 3 h OGD and 24 h reoxygenation, cell apoptotic rate and cleaved caspase-3 expression were evaluated by using flow cytometry and western blot, respectively. (a) Flow cytometry results of cells. (b) SOD2-siRNA reversed curcumin-induced antiapoptotic effect ($n = 6$). (c) SOD2-siRNA reversed curcumin-induced downregulation of cleaved caspase-3 expression ($n = 4$). Results are expressed as means ± SD. $^*P < 0.05$; NS: no significance.

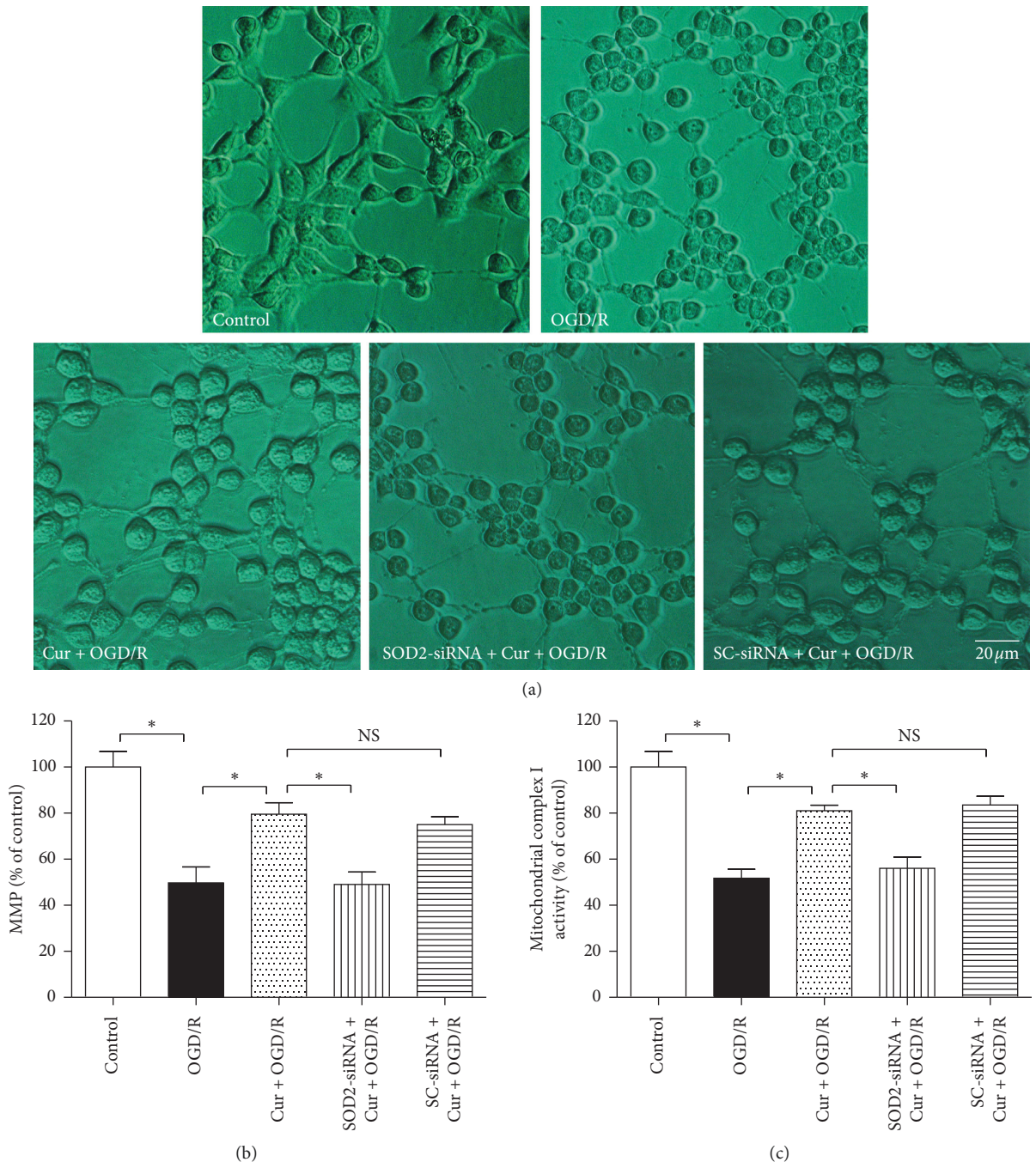

Figure 5: SOD2-siRNA reversed curcumin-induced ameliorations of cell morphology and mitochondrial functions in HT22 cells exposed to OGD/R. The cells were divided into 5 groups, including control, OGD/R, Cur + OGD/R, SOD2-siRNA + Cur + OGD/R, and SC-siRNA + Cur + OGD/R; after 3 h OGD and 24 h reoxygenation, cell morphology and mitochondrial functions were evaluated. (a) SOD2-siRNA reversed curcumin-induced cell morphology amelioration. (b) SOD2-siRNA reversed curcumin-induced amelioration of mitochondrial membrane potential (MMP) ($n = 8$). (c) SOD2-siRNA reversed curcumin-induced amelioration of mitochondrial complex I activity ($n = 8$). Results are expressed as means ± SD. $^*P < 0.05$; NS: no significance; Bar = 20 μm.

ameliorate mitochondrial functions in neuronal cells [27]. Xie et al. [28] reported that curcumin can reduce neuronal injury against I/R and OGD/R in vivo and in vitro, and restricting Bax activation may be the key neuroprotective mechanism of curcumin. In another two investigations, nuclear factor erythroid-2-related factor 2 (Nrf2), a nuclear transcription factor with neuroprotective effects against central nervous system disease, was reported to be involved in curcumin-induced neuroprotection against hypoxic-ischemic brain injury in neonatal rats and against OGD/R injury in primary cultured cortical neurons [29, 30]. In the present study, we explored the role of curcumin in OGD/R-

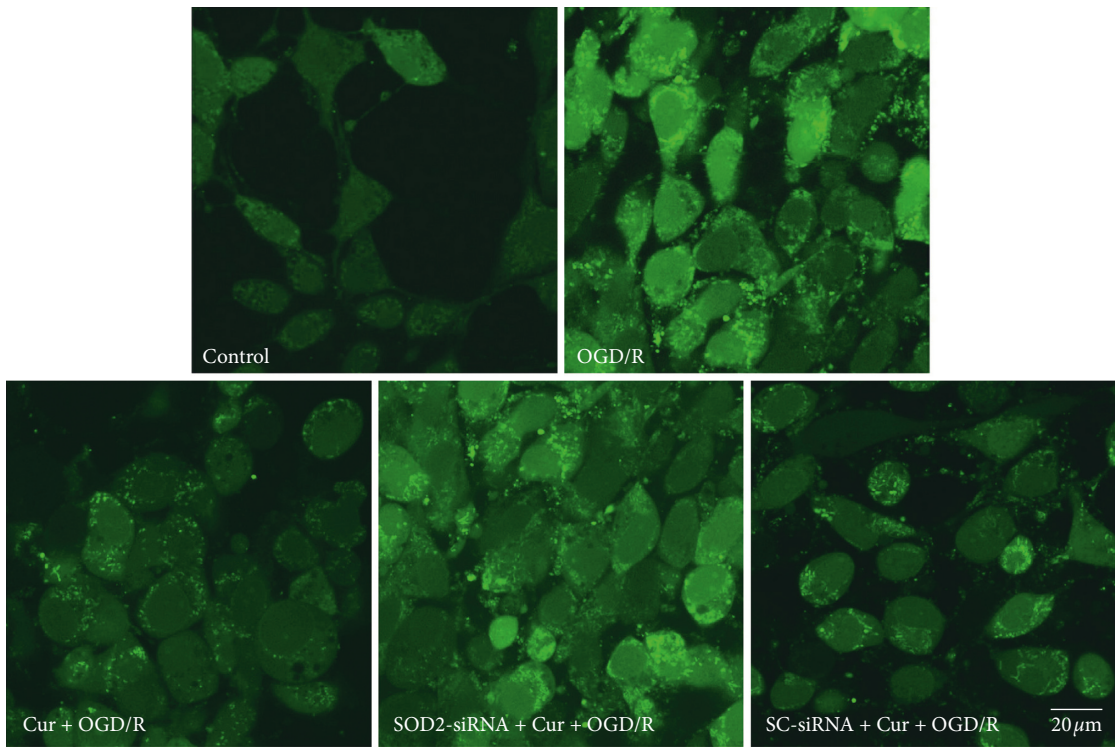

(a)

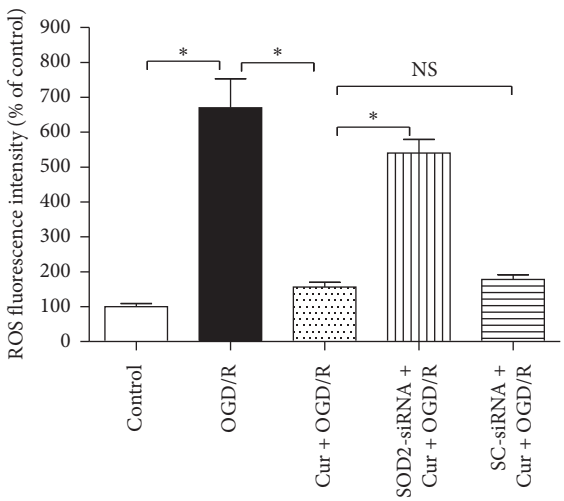

(b)

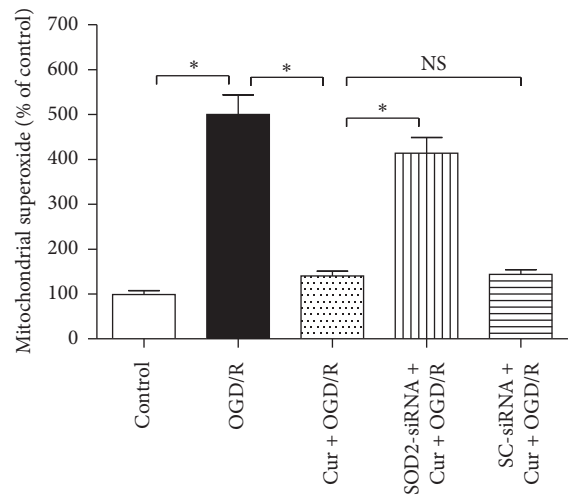

(c)

Figure 6: Continued.

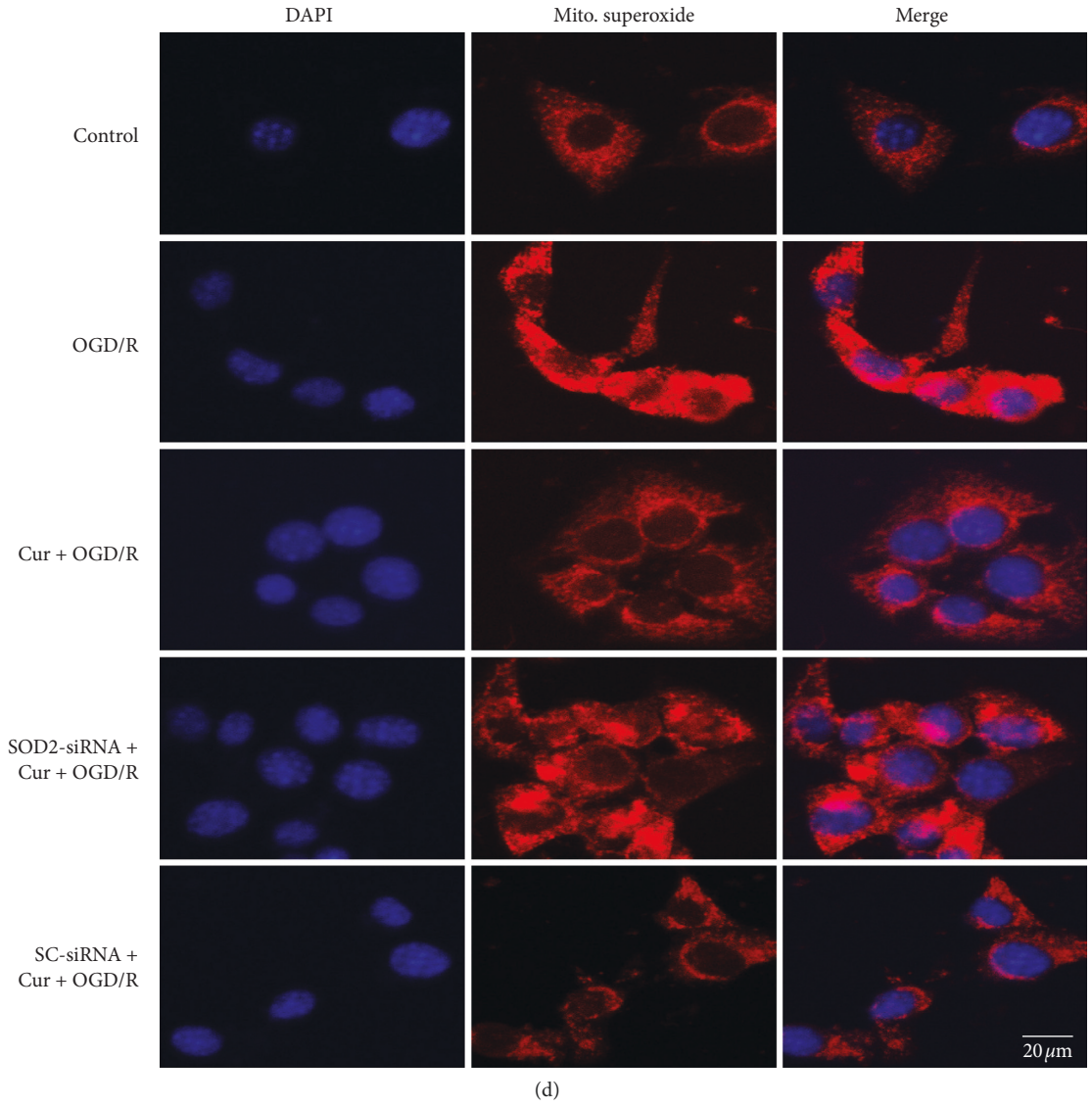

Figure 6: SOD2-siRNA reversed curcumin-induced reduction of intracellular ROS and mitochondrial superoxide in HT22 cells exposed to OGD/R. The cells were divided into 5 groups, including control, OGD/R, Cur + OGD/R, SOD2-siRNA + Cur + OGD/R, and SC-siRNA + Cur + OGD/R; after 3 h OGD and 24 h reoxygenation, intracellular ROS and mitochondrial superoxide were evaluated. (a) Intracellular ROS fluorescence staining results. (b) SOD2-siRNA reversed curcumin-induced intracellular ROS reduction ($n = 8$). (c) SOD2-siRNA reversed curcumin-induced mitochondrial superoxide reduction ($n = 8$). (d) Mitochondrial superoxide fluorescence staining results. Results are expressed as means ± SD. $^*P < 0.05$; NS: no significance; Bar = 20 μm.

induced neuronal injury and determined whether SOD2 protein mediates curcumin-induced potential protection against OGD/R. We found that curcumin alleviated the OGD/R-induced cell injury and apoptosis, maintained cell morphology and mitochondrial functions, and increased SOD2 expression, ROS, and mitochondrial superoxide in the cells. Downregulating SOD2 expression, however, obviously abolished the curcumin-induced cytoprotection and mitochondrial function improvement and also reversed the curcumin-induced reductions on intracellular ROS and mitochondrial superoxide. High-level ROS and mitochondrial superoxide accumulation can oxidize and damage cell membrane and mitochondria. SOD2 is a protein expressed in mitochondria. Too much consumption of SOD2 can damage mitochondria and inhibit mitochondrial functions, leading to a reduction in mitochondrial energy generation [31]. Then, without enough energy supply, general functions of neuronal cells, including proliferation, action potential, excitability, and activation, could be abnormal. For the neuronal cells, energy supply deficiency can increase glutamate (an excitatory neurotransmitter) release, and the neuronal excitability may be upregulated, and long-term exposure to glutamate can activate the N-methyl-D-aspartic acid (NMDA) receptors expressed in the neuronal membrane, causing neural death and dysfunction ultimately [32]. In this study, we measured the MMP and mitochondrial complex I levels in the cells. The activation of NMDA receptors can induce overload of intracellular calcium [32].

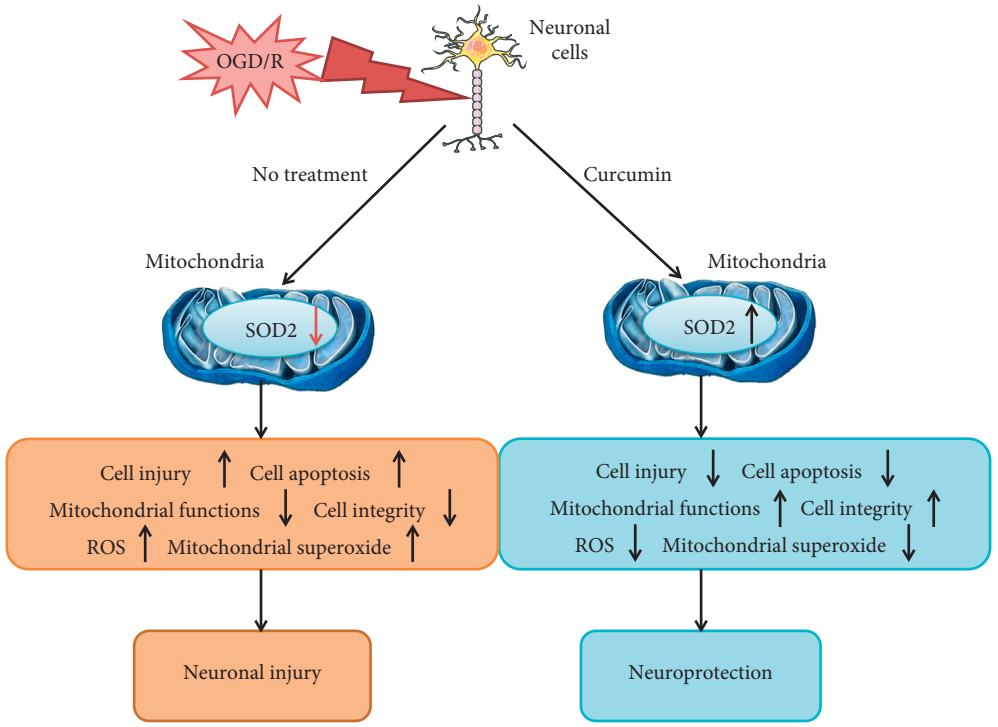

Figure 7: Curcumin induces neuroprotection against OGD/R in neuronal cells via upregulating SOD2 protein. Oxygen-glucose deprivation and reoxygenation (OGD/R) injury can downregulate SOD2 expression, increase intracellular ROS and mitochondrial superoxide accumulations, then damage neuronal cells, increase cell apoptosis, cause mitochondrial dysfunctions, and undermine cell integrity, leading to neuronal injury ultimately. Coadministration of curcumin, however, could upregulate SOD2 expression, reduce intracellular ROS and mitochondrial superoxide accumulations, and ameliorate mitochondrial functions and cell integrity, causing neuroprotection.

Then, high concentration of intracellular calcium may inhibit oxidative phosphorylation and MMP, and the ability of mitochondria to produce energy (ATP) will decrease, leading to chloride ion infusion and cell death ultimately [33]. Mitochondrial respiratory chain consists of five complexes, including mitochondrial complex I-V, which are also called mitochondrial complex enzymes, and complex I is the most sensitive respiratory enzyme to ischemia among the five. Mitochondrial complex I can oxidize tricarboxylic acid cycle-produced NADH in the inner mitochondrial membrane, and it participates in producing ATP with ATPase. And brain ischemia results in greater complex I injury after brain oxygen deprivation [34]. Therefore, we evaluated MMP and mitochondrial complex I levels in the OGD/R-treated cells to determine the protective effects of curcumin in mitochondrial functions. Except for SOD2, SOD1 and SOD3 also induce protection against oxidative injury, and SOD1 is expressed in intercellular space, while SOD3 is in the cytoplasm [35]. In addition, evaluating the change of mitochondrial function is another aim of this study. Therefore, we explored SOD2, but not SOD1 or SOD3. In one study about osteoblasts in mice, SOD2 protected mitochondria against oxidative injury and increased osteoblast differentiation [36]. Another study reported that curcumin increased intracellular SOD2 level in human hepatoma cells [37]. In one of our studies, we found that curcumin can protect HT22 cells against Aβ-induced injury, and SOD2 protein mediates the curcumin-induced protection [12]. The findings of the present study explained, to some extent, the neuroprotective mechanism of curcumin against brain I/R. However, there are several limitations in our investigation. In the first place, the findings of this study were from in vitro and neuronal cell line, and whether similar results can be observed in vivo or in primary cultured neurons is unknown. In addition, except for SOD2, whether SOD1 or SOD3 mediates curcumin-induced neuroprotection is also not clear.

Taken together, in the present study, we found that curcumin can reduce OGD/R-induced cell injury in HT22 cells, and SOD2 protein mediates the curcumin-induced neuroprotection.

Data Availability

All datasets analyzed during the current study are available from the corresponding author upon reasonable request.

Conflicts of Interest

The authors declare no conflicts of interest.

Authors' Contributions

Yuqing Wang, Yuanyuan Zhang, and Liang Yang contributed equally to this work.

Acknowledgments

This study was supported by the Natural Science Foundation of Guangdong Province, China (no. 2016A030313613), the Science and Technology Program of Guangdong Province, China (no. 2016A020215132), and the Science and Technology Program of Guangzhou, China (nos. 201707010027 and 201707010474).

References

[1] C. S. Anderson, Y. Huang, R. I. Lindley et al., "Intensive blood pressure reduction with intravenous thrombolysis therapy for acute ischaemic stroke (ENCHANTED): an international, randomised, open-label, blinded-endpoint, phase 3 trial," *Lancet*, vol. 393, no. 10174, pp. 877–888, 2019.

[2] L. Ma, W. Niu, S. Yang et al., "Inhibition of mitochondrial permeability transition pore opening contributes to cannabinoid type 1 receptor agonist ACEA-induced neuroprotection," *Neuropharmacology*, vol. 135, pp. 211–222, 2018.

[3] S. J. Snow, "Stroke and t-PA-triggering new paradigms of care," *New England Journal of Medicine*, vol. 374, no. 9, pp. 809–811, 2016.

[4] K. Murakami, M. Suzuki, N. Suzuki, K. Hamajo, T. Tsukamoto, and M. Shimojo, "Cerebroprotective effects of TAK-937, a novel cannabinoid receptor agonist, in permanent and thrombotic focal cerebral ischemia in rats: therapeutic time window, combination with t-PA and efficacy in aged rats," *Brain Research*, vol. 1526, pp. 84–93, 2013.

[5] A. Mukherjee, S. Sarkar, S. Jana, S. Swarnakar, and N. Das, "Neuro-protective role of nanocapsulated curcumin against cerebral ischemia-reperfusion induced oxidative injury," *Brain Research*, vol. 1704, pp. 164–173, 2019.

[6] K. Bavarsad, G. E. Barreto, M.-A.-R. Hadjzadeh, and A. Sahebkar, "Protective effects of curcumin against ischemia-reperfusion injury in the nervous system," *Molecular Neurobiology*, vol. 56, no. 2, pp. 1391–1404, 2019.

[7] Y. Zhang, X. Yang, X. Ge, and F. Zhang, "Puerarin attenuates neurological deficits via Bcl-2/Bax/cleaved caspase-3 and Sirt3/SOD2 apoptotic pathways in subarachnoid hemorrhage mice," *Biomedicine & Pharmacotherapy*, vol. 109, pp. 726–733, 2019.

[8] L. Xu, J. F. Emery, Y.-B. Ouyang, L. A. Voloboueva, and R. G. Giffard, "Astrocyte targeted overexpression of Hsp72 or SOD2 reduces neuronal vulnerability to forebrain ischemia," *Glia*, vol. 58, no. 9, pp. 1042–1049, 2010.

[9] J. Yin, P. Han, Z. Tang, Q. Liu, and J. Shi, "Sirtuin 3 mediates neuroprotection of ketones against ischemic stroke," *Journal of Cerebral Blood Flow & Metabolism*, vol. 35, no. 11, pp. 1783–1789, 2015.

[10] O. Akpınar, M. Nazıroğlu, and H. Akpınar, "Different doses of dexmedetomidine reduce plasma cytokine production, brain oxidative injury, PARP and caspase expression levels but increase liver oxidative toxicity in cerebral ischemia-induced rats," *Brain Research Bulletin*, vol. 130, pp. 1–9, 2017.

[11] S. S. Andrabi, S. Parvez, and H. Tabassum, "Progesterone induces neuroprotection following reperfusion-promoted mitochondrial dysfunction after focal cerebral ischemia in rats," *Disease Models & Mechanisms*, vol. 10, no. 6, pp. 787–796, 2017.

[12] S. Du, Y. Zhang, J. Yang et al., "Curcumin alleviates β amyloid-induced neurotoxicity in HT22 cells via upregulating SOD2," *Journal of Molecular Neuroscience*, vol. 67, no. 4, pp. 540–549, 2019.

[13] S.-P. Lin, S. Ye, Y. Long et al., "Circular RNA expression alterations are involved in OGD/R-induced neuron injury," *Biochemical and Biophysical Research Communications*, vol. 471, no. 1, pp. 52–56, 2016.

[14] J. Jia, L. Ma, M. Wu et al., "Anandamide protects HT22 cells exposed to hydrogen peroxide by inhibiting CB1 receptor-mediated type 2 NADPH oxidase," *Oxidative Medicine and Cellular Longevity*, vol. 2014, Article ID 893516, 16 pages, 2014.

[15] J. Jia, L. Zhang, X. Shi et al., "SOD2 mediates amifostine-induced protection against glutamate in PC12 cells," *Oxidative Medicine and Cellular Longevity*, vol. 2016, Article ID 4202437, 11 pages, 2016.

[16] Z. Han, Y.-R. Chen, C. I. Jones 3III, G. Meenakshisundaram, J. L. Zweier, and B. R. Alevriadou, "Shear-induced reactive nitrogen species inhibit mitochondrial respiratory complex activities in cultured vascular endothelial cells," *American Journal of Physiology-Cell Physiology*, vol. 292, no. 3, pp. C1103–C1112, 2007.

[17] J. Dąbrowski, A. Czajka, J. Zielińska-Turek et al., "Brain functional reserve in the context of neuroplasticity after stroke," *Neural Plasticity*, vol. 2019, Article ID 9708905, 10 pages, 2019.

[18] Y. Zhang, Z. Cheng, C. Wang, H. Ma, W. Meng, and Q. Zhao, "Neuroprotective effects of kukoamine a against radiation-induced rat brain injury through inhibition of oxidative stress and neuronal apoptosis," *Neurochemical Research*, vol. 41, no. 10, pp. 2549–2558, 2016.

[19] O. Rebai, M. Belkhir, M. V. Sanchez-Gomez, C. Matute, S. Fattouch, and M. Amri, "Differential molecular targets for neuroprotective effect of chlorogenic acid and its related compounds against glutamate induced excitotoxicity and oxidative stress in rat cortical neurons," *Neurochemical Research*, vol. 42, no. 12, pp. 3559–3572, 2017.

[20] M. S. Sun, H. Jin, X. Sun et al., "Free radical damage in ischemia-reperfusion injury: an obstacle in acute ischemic stroke after revascularization therapy," *Oxidative Medicine and Cellular Longevity*, vol. 2018, Article ID 3804979, 17 pages, 2018.

[21] S. Sun, X. Chen, Y. Gao et al., "Mn-SOD upregulation by electroacupuncture attenuates ischemic oxidative damage via CB1r-mediated STAT3 phosphorylation," *Molecular Neurobiology*, vol. 53, no. 1, pp. 331–343, 2016.

[22] Z. Li, H. Chen, J. Lv, and R. Zhao, "The application and neuroprotective mechanisms of cerebral ischemic post-conditioning: a review," *Brain Research Bulletin*, vol. 131, pp. 39–46, 2017.

[23] D. Hernandez-Baltazar, M. E. Mendoza-Garrido, and D. Martinez-Fong, "Activation of GSK-3β and caspase-3 occurs in nigral dopamine neurons during the development of apoptosis activated by a striatal injection of 6-hydroxydopamine," *PLoS One*, vol. 8, no. 8, Article ID e70951, 2013.

[24] W. R. García-Niño, E. Tapia, C. Zazueta et al., "Curcumin pretreatment prevents potassium dichromate-induced hepatotoxicity, oxidative stress, decreased respiratory complex I activity, and membrane permeability transition pore opening," *Evidence-Based Complementary and Alternative Medicine*, vol. 2013, Article ID 424692, 19 pages, 2013.

[25] Z. Fan, J. Li, J. Liu, H. Jiao, and B. Liu, "Anti-inflammation and joint lubrication dual effects of a novel hyaluronic acid/curcumin nanomicelle improve the efficacy of rheumatoid arthritis therapy," *ACS Applied Materials & Interfaces*, vol. 10, no. 28, pp. 23595–23604, 2018.

[26] Z. J. Liu, W. Liu, L. Liu et al., "Curcumin protects neuron against cerebral ischemia-induced inflammation through improving PPAR-gamma function," *Evidence-Based Complementary and Alternative Medicine*, vol. 2013, Article ID 470975, 10 pages, 2013.

[27] P. Dai, Y. Mao, X. Sun et al., "Attenuation of oxidative stress-induced osteoblast apoptosis by curcumin is associated with preservation of mitochondrial functions and increased akt-GSK3β signaling," *Cellular Physiology and Biochemistry*, vol. 41, no. 2, pp. 661–677, 2017.

[28] C. J. Xie, A. P. Gu, J. Cai, Y. Wu, and R.-C. Chen, "Curcumin protects neural cells against ischemic injury in N2a cells and mouse brain with ischemic stroke," *Brain and Behavior*, vol. 8, no. 2, Article ID e00921, 12 pages, 2018.

[29] J. Wu, Q. Li, X. Wang et al., "Neuroprotection by curcumin in ischemic brain injury involves the Akt/Nrf2 pathway," *PLoS One*, vol. 8, no. 3, Article ID e59843, 9 pages, 2013.

[30] X. Cui, H. Song, and J. Su, "Curcumin attenuates hypoxic-ischemic brain injury in neonatal rats through induction of nuclear factor erythroid-2-related factor 2 and heme oxygenase-1," *Experimental and Therapeutic Medicine*, vol. 14, no. 2, pp. 1512–1518, 2017.

[31] J. Gao, S. Liu, F. Xu et al., "Trilobatin protects against oxidative injury in neuronal PC12 cells through regulating mitochondrial ROS homeostasis mediated by AMPK/Nrf2/Sirt3 signaling pathway," *Frontiers in Molecular Neuroscience*, vol. 11, p. 16, 2018.

[32] J. Allyson, E. Dontigny, Y. Auberson, M. Cyr, and G. Massicotte, "Blockade of NR2A-containing NMDA receptors induces tau phosphorylation in rat hippocampal slices," *Neural Plasticity*, vol. 2010, Article ID 340168, 10 pages, 2010.

[33] Y. Zhang, X. Zhao, Y. Chang et al., "Calcium channel blockers ameliorate iron overload-associated hepatic fibrosis by altering iron transport and stellate cell apoptosis," *Toxicology and Applied Pharmacology*, vol. 301, pp. 50–60, 2016.

[34] A. Stepanova, A. Kahl, C. Konrad, V. Ten, A. S. Starkov, and A. Galkin, "Reverse electron transfer results in a loss of flavin from mitochondrial complex I: potential mechanism for brain ischemia reperfusion injury," *Journal of Cerebral Blood Flow & Metabolism*, vol. 37, no. 12, pp. 3649–3658, 2017.

[35] E. Barcińska, J. Wierzbicka, A. Zauszkiewicz-Pawlak, D. Jacewicz, A. Dabrowska, and I. Inkielewicz-Stepniak, "Role of oxidative and nitro-oxidative damage in silver nanoparticles cytotoxic effect against human pancreatic ductal adenocarcinoma cells," *Oxidative Medicine and Cellular Longevity*, vol. 2018, Article ID 8251961, 15 pages, 2018.

[36] J. Gao, Z. Feng, X. Wang et al., "SIRT3/SOD2 maintains osteoblast differentiation and bone formation by regulating mitochondrial stress," *Cell Death & Differentiation*, vol. 25, no. 2, pp. 229–240, 2018.

[37] S. Gounden and A. Chuturgoon, "Curcumin upregulates antioxidant defense, lon protease, and heat-shock protein 70 under hyperglycemic conditions in human hepatoma cells," *Journal of Medicinal Food*, vol. 20, no. 5, pp. 465–473, 2017.

Hindawi
Evidence-Based Complementary and Alternative Medicine
Volume 2019, Article ID 1685128, 9 pages
https://doi.org/10.1155/2019/1685128

Research Article

The Variant at TGFBRAP1 but Not TGFBR2 Is Associated with Antituberculosis Drug-Induced Liver Injury

Jingwei Zhang, Zhenzhen Zhao, Hao Bai, Lin Jiao, Qian Wu, Tao Wu, Tangyuheng Liu, Xuejiao Hu, Jiajia Song, Mengyuan Lyv, and Binwu Ying

Department of Laboratory Medicine, West China Hospital, Sichuan University, Chengdu, Sichuan, China

Correspondence should be addressed to Binwu Ying; docbwy@126.com

Received 14 May 2019; Revised 12 July 2019; Accepted 4 August 2019; Published 22 August 2019

Academic Editor: Mario Ledda

Background. TGFBRAP1 and TGFBR2 play important roles in the TGF-β/smad signalling pathway and may disturb liver homeostasis by regulating liver injury and renewal. However, little is known about the association between their genetic polymorphisms and antituberculosis drug-induced liver injury (ATDILI), so we explored the association between their variants and the susceptibility to ATDILI. *Materials and Methods*. A total of 746 tuberculosis patients were prospectively enrolled, and fifteen selected SNPs were genotyped. The allele, genotype, and genetic model frequencies of the variants were compared between patients with or without ATDILI, as well as the joint effect analysis of SNP-SNP interactions. The odds ratio (OR) with the corresponding 95% confidence interval (CI) was calculated. *Results*. The A variant at rs17687727 was significantly associated with an increased risk for ATDILI (OR 1.55; 95% CI: 1.08–2.22; $p = 0.016$), which is consistent with the results in the additive and dominant models. Other allele, genotype, and genetic model frequencies were similar in the two groups for the other fourteen SNPs (all $p > 0.05$). *Conclusion*. Our study first implied that the A variant of rs17687727 in TGFBRAP1 influenced the susceptibility to ATDILI in first-line antituberculosis combination treatment in the Han Chinese population in a dependent manner.

1. Introduction

Tuberculosis (TB) is a leading infectious disease, with approximately 10 million new cases and 1.6 million deaths in 2017 as reported by the WHO [1]. In addition, China had the second largest number of new TB cases in the world in 2017 [1]. At present, although significant progress has been made in the treatment of antituberculosis drugs, the combination of isoniazid, rifampicin, pyrazinamide, and streptomycin is still recommended by the WHO as the standard chemotherapy to cure tuberculosis effectively and prevent the production of resistant bacteria [1]. Although effective, 2.0–28.0% of patients receiving the combination therapy developed antituberculosis drug-induced liver injury (ATDILI). The incidence fluctuates depending on the characteristics of the particular cohort, drug regimens involved, threshold used to define hepatotoxicity, and monitoring and reporting practices [2, 3]. Because of atypical symptoms and nonspecific diagnostic criteria, it is difficult to make an early and accurate diagnosis of ATDILI, which can result in delayed treatment. Whereas mild ATDILI can recover by itself after withdrawing related drugs, severe ATDILI can cause fulminant hepatic failure, liver transplantation, or even death, resulting in a heavy social burden [4]. Prediction of hepatotoxicity is critical in the treatment of TB and can guide the choice of safe medicines.

The pathogenesis of ATDILI mainly involves four mechanisms: drug metabolism, oxidative stress, mitochondrial dysfunction, and immune regulation and inflammatory response [3, 5]. Although the exact mechanisms are not yet fully understood, genetic polymorphisms of genes related to hypothesis have been extensively studied, which helped to clarify the pathogenic mechanisms, and there is growing evidence that genetic vulnerability of related genes may be involved in the pathogenesis [6]. Single nucleotide polymorphisms (SNPs), which are the most common genetic variants, have been shown to have ATDILI clinical guidance value. For example, the associations of

"slow acetylation" phenotypes of the NAT gene with increased rates of toxic reactions have been incorporated into the FDA's drug label for isoniazid treatment [7]. In addition, in studies of other genes, such as drug metabolizing enzymes, accumulation of bile acids, lipids, and haem metabolites, immune adaptation, and oxidant challenge, the association still needs further verification [7]. However, these studies also provide novel insight into our better understanding of ATDILI. It is necessary and urgent to clarify the pathogenesis of ATDILI and discover key molecules in the progression as targets for diagnosis and treatment.

Transforming growth factor-beta (TGF-β) is a key regulator of liver physiology and pathology, contributing to all stages of disease progression, from initial liver injury through inflammation, wound healing, tissue homeostasis, fibrosis, immune modulation, and hepatocellular carcinoma (HCC) [8]. The TGF-β/smad signalling pathway can regulate the function of lymphocytes and macrophages; as a result, inflammatory-related cytokine changes in dose and time-space effects may be involved in liver homeostasis [9]. Therefore, it is reasonable to infer the potential involvement of the TGF-β/smad signalling pathway in ATDILI. There are three types of TGF-β transmembrane receptors: TGF-β receptor 1 (TGFBR1), TGF-β receptor 2 (TGFBR2), and TGF-β receptor 3 (TGFBR3). Only TGFBR2 can bind TGF-β1, and then, it promotes TGFBR1 phosphorylation and recruitment to trigger the formation of a heterotetrameric complex of TGFBR1 and TGFBR2. Then, activated receptor complexes mediate canonical TGF-β signalling through phosphorylation of the receptor-associated SMADs (smad2/3). After phosphorylation, smad2/3 forms a trimeric complex with smad4, which translocates to the nucleus and associates with other transcription factors to regulate gene expression. TGF-β receptor-associated protein 1 (TGFBRAP1) was recently shown to be the molecular chaperone of smad 4. TGFBRAP1 carries smad 4 to the activated TGFBR2 complex and promotes the phosphorylation of smad 2/3 [10]. The mutant form of TGFBRAP1 may inhibit the signalling pathway through interference complex formation [10]. Therefore, as the important role of TGFBRAP1 and TGFBR2 in the signalling pathway, genetic gene polymorphisms of TGFBRAP1 and TGFBR2 have been researched in hepatocellular carcinomas and hepatitis C infection, which indicated that genetic polymorphisms of TGFBRAP1 and TGFBR2 may disturb the regulation in liver injury and renewal [11–13]. However, to the best of our knowledge, no genetic associations between TGFBRAP1 and TGFBR2 variants and ATDILI have been reported.

Therefore, considering the heavy load of tuberculosis in China, the aim of the present study was to explore the possible association between TGFBRAP1 and TGFBR2 gene polymorphisms with the risk of ATDILI in the Han Chinese population.

2. Subjects and Methods

2.1. Subjects. Ethical approval for this study was obtained from the Institutional Review Board of the West China Hospital of Sichuan University. We recruited 1060 highly suspicious tuberculosis patients at the West China Hospital between December 2014 and April 2018 consecutively. In total, 817 tuberculosis patients were confirmed by experienced respiratory physicians with a clear tuberculosis diagnosis. All patients underwent standard short-course chemotherapy consisting of isoniazid, rifampicin, pyrazinamide, and ethambutol for six months in accordance with the approved guidelines. Treatments were adjusted accordingly if any patient developed definite ATDILI. The definition of drug-induced liver injury we used was based on the National Institutes of Health and Common Toxicity Criteria for Adverse Events v5.0 (CTCAE v5.0), unless stated otherwise [14]. The inclusion criteria for the ATDILI group were as follows: (a) normal serum alanine aminotransferase (ALT) (0–40 IU/L) and aspartate aminotransferase (AST) (0–40 IU/L) before treatment; (b) ALT and/or AST levels $\geq 3 \times$ upper limit of normal (ULN) (120 IU/L) with hepatitis symptoms such as jaundice, nausea, vomiting, and abdominal pain; (c) ALT and/or AST levels $\geq 5 \times$ ULN (200 IU/L), with or without symptoms; (d) total bilirubin (TBIL) $\geq 1.5 \times$ ULN (42 μmol/L); and (e) no administration of other potentially hepatotoxic drugs two weeks before the occurrence of ATDI (LIDI/> HIV) (no history of HIV treatment [14, 15]). The inclusion criteria for the non-ATDILI group were normal serum ALT, AST, and TBIL before and after treatment. Ultimately, 746 tuberculosis patients receiving first-line treatment were enrolled. The process of study enrolment is shown in S1 Figure. Demographic and clinical characteristics of the enrolled patients were obtained from electronic medical records.

2.2. Sample Genotyping and Data Collection. Genomic DNA was extracted from three millilitres (ml) of EDTA anticoagulated whole blood obtained from all participants for genotyping by the QIAamp® DNA Blood Mini Kit (Qiagen, Germany) according to the manufacturer's instructions. The DNA samples were stored at −80°C until further analysis. The SNP genotyping work was conducted by a custom-by-design 2x48-Plex SNP scan TM Kit (Cat#: G0104, Gene sky Biotechnologies Inc, Shanghai, China), as described previously [16]. Along with treatment, biochemical and haematological analyses were performed twice a month during the first two months and monthly in the subsequent four months. Test results and clinical symptoms were recorded to assess ATDILI.

2.3. The Clinical Definition of ATDILI Severity. The severity of hepatotoxicity is classified into three major categories according to the WHO Toxicity Classification Standards: grade 1 (mild) ALT $< 5 \times$ ULN (200 IU/L), grade 2 (moderate) ALT level higher than $5 \times$ ULN but less than $10 \times$ ULN, and grade 3 (severe) ALT levels $\geq 10 \times$ ULN (400 IU/L) [17].

2.4. Candidate Single Nucleotide Polymorphism Selection. Candidate SNPs were selected by the following strategies: (a) searching the dbSNP database (http://www.ncbi.nlm.nih.gov/projects/SNP/), 1000 Genomes (http://www.1000genomes.org/)

and finding SNPs with minor allele frequencies ≥0.02 among Han Chinese in Beijing and located within 2000 bp upstream and 300 bp downstream of the TGFBR2 and TGFBRAP1 genomic regions [18]; (b) under the experimental conditions for genotyping; and (c) a minor allele frequency (MAF) ≥0.05 and linkage disequilibrium (LD) $r^2 \geq 0.8$. Four TGFBRAP1 SNPs (rs17687727, rs75725426, rs2241797, and rs12476720) and eleven TGFBR2 SNPs (rs1835538, rs9881945, rs4522809, rs11924422, rs12493607, rs1808602, rs114342639, rs3773644, rs3773652, rs2043136, and rs876688) were examined in the current study (S1 Table).

2.5. Statistical Analysis. The demographic and clinical data of the enrolled patients in the ATDILI group and in the non-ATDILI group were compared using the chi-square test and *t*-test by SPSS version 17.0. The Hardy–Weinberg equilibrium (HWE) for all SNPs in the controls was assessed by Plink version 1.07. Associations between SNPs and ATDILI were evaluated using the unconditional logistic regression after adjusting for age and gender by Plink version 1.07. The odds ratio (OR) with 95% confidence interval (CI) was used as a measure of associations. The linkage disequilibrium (LD) and haplotype analysis were conducted by Haplotype version 4.2. Multifactor Dimensionality Reduction Software (version 3.0.2) was used to analyse the SNP-SNP interactions associated with ATDILI [19]. Two-sided values of $p < 0.05$ were considered statistically significant.

3. Results

3.1. Demographic and Clinical Characteristics of the Subjects. In total, 746 TB patients were included in this prospective study. The overall incidence rate of ATDILI was 15.82% (118/746) among the patients. There was no difference in age ($p = 0.285$) or gender ($p = 0.801$) between the patients with ATDILI and patients without ATDILI. Compared with patients without ATDILI, patients with ATDILI showed a tendency of higher percentage of fever and weight loss ($p = 0.016$ and $p = 0.036$) and a different proportion of tuberculosis subtype ($p < 0.001$). The ATDILI group also had a higher frequency of elevated serum levels of ALT ($p < 0.001$), AST ($p < 0.001$), ALP ($p < 0.001$), TBIL ($p = 0.002$), IBIL ($p = 0.049$), uric ($p = 0.008$), and GGT ($p = 0.021$). Among the ATDILI group, 70.34%, 17.80%, and 11.86% patients presented mild, moderate, and severe hepatotoxicity, respectively, without differences in age or gender; 39.83%, 16.10%, 17.80%, and 26.27% patients developed hepatocellular injury, cholestatic injury, mixed injury, and injury, respectively, with unknown classification. Demographic, clinical characteristics, laboratory indicators, severity, and clinical phenotype of patients are displayed in Table 1.

3.2. SNP Allele, Genotype, Genetic Model, and Haplotype Analysis. Genotyping of selected SNPs was successfully completed for all 118 patients in the ATDILI group and 628 patients in the non-ATDILI group. To ensure the repeatability and stability of genotyping, 30 samples were randomly selected for double-blind experiments, and all the genotype calling success rates were greater than 99.0%. None of the SNP genotype distributions deviated from the Hardy–Weinberg equilibrium (HWE), except rs2043136 ($p = 0.033$). The distributions of genotype and allele frequencies of all fifteen SNPs are depicted in Table 2. For the rs17687727 locus, the proportions of the A allele were 46/234 (19.66%) in the ATDILI group and 171/1253 (13.73%) in the non-ATDILI group compared with the G allele (OR 1.55; 95% CI: 1.08–2.22, $p = 0.016$). The occurrence of the AA genotype seemed more common in the ATDILI group (4/117, 3.42%) compared with the non-ATDILI group (11/627, 1.75%), but there was no significant difference ($p = 0.055$). For other SNPs, no allele or genotype differences were found between the two groups (all $p > 0.05$).

Three genetic models were constructed to compare the significance of each SNP: dominant, recessive, and additive patterns. In line with the abovementioned findings, as shown in Table 3, rs17687727 in the dominant model (OR 1.634; 95% CI: 1.076–1.634; $p = 0.021$) and additive model (OR 1.559; 95% CI: 1.083–2.246; $p = 0.017$) showed statistical significance between the two groups. No genetic model was associated with ATDILI in other SNPs, even marginally.

We next constructed the haplotype to analyse whether there was additive association among selected SNPs. One haplotype consisted of rs2241797 and rs12476720 in TGFBRAP1, and three haplotypes consisting of rs11924422 and rs12493607, rs1808602 and rs114342639, and rs3773652 and rs2043136 in TGFBR2 ($D' > 0.80$) were constructed with a frequency >0.05 and in a strong linkage disequilibrium state by calculating the pairwise r^2 coefficient ($r^2 > 0.80$). However, none was associated with ATDILI ($p > 0.05$). Table 4 shows the association of the haplotypes of TGFBRAP1 and TGFBR2 with the risk of ATDILI. S2 Figure and S3 Figure depict the loci of TGFBRAP1 and TGFBR2 in the linkage disequilibrium block risk.

3.3. SNP-SNP Interactions with the Risk of ATDILI. We carried out a multifactor dimensionality reduction (MDR) analysis with all fifteen SNPs to investigate potential genetic interactions associated with ATDILI. We limited the interaction models from two-way to nine-way and linear regression for score calculation. However, we did not identify any multilocus model with receivable cross-validation consistency (from 3/10 to 6/10). Moreover, all these models did not reach the threshold value of statistical significance (all $p > 0.05$ in S2 Table).

3.4. The Relationship between Genetic Polymorphism and ATDILI Laboratory Test Indicators. Genetic polymorphism not only affects disease susceptibility but also has a certain correlation with the clinical features of the disease, which may affect different clinical characteristics of individuals. In this study, as shown in Table 5, the

Table 1: Demographic characteristics, clinical characteristics, and laboratory indicators of enrolled patients.

Group	Non-ATDILI ($n = 628$)		ATDILI ($n = 118$)		p value
General data					
Age (years)[a]	40.92 ± 15.72		42.85 ± 18.44		0.284
Gender (male/female)[c]	375 (59.71%)	253 (40.28%)	69 (58.47%)	49 (41.52%)	0.801
Smoking (no/yes)[c]	407 (64.80%)	221 (35.19%)	80 (67.79%)	38 (32.20%)	0.532
Drinking (no/yes)[c]	465 (74.04%)	163 (25.95%)	83 (70.33%)	35 (29.66%)	0.464
Tuberculosis subtype, n (%)					
PTB[c]	520	82.80%	79	66.95%	<**0.001**
EPTB[c]	43	6.85%	15	12.71%	
PTB and EPTB[c]	65	10.35%	24	20.34%	
General symptoms (no/yes)[c]	135 (19.62%)	492 (80.37%)	23 (19.49%)	95 (80.51%)	0.567
Fever (no/yes)[c]	344 (54.78%)	284 (45.22%)	50 (42.37%)	68 (57.62%)	**0.016**
Weight loss (no/yes)[c]	367 (58.43%)	261 (41.56%)	82 (69.49%)	36 (30.50%)	**0.036**
Night sweat (no/yes)[c]	433 (68.94%)	195 (31.05%)	86 (72.88%)	32 (21.12%)	0.446
Fatigue (no/yes)[c]	462 (73.57%)	166 (26.43%)	85 (72.03%)	33 (27.97%)	0.716
Poor appetite (no/yes)[c]	374 (59.55%)	254 (40.45%)	69 (58.47%)	49 (41.52%)	0.859
Local infection (no/yes)[c]	134 (21.34%)	494 (78.66%)	24 (20.34)	94 (79.66%)	0.758
Laboratory examinations	Mean ± SD or $p50$ ($p25$–$p75$)				
RBC (×1012/L)[a]	4.28 ± 0.68		4.31 ± 0.74		0.481
HB (g/L)[a]	122.06 ± 20.58		122.87 ± 22.11		0.717
HCT (L/L)[a]	0.36 ± 0.06		0.38 ± 0.06		0.069
PLT ($\times 10^9$/L)[b]	232.50 (172.75–297.25)		236.50 (184.00–321.75)		0.134
WBC ($\times 10^9$/L)[b]	6.51 (5.17–8.44)		6.57 (4.99–7.96)		0.761
Neutrophils ($\times 10^9$/L)[a]	5.10 ± 2.73		5.23 ± 2.89		0.631
Monocytes ($\times 10^9$/L)[a]	1.26 ± 0.62		1.29 ± 0.79		0.625
Lymphocytes ($\times 10^9$/L)[a]	0.50 ± 0.25		0.55 ± 0.29		0.099
Neutrophils (%)[a]	70.13 ± 11.54		70.49 ± 11.50		0.760
Monocytes (%)[a]	7.30 ± 2.37		7.74 ± 2.62		0.077
Lymphocytes (%)[b]	17.5 (12.18–25.68)		16.25 (12.58–25.58)		0.527
TBIL (μmol/L)[b]	8.70 (6.30–12.10)		10.05 (7.50–14.13)		0.002
DBIL (μmol/L)[b]	3.45 (2.50–5.40)		3.55 (2.38–5.60)		0.126
IBIL (μmol/L)[b]	4.80 (3.40–7.03)		5.70 (3.98–7.95)		**0.049**
ALT (IU/L)[b]	15.00 (10.00–21.00)		28.00 (15.75–38.00)		<**0.001**
AST (IU/L)[b]	19.50 (16.00–25.00)		27.00 (20.00–34.00)		<**0.001**
TP (g/L)[a]	68.82 ± 9.15		69.42 ± 8.42		0.508
ALB (g/L)[a]	37.89 ± 6.90		38.64 ± 7.35		0.248
GLB (g/L)[a]	30.93 ± 7.02		30.78 ± 6.65		0.829
GLU (mmol/L)[b]	5.14 (4.71–5.89)		5.15 (4.64–5.95)		0.41
UREA (mmol/L)[b]	4.05 (3.15–5.30)		3.92 (2.90–5.24)		0.299
CREA (μmol/L)[b]	60.45 (49.00–73.20)		57.50 (47.78–67.00)		0.601
CYS-C (mg/L)[b]	0.92 (0.79–1.06)		0.91 (0.81–1.04)		0.975
Uric (μmol/L)[a]	331.51 ± 155.30		291.29 ± 125.98		**0.008**
TG (mmol/L)[b]	1.06 (0.80–1.43)		0.99 (0.81–1.31)		0.469
CHOL (mmol/L)[a]	3.96 ± 1.058		3.96 ± 1.206		0.966
HDL-C (mmol/L)[a]	1.08 (0.82–1.41)		1.12 (0.85–1.48)		0.811
LDL-C (mmol/L)[b]	2.21 (1.69–2.77)		2.20 (1.79–2.72)		0.575
ALP (IU/L)[b]	79.00 (64.00–98.00)		85.50 (68.50–106.00)		**0.021**
GGT (IU/L)[b]	29.00 (19.00–48.00)		42.50 (26.00–78.00)		<**0.001**
CRP (mg/L)[b]	12.25 (2.67–37.43)		9.74 (2.30–39.23)		0.961
ESR (mm/h)[b]	33.50 (14.75–64.00)		38.50 (20.50–63.00)		0.173

Severity	*N*	Age (years)	*p*	Gender (*N*)		*p*
				Male	Female	
Mild	83	40.42 ± 16.48	0.888	53	30	0.117
Moderate	21	42.19 ± 14.04		11	10	
Severe	14	41.57 ± 14.78		5	9	

TB, tuberculosis; PTB, pulmonary tuberculosis; EPTB, extrapulmonary tuberculosis. [a]Data are shown as mean ± standard deviation; [b]data are shown as median (interquartile range); [c]data are shown as number of cases (frequency).

positive site rs17687727 in TGFBRAP1 and liver function-related laboratory test indicators indicated that the patients with the AA genotype had the highest AST 200.50 (100.50–276.50), whereas patients with the GA and GG genotypes had AST values of 83.00 (38.50–160.25) and 115.00 (72.50–217.00), respectively.

Table 2: The distributions of allele and genotype frequencies of all fifteen SNPs.

Gene	dbSNP	Allele	Allele					Genotype		
			ATDILI (n, %)	Non-ATDILI (n, %)	OR (95% CI)	p	p^{HWE}	ATDILI	Non-ATDIH	p
			1/2	1/2				11/12/22	11/12/22	
TGFBRAP1	rs17687727	G > A	46/188	171/1083	1.55 (1.08–2.22)	**0.016**	0.883	4/38/75	11/149/467	0.055
	rs75725426	A > G	27/205	140/1116	1.05 (0.67–1.62)	0.827	0.096	2/23/91	12/116/500	0.936
	rs2241797	T > C	64/170	340/912	1.01 (0.73–1.38)	0.951	0.578	8/48/61	50/240/336	0.821
	rs12476720	A > G	113/123	622/634	0.93 (0.70–1.23)	0.643	1.000	28/57/33	153/316/159	0.832
TGFBR2	rs1835538	G > A	29/207	188/1068	0.79 (0.52–1.20)	0.283	0.638	2/25/91	12/164/452	0.512
	rs9881945	G > T	36/200	180/1074	1.07 (0.72–1.58)	0.718	0.744	3/30/85	14/152/461	0.937
	rs4522809	A > G	69/167	382/868	0.93 (0.69–1.27)	0.685	0.924	6/57/55	59/264/302	0.216
	rs11924422	C > A	69/167	383/869	0.93 (0.69–1.27)	0.678	0.258	9/51/58	52/279/295	0.912
	rs12493607	C > G	78/158	412/838	1.00 (0.74–1.35)	0.978	0.651	11/56/51	65/282/278	0.874
	rs1808602	A > G	102/134	575/677	0.89 (0.67–1.18)	0.443	0.809	19/64/35	130/315/181	0.497
	rs114342639	G > T	46/190	260/994	0.92 (0.65–1.31)	0.664	0.903	4/38/76	26/208/393	0.897
	rs3773644	C > T	88/148	500/754	0.89 (0.67–1.19)	0.456	0.454	18/52/48	95/310/222	0.508
	rs3773652	G > A	123/113	602/648	1.17 (0.88–1.54)	0.264	0.575	32/59/27	141/320/164	0.509
	rs2043136	A > G	17/101	102/524	0.94 (0.71–1.25)	0.680	0.033	17/64/37	102/334/190	0.874
	rs876688	G > A	66/170	297/959	1.25 (0.91–1.71)	0.155	0.438	11/44/63	31/235/362	0.156

p: p value was calculated using logistic regression analysis. p^{HWE}: p value of Hardy–Weinberg equilibrium. HWE was assessed by the χ^2 goodness-of-fit test based on the genotype distributions in this study. The significance of bold in the table means p value < 0.05. "1" designates the mutant allele and "2" designates the wild allele; 11 = mutant homozygote; 12 = heterozygote; 22 = wild homozygote.

4. Discussion

The TGF-β1/smad signalling pathway can regulate liver homeostasis [9], although the distinct role of TGFBR2 and TGFBRAP1 in the TGF-β1/smad signalling pathway had been observed previously, playing a vital role in liver fibrosis and hepatocarcinogenesis [9]. No genetic association study was conducted to evaluate the correlation of TGFRB2 and TGFBRAP1 polymorphisms with ATDILI. In the present study, we first revealed that the A variants at rs17687727 loci were significantly associated with an increased risk for ATDILI in the Han Chinese population.

The TGFBRAP1 gene (Gene ID: 9392) maps to chromosome 2 at q12.1 and spans 80.29 kbp. No study on rs17687727 has been reported yet. A G > A mutation of rs17687727 located at the 3′ UTR of the TGFBRAP1 gene would influence the combined functions of the miRNAs. We searched the miRNA target gene prediction website database (http://www.targetscan.org) and found that TGFBRAP1 and miR-122 had potential binding sites (S3 Figure). MiR-122, which accounts for approximately 70% of the total miRNA in the adult liver, is involved in cell cycle progression, hepatocellular carcinogenesis, lipid metabolism, and fibrosis [20], so it was considered to have a high specificity in drug-induced liver injury with modest positive diagnostic effects [20, 21]. MiR-122 might inhibit hepatocellular carcinoma progression by downregulating TGFBRAP1 in the presence of the hepatitis C virus core, suggesting that the TGF-β/smad signalling pathway may be related to the expression level of miR-122, which plays an important role in drug-induced liver injury [22–24]. Exposure to TGF-β led to significant downregulation of miR-122. Furthermore, reintroduction of miR-122 suppressed TGF-β-induced expression of fibrosis-related genes in hepatic fibrogenesis [25]. Investigations have identified the ratio of miR-122/miR-155 as potential biomarkers for the early diagnosis of isoniazid-induced liver injury in mice [26]. In our study, we also found that the genetic polymorphism of TGFBRAP1 was related to the clinical features of liver injury and that patients with the AA genotype had a higher AST than patients with the GA and GG genotypes. Whether this regulation is also modified by miR-122 is worth exploring. Considering the haplotype is a combination of specific alleles at neighbouring genes that tend to be inherited together, multiple SNPs may "tag" an untyped variant more effectively than a single-typed variant. The subset of SNPs used in such an approach is called "haplotype tagging" SNPs [27]. We also generated a regional LD plot (http://www.internationalgenome.org) for rs17687727 to search for the "haplotype tagging" SNPs. Two estimated loci (rs34686799 and rs10176000) with high LD ($r^2 > 0.8$) were found in the intron region, but no clear biological significance was found in these sites. In summary, taking the spatiotemporal orchestration of TGF-β signalling at different stages of liver injury, its cross-talk with several signalling pathways, and even its interplay with posttranslational modification into consideration [8], the role

Table 3: Genetic models of related SNPs associated with ATDILI in tuberculosis patients.

Gene	dbSNP	Dominant model		Recessive model		Additive model	
		OR (95% CI)	p	OR (95% CI)	p	OR (95% CI)	p
TGFBRAP1	rs17687727	1.634 (1.076–1.634)	**0.021**	1.982 (0.620–6.335)	0.248	1.559 (1.083–2.246)	**0.017**
	rs75725426	1.073 (0.661–1.073)	0.774	0.900 (0.198–4.078)	0.891	1.047 (0.684–1.601)	0.832
	rs2241797	1.064 (0.716–1.064)	0.759	0.845 (0.390–1.833)	0.670	1.010 (0.740–1.377)	0.951
	rs2576736	0.793 (0.526–0.793)	0.268	0.908 (0.397–2.076)	0.819	0.847 (0.607–1.182)	0.329
	rs12476720	0.873 (0.562–0.873)	0.546	0.965 (0.608–1.532)	0.882	0.936 (0.708–1.237)	0.643
	rs2679876	0.816 (0.537–0.816)	0.342	0.632 (0.219–1.820)	0.395	0.820 (0.576–1.168)	0.272
TGFBR2	rs1835538	0.762 (0.479–1.211)	0.250	0.885 (0.195–4.007)	0.874	0.792 (0.519–1.209)	0.280
	rs9881945	1.078 (0.694–1.673)	0.737	1.142 (0.323–4.038)	0.836	1.073 (0.729–1.578)	0.720
	rs4522809	1.071 (0.722–1.589)	0.733	0.513 (0.216–1.219)	0.131	0.937 (0.688–1.276)	0.682
	rs11924422	0.922 (0.622–1.367)	0.685	0.911 (0.436–1.904)	0.805	0.934 (0.683–1.278)	0.670
	rs12493607	1.052 (0.707–1.565)	0.800	0.885 (0.452–1.734)	0.723	1.004 (0.743–1.356)	0.978
	rs1808602	0.964 (0.626–1.484)	0.869	0.732 (0.432–1.241)	0.246	0.893 (0.672–1.188)	0.437
	rs1078985	0.959 (0.619–1.487)	0.854	1.583 (0.572–4.376)	0.376	1.025 (0.706–1.488)	0.896
	rs9847368	0.864 (0.535–1.394)	0.549	1.066 (0.230–4.926)	0.935	0.891 (0.578–1.375)	0.604
	rs114342639	0.929 (0.615–1.399)	0.721	0.811 (0.277–2.368)	0.701	0.924 (0.650–1.315)	0.663
	rs3773644	0.799 (0.534–1.195)	0.275	1.008 (0.583–1.742)	0.977	0.894 (0.669–1.196)	0.452
	rs3773652	1.199 (0.753–1.909)	0.444	1.277 (0.816–1.997)	0.283	1.176 (0.887–1.558)	0.260
	rs2043136	0.954 (0.624–1.459)	0.827	0.864 (0.496–1.508)	0.608	0.936 (0.696–1.26)	0.665
	rs876688	1.188 (0.800–1.763)	0.392	1.98 (0.965–4.059)	0.062	1.259 (0.917–1.727)	0.153

p: p value was calculated using logistic regression analysis.

Table 4: Analysis of haplotypes with the risk of ATDILI.

Gene	SNP	Haplotype*	Frequency	p
TGFBRAP1	rs2241797 : rs12476720	GA	0.497	0.575
		AG	0.261	0.963
		GG	0.231	0.457
TGFBR2	rs11924422 : rs12493607	AG	0.649	0.804
		CC	0.281	0.922
		AC	0.048	0.734
	rs1808602 : rs114342639	AC	0.536	0.485
		GC	0.259	0.682
		GA	0.196	0.618
		AA	0.483	0.332
	rs3773652 : rs2043136	GG	0.423	0.573
		GA	0.089	0.325

*Ratio is shown by CC frequencies.

Table 5: Quantitative indicator comparisons among genotypes of rs17687727 in TGFBRAP1.

Laboratory indicators	Genotype			p
	GG	GA	AA	
TBIL (μmol/L)[a]	12.15 (7.15–18.44)	13.40 (9.70–19.55)	10.35 (6.85–17.67)	0.48
DBIL (μmol/L)[a]	5.65 (3.25–10.40)	5.60 (3.95–8.79)	3.90 (3.80–4.98)	0.45
IBIL (μmol/L)[a]	4.90 (3.57–8.12)	6.60 (4.74–10.2)	6.45 (3.00–12.75)	0.08
ALT (IU/L)[a]	108.00 (50.50–191.75)	164.00 (105.00–316.00)	91.00 (38.00–250.50)	0.03
AST (IU/L)[a]	83.00 (38.50–160.25)	115.00 (72.50–217.00)	200.50 (100.50–276.50)	0.03
ALP (IU/L)[a]	108.5 (75.25–189.25)	98.00 (71.50–126.50)	97.50 (77.75–129.25)	0.32

[a]Data are shown as median (interquartile range).

of the TGF-β/smad signalling pathway in ATDILI is obscure. Our study found that a variant of rs17687727 in the 3′ UTR region of the TGFBRAP1 gene was associated with susceptibility to ATDILI and suggested that fine mapping and further functional studies are necessary to evaluate the genetic effect of TGFBRAP1 and its potential regulatory mechanism on ATDILI.

The TGFBR2 gene (gene ID: 7048) is located on chromosome 3 at p24.1 and spans 87.65 kbp. Genotyping results showed that the rs4522809G allele was associated with ascending thoracic aorta with significantly higher TGF-β1 concentrations [28]. rs4522809 was found to have a strong predictive role in the regulation of osteopontin expression [29]. Associations of rs4522809 were meta-analysed with

data from the NCI Polish Breast Cancer Study and published data from the Breast Cancer Association Consortium, which found a weak association [29]. For rs12493607, studies focused on the susceptibility to breast cancer with controversial results [30–32]. rs876688 has been researched in oral facial clefts, and no correlation was found [33]. We did not find any positive results for the SNPs in the TGFBR2 genetic region. One possible reason to explain this lack of association is that the TGF-β/smad signalling pathway involves different mechanisms in acute and chronic liver injuries. In brief, TGF-β plays a dual role in the control of proliferation and apoptosis. On the one hand, early on, it induces intracellular signals that mediate cell cycle arrest and apoptosis; on the other hand, at later times, it activates proliferative and antiapoptotic signals through activation of the EGFR pathway, especially as a central regulator in chronic liver disease contributing to fibrogenesis through inflammation [34]. As most of the ATDILI cases appeared within sixteen weeks (range: 6 weeks–6 months) after the start of the combined therapy, it is reasonable to speculate that it was mainly acute liver injury [3]. Therefore, TGFBR2 or its genetic variation may not play a pivotal role in this specific pathway. Second, TGF-β alone does not direct normal liver development. A hepatocyte growth factor (HGF) mediated smad-independent pathway is able to rescue the liver phenotype in SMAD2/3 mutants [35].

Given that combined analyses of SNPs may display a more complete picture of the candidate genes [27], we further conducted a haplotype analysis and a SNP-SNP interaction analysis of the selected tagSNPs. Neither a haplotype nor a joint effect was found in association with ATDILI, which explained on another level that the TGF-β/smad signalling pathway is related to ATDILI but may not be the main pathway.

There are several strengths of our study. First, our prospective study included patients from the West China Hospital, the largest medical centre in western China, which has surveillance of ATDILI with strict criteria to avoid misclassification and inclusion criteria. We excluded people with hepatitis B virus (HCV) or hepatitis C virus (HCV), as well as HIV coinfection, which were shown to be risk factors for ATDILI. Second, the laboratory for testing is one of the advanced and comprehensive laboratories integrating clinical, scientific research and teaching in China. The laboratory is also certified by the American Association of Pathologists (CAP). All the test data had good quality control and reliability. Third, people who were collecting and sorting clinical data and people who were responsible for laboratory data worked independently in this study to minimize potential bias. These differences may make the conclusions of our study more persuasive and representative to some degree.

There were several limitations in our study. First, we focused on ATDILI induced by first-line antituberculosis regimens and the genetic risk factors of TGFBR2 and TGFBRAP1 only, without assessment of other relevant genes, environmental risks, and comorbid conditions (malnutrition, alcoholism, chronic hepatitis C and chronic hepatitis B infection, HIV infection, and preexisting liver disease), as well as epigenetic modification. For example, association of genetic polymorphisms of the NAT2 gene with "slow acetylation" phenotypes has been clearly documented to increased risk of ATDILI [7]. It is an excellent discovery on the drug metabolism pathway. However, TGFBRAP1 and TGFBR2 may play a role in ATDILI by the TGF-β/smad signalling pathway through potential immune regulation. In our study, we did not analyse the gene polymorphisms of NAT2 gene simultaneously, so we did not analyse the relationship between rs17687727 and slow acetylator status, and the correlation between the TGF-β/smad signalling pathway and isoniazid acetylation is still poorly understood. Concomitant viral hepatitis infection may be another confounding factor in ATDILI, and the risk of ATDILI is directly related to the viral load [3]. It is difficult to perform real-time fluorescent PCR testing for every patient to detect the precise level of HBV-DNA/HCV-RNA concentration. Meanwhile, the ALT, AST, and ALP levels of patients with viral hepatitis also have an increased likelihood, which makes it more difficult to do causal judgement of liver damage caused by antituberculosis drugs or hepatitis. To avoid bias and confounding variables caused by different viral loads and/or hepatitis progression itself, we excluded patients with hepatitis B virus or hepatitis C virus in the study. Second, all the samples in our study were Han Chinese in western China and not large enough to detect a rare risk allele in other ethnicities. No differences in age and gender were found between the ATDILI group and the control group in our population. Older age is associated with decreased liver blood flow and changes in the drug distribution and metabolism, thus potentially reducing the effective clearance of the drugs [3]. To make this point clear, we further analysed the age composition according to the severity of liver injuries, and no significant differences were observed (Table 1). To explore the correlation between age and ATDILI in the Chinese population, we looked for genetic polymorphism studies of ATDILI based on the Chinese Han population. Although the target genes of the study are different, these studies did not have a significant difference in gender or age, neither [36–39]. Taken together, we hypothesized that due to the genetic backgrounds of different ethnic groups, perhaps the correlation between age and ATDILI for the Chinese Han population is not as obvious as other ethnic groups. However, it cannot be ruled out that the undetected correlation between age and ATDILI is due to the limited sample size. Furthermore, extended validation in multicentre and enlarged sample studies in other cohorts is needed to identify the association between target and ATDILI, plus functional verification test in vitro and vivo.

In conclusion, we found that genetic polymorphisms of rs17687727 in the TGFBRAP1 gene influenced the susceptibility to ATDILI in first-line antituberculosis combination treatment in a Chinese population. We believe that mapping the TGFBRAP1 variants in a larger population along with functional verifications will further explore the important role of the TGF-β1/smad signalling pathway in the process. These findings provide novel insight into better understanding the molecular mechanisms

of ATDILI and shed light on still unrecognized candidate targets for developing better personalized therapy and successful treatment in ATDILI.

Data Availability

The data used to support the findings of this study are included with in the article and the supplementary information file.

Ethical Approval

Ethical approval for this study was obtained from the Institutional Review Board of the West China Hospital of Sichuan University.

Conflicts of Interest

The authors declare that they have no conflicts of interest.

Acknowledgments

This work was supported by the National Natural Science Foundation of China (Grant no. 81472026) and University-City Science and Technology Cooperation Project of Sichuan University and Panzhihua City (2018CDPZH-13).

Supplementary Materials

S1 Table: Candidate single nucleotide polymorphism of TGFBRAP1 and TGFBR2. The location (GRCh38.p7) and region of the SNPs, and the MAF of the SNPs in 1000 Genomes (East Asia) and in our study. S2 Table: SNP-SNP interactions analysed with Multifactor Dimensionality Reduction Software (version 3.0.2). S1 Figure: Flow diagram of the enrolment of the study population. S2 Figure: Haplotype analysis for the candidate SNPs of TGFBRAP1 based on linkage disequilibrium (LD) plots. S3 Figure: Haplotype analysis for the candidate SNPs of TGFBR2 based on linkage disequilibrium (LD) plots. (*Supplementary Materials*)

References

[1] World Health Organanization, "Global tuberculosis," Report World Health Organanization, Geneva, Switzerland, 2018, http://www.who.int/tb/publications_report/en.

[2] Y. Wang, X. Xiang, S.-Q. Wu et al., "Association of CYP2B6 gene polymorphisms and anti-tuberculosis drug-induced hepatotoxicity in a Chinese population," *Infection, Genetics and Evolution*, vol. 51, pp. 198–202, 2017.

[3] V. Ramappa and G. P. Aithal, "Hepatotoxicity related to anti-tuberculosis drugs: mechanisms and management," *Journal of Clinical and Experimental Hepatology*, vol. 3, no. 1, pp. 37–49, 2013.

[4] X. Hu, M. Zhang, H. Bai et al., "Antituberculosis drug-induced adverse events in the liver, kidneys, and blood: clinical profiles and pharmacogenetic predictors," *Clinical Pharmacology & Therapeutics*, vol. 104, no. 2, pp. 1–9, 2018.

[5] W. W. Yew, K. C. Chang, and D. P. Chan, "Oxidative stress and first-line antituberculosis drug-induced hepatotoxicity," *Antimicrobial Agents and Chemotherapy*, vol. 62, no. 8, pp. 1–36, 2018.

[6] O. E. Bouazzi, S. Hammi, J. E. Bourkadi et al., "First line anti-tuberculosis induced hepatotoxicity: incidence and risk factors," *Pan African Medical Journal*, vol. 25, pp. 167–176, 2016.

[7] Y. Bao, X. Ma, T. P. Rasmussen, and X.-B. Zhong, "Genetic variations associated with anti-tuberculosis drug-induced liver injury," *Current Pharmacology Reports*, vol. 4, no. 3, pp. 171–181, 2018.

[8] I. Fabregat and D. Caballero-Diaz, "Transforming growth factor-beta-induced cell plasticity in liver fibrosis and hepatocarcinogenesis," *Frontiers in Oncology*, vol. 8, p. 357, 2018.

[9] I. Fabregat, J. Moreno-Càceres, A. Sánchez et al., "TGF-β signalling and liver disease," *The FEBS Journal*, vol. 283, no. 12, pp. 2219–2232, 2016.

[10] J. U. Wurthner, D. B. Frank, A. Felici et al., "Transforming growth factor-β receptor-associated protein 1 is a Smad4 chaperone," *Journal of Biological Chemistry*, vol. 276, no. 22, pp. 19495–19502, 2001.

[11] B. Ziarkiewicz-Wroblewska, E. Sajjad, M. Ciszek et al., "Association of 49245A>G (rs868) polymorphism in the 3′ UTR of donor TGFBR1 gene with course of hepatitis C following orthotopic liver transplantation," *Annals of Transplantation*, vol. 19, pp. 643–651, 2014.

[12] S. Kawate, S. Takenoshita, S. Ohwada et al., "Mutation analysis of transforming growth factor beta type II receptor, Smad2, and Smad4 in hepatocellular carcinoma," *International Journal of Oncology*, vol. 14, no. 1, pp. 127–131, 1999.

[13] Y.-S. Huang, Y. Zhong, L. Yu, and L. Wang, "Association between the TGFBR2 G-875A polymorphism and cancer risk: evidence from a meta-analysis," *Asian Pacific Journal of Cancer Prevention*, vol. 15, no. 20, pp. 8705–8708, 2014.

[14] World Health Organization, *Common Terminology Criteria for Adverse Events (CTCAE) Version 5.0*, U.S. Department of Health and Human Services, Washington, DC, USA, 2017, https://www.who-umc.org/media/2768/standardised-case-causality-assessment.pdf.

[15] P. Nahid, S. E. Dorman, N. Alipanah et al., "Executive summary: official American thoracic society/centers for disease control and prevention/infectious diseases society of America clinical practice guidelines: treatment of drug-susceptible tuberculosis," *Clinical Infectious Diseases*, vol. 63, no. 7, pp. 853–867, 2016.

[16] J. Zhang, Z. Zhao, H. Zhong et al., "Importance of common TLR2 genetic variants on clinical phenotypes and risk in tuberculosis disease in a Western Chinese population," *Infection, Genetics and Evolution*, vol. 60, pp. 173–180, 2018.

[17] A. Tostmann, M. J. Boeree, R. E. Aarnoutse, W. C. de Lange, A. J. A. M. van der Ven, and R. Dekhuijzen, "Antituberculosis drug-induced hepatotoxicity: concise up-to-date review," *Journal of Gastroenterology and Hepatology*, vol. 23, no. 2, pp. 192–202, 2008.

[18] Z. Zhao, W. Peng, X. Hu et al., "SFRP1 variations influence susceptibility and immune response to mycobacterium tuberculosis in a Chinese Han population," *Infection, Genetics and Evolution*, vol. 37, pp. 259–265, 2016.

[19] L. W. Hahn, M. D. Ritchie, and J. H. Moore, "Multifactor dimensionality reduction software for detecting gene-gene and gene-environment interactions," *Bioinformatics*, vol. 19, no. 3, pp. 376–382, 2003.

[20] Y. Liu, P. Li, L. Liu, and Y. Zhang, "The diagnostic role of miR-122 in drug-induced liver injury: a systematic review and meta-analysis," *Medicine*, vol. 97, no. 49, article e13478, 2018.

[21] C. Munakata, Y. Fuchigami, S. Hiroishi et al., "Evaluation of miR-122 to predict high dose acetaminophen-induced liver injury in mice: the combination uses of 5-fluorouracil,"

Biological and Pharmaceutical Bulletin, vol. 41, no. 11, pp. 1732–1735, 2018.

[22] L. S. Howell, L. Ireland, B. K. Park, and C. E. Goldring, "MiR-122 and other microRNAs as potential circulating biomarkers of drug-induced liver injury," *Expert Review of Molecular Diagnostics*, vol. 18, no. 1, pp. 47–54, 2018.

[23] R. T. Marquez, S. Bandyopadhyay, E. B. Wendlandt et al., "Correlation between microRNA expression levels and clinical parameters associated with chronic hepatitis C viral infection in humans," *Laboratory Investigation*, vol. 90, no. 12, pp. 1727–1736, 2010.

[24] X. Wang, J. Peng, J. Wang et al., "Hepatitis C virus core impacts expression of miR122 and miR204 involved in carcinogenic progression via regulation of TGFBRAP1 and HOTTIP expression," *OncoTargets and Therapy*, vol. 11, pp. 1173–1182, 2018.

[25] C. Zeng, Y.-L. Wang, C. Xie et al., "Identification of a novel TGF-beta-miR-122-fibronectin 1/serum response factor signaling cascade and its implication in hepatic fibrogenesis," *Oncotarget*, vol. 6, no. 14, pp. 12224–12233, 2015.

[26] L. Song, Z. Zhang, J. Zhang et al., "Ratio of microRNA-122/155 in isoniazid-induced acute liver injury in mice," *Experimental and Therapeutic Medicine*, vol. 12, no. 2, pp. 889–894, 2016.

[27] J. Little, J. P. T. Higgins, J. P. A. Ioannidis et al., "Strengthening the reporting of genetic association studies (STREGA)—an extension of the STROBE statement," *PLoS Medicine*, vol. 6, no. 2, article e1000022, 2009.

[28] Z. Staneviciute, R. Sepetiene, I. Grabauskyte, V. Patamsyte, and V. Lesauskaite, "Investigation of TGFβR2 SNP rs4522809, osteopontin, TGF β1 and their association with dilatative pathology of ascending thoracic aorta," *Cytokine*, vol. 107, pp. 70–73, 2018.

[29] L. Piva, B. F. Gavassini, L. Bello et al., "TGFBR2 but not SPP1 genotype modulates osteopontin expression in duchenne muscular dystrophy muscle," *The Journal of Pathology*, vol. 228, no. 2, pp. 251–259, 2012.

[30] C. P. Lee, A. Irwanto, A. Salim et al., "Breast cancer risk assessment using genetic variants and risk factors in a Singapore Chinese population," *Breast Cancer Research*, vol. 16, no. 3, p. R64, 2014.

[31] C. Petridis, M. N. Brook, V. Shah et al., "Genetic predisposition to ductal carcinoma in situ of the breast," *Breast Cancer Research*, vol. 18, no. 1, p. 22, 2016.

[32] L. Dorling, S. Kar, K. Michailidou et al., "The relationship between common genetic markers of breast cancer risk and chemotherapy-induced toxicity: a case-control study," *PLoS One*, vol. 11, no. 7, Article ID e0158984, 2016.

[33] A. L. Boyles, A. J. Wilcox, J. A. Taylor et al., "Oral facial clefts and gene polymorphisms in metabolism of folate/one-carbon and vitamin A: a pathway-wide association study," *Genetic Epidemiology*, vol. 33, no. 3, pp. 247–255, 2009.

[34] K. Yoshida and K. Matsuzaki, "Differential regulation of TGF-β/Smad signaling in hepatic stellate cells between acute and chronic liver injuries," *Frontiers in Physiology*, vol. 3, p. 53, 2012.

[35] M. Weinstein, S. P. S. Monga, Y. Liu et al., "Smad proteins and hepatocyte growth factor control parallel regulatory pathways that converge on β1-integrin to promote normal liver development," *Molecular and Cellular Biology*, vol. 21, no. 15, pp. 5122–5131, article 300060518811512, 2001.

[36] S. Wang, Y. Shangguan, C. Ding et al., "Risk factors for acute liver failure among inpatients with anti-tuberculosis drug-induced liver injury," *Journal of International Medical Research*, 2018.

[37] G. Chen, S.-Q. Wu, M. Feng et al., "Association of UGT2B7 polymorphisms with risk of induced liver injury by anti-tuberculosis drugs in Chinese Han," *International Journal of Immunopathology and Pharmacology*, vol. 30, no. 4, pp. 434–438, 2017.

[38] J. Zhang, X. Zhu, Y. Li et al., "Correlation of CpG island methylation of the cytochrome P450 2E1/2D6 genes with liver injury induced by anti-tuberculosis drugs: a nested case-control study," *International Journal of Environmental Research and Public Health*, vol. 13, no. 8, p. 776, 2016.

[39] Y. Wang, X. Xiang, W.-W. Huang et al., "Association of PXR and CAR polymorphisms and antituberculosis drug-induced hepatotoxicity," *Scientific Reports*, vol. 9, no. 1, p. 2217, 2019.

Hindawi
Evidence-Based Complementary and Alternative Medicine
Volume 2019, Article ID 1390795, 9 pages
https://doi.org/10.1155/2019/1390795

Review Article

Effects of Curcumin on Vessel Formation Insight into the Pro- and Antiangiogenesis of Curcumin

Ting-ye Wang and Jia-xu Chen

School of Traditional Chinese Medicine, Beijing University of Chinese Medicine, Beijing 100029, China

Correspondence should be addressed to Jia-xu Chen; chenjiaxu@hotmail.com

Received 21 February 2019; Revised 2 May 2019; Accepted 2 June 2019; Published 19 June 2019

Academic Editor: Jamal A. Mahajna

Curcumin is a compound extracted from the *Curcuma longa L,* which possesses a wide range of pharmacological effects. However, few studies have collected scientific evidence on its dual effect on angiogenesis. The present review gathered the fragmented information available in the literature to discuss the dual effect and possible mechanisms of curcumin on angiogenesis. Available information concerning the effect of curcumin on angiogenesis is compiled from scientific databases, including PubMed and Web of Science using the key term (curcumin and angiogenesis). The results were reviewed to identify relevant articles. Related literature demonstrated that curcumin has antiangiogenesis effect via regulating multiple factors, including proangiogenesis factor VEGF, MMPs, and FGF, both *in vivo* and *in vitro*, and could promote angiogenesis under certain circumstances via these factors. This paper provided a short review on bidirectional action of curcumin, which should be useful for further study and application of this compound that require further studies.

1. Introduction

Curcumin, one of the most promising natural compounds, is the major polyphenol compound found in *Curcuma longa L* with the symmetric chemical structure [1, 2]. Since its first isolation in impure in 1815 by Vogel and Pelletier [3], Lampe et al. confirmed its chemical structure and synthesis in 1910 and 1913, respectively [4], and identified the use of curcumin in human diseases in 1937 for the first time [5]; extensive studies over the last half century have clearly confirmed the pharmacological and biological effects of curcumin including antiproliferation, anti-inflammatory, antioxidant, anti-HIV, antibacterial, antifungal, nematocidal, antispasmodic, antiparasitic, antimutagenic, antidiabetic, antifibrinolytic, antithrombotic, radioprotective, and anticarcinogenic activity as well as wound healing, lipid lowering, and immunomodulating (Figure 1) [2, 6–11]. Preclinical and clinical researches demonstrated that curcumin could be utilized in the treatment of cancer, diabetes, and other diseases [12]. Cancer is one of the research hotspots in recent years; as a natural compound with no toxicity and promising feature on tumor therapy, attention have been paid on curcumin.

Angiogenesis is the process of new vessel formation and hallmark of tumor progression [13], which is crucial for tumor growth and expansion [14]. It was reported that solid tumor cannot grow well without inducing blood supply [15]. As a result of the hotspot of cancer therapy, the anticarcinogenic effect of curcumin has been investigated systematically, where angiogenesis plays an important role. Studies have found that the anticancer effect of curcumin is achieved by inhibiting angiogenesis partly [16–19]; naturally, effects of curcumin on angiogenesis draw the attention of researchers. At the same time, angiogenesis represents a critical determinant in wound repair where curcumin plays a role because new blood vessels act as a route for delivering oxygen and nutrients to cells at the wound points [20]; effects of curcumin on promoting angiogenesis in wound healing process have been studied. Altogether, curcumin has bidirectional action on angiogenesis.

This article is aimed at reviewing the bidirectional action of curcumin and curcuminoids as well as synthetic curcumin analog on angiogenesis based on current research findings, focusing on regulation of curcumin on proangiogenesis factors in antiangiogenesis and proangiogenesis process;

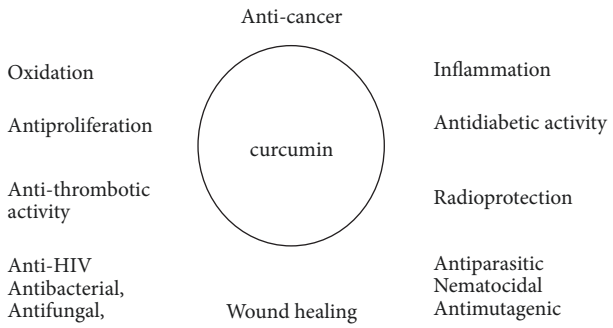

Figure 1: Biological effect of curcumin.

Figure 2: Curcuma rhizome and curcumin powder.

some of the mechanisms were summarized and discussed. Furthermore, this article provided some information and insights which could be interesting to researchers in related areas.

2. Traditional Uses of Curcumin

Curcumin (Figure 2) is a member of the ginger family and is prescribed abundantly for ailments in both traditional Chinese and Indian medicine [21]. In China, *Curcuma longa L* has been used as a commonly used traditional Chinese medicine for thousands of years with the effect of activating qi flowing, removing blood stasis, benefiting menstruation, and relieving pain. In India, turmeric is commonly used in the Indian subcontinent as a spice, concurrently used for health care including various respiratory diseases [22, 23]. Besides, turmeric preparations could be applied to treat fresh wounds and anticancer effect of turmeric was also documented in Indian medical literature [24].

3. Chemistry of Curcumin

Chemically, curcumin is a bis-α,β-unsaturated β-diketone [4] (Figure 3). Based on its β-diketone moiety, curcumin exists in keto-enol tautomers, and this tautomerism favors interaction and binding with a wide range of enzymes [25]. Some researchers have reported that the potency for the suppression of nuclear factor-kappaB (NF-κB) differ between curcuminoids, suggesting that the methoxy groups on the phenyl rings in curcumin are important to have health effects [26]. In the same time, the 4,4′-free phenolic groups is found to be another important groups in curcumin structure, studies have confirmed 4,4′-free phenolic groups to be associated with curcumin activities [27, 28], and these findings draw attention to the researches on the synthetic analogs of curcumin.

4. Bioactivity of Curcumin

Studies over the past thirty years have revealed that low bioavailability of curcumin mainly due to poor absorption and rapid metabolism [29]; metabolism has been considered to be the main reasons of poor bioavailability [30]. Because of the low bioavailability, innovative methods of increasing solution of curcumin have been used, resulting in the highlight on curcumin nanoformulations. During the last decades, various types of nanocarriers of curcumin have been investigated to improve the bioavailability of curcumin and some systems have reached clinical evaluations and applications [31–33]; these achievements can facilitate the better use of curcumin.

5. Curcumin and Angiogenesis

In adult, angiogenesis is required for wound healing and female reproductive organs actions [34]. Generally, the angiogenesis process is activated by growth factors such as basic fibroblast growth factor (bFGF), vascular endothelia growth factor (VEGF), or placental growth factor [35]. In adults, the formation and growth of new blood vessels are tightly controlled. These processes are triggered only under strictly defined conditions like wound healing. The function of strict system regulation and balance is very important for the body, because both excessive formation of blood vessels and underdevelopment of blood vessels could lead to serious diseases [36], such as neurological disease and tumor. There are three stages of angiogenesis: the first stage: some endothelial cells, namely, "tip cells" inside the capillary that react to the angiogenesis factor VEGF-A, are selected as the starting point to begin angiogenesis expansion. The second stage: the tip cells only respond to VEGF-A through guided migration; in the sprout stalks, the proliferative response to VEGF-A occurs. Both of these two cellular responses are mediated by the activation of VEGF-A on VEGFR-2 [37]. The third stage: maturation of newly formed vessels consists of endothelial proliferation inhibition, new capillaries migration, and new vascular tubes that already existing stabilization [38, 39]. During the process of angiogenesis, various signaling pathways, related factors, and receptors are involved. VEGF is part of the most important ligand among them. Others as epidermal growth factor (EGF), transforming growth factors (TGF), fibroblast growth factors (FGF), angiopoietin-1 and 2, and matrix metalloproteinases (MMPs) also play a role in the process of angiogenesis [34, 40].

5.1. Antiangiogenesis Effects of Curcumin. It was showed that pathological angiogenesis is a mark of cancer and several ischaemic and inflammatory disease [41]. During the past years, great progress has been made in comprehending the mechanism of angiogenesis in different pathophysiological conditions, the antiangiogenesis effect of curcumin is

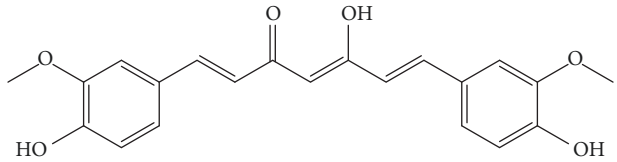

Figure 3: Chemical structure of curcumin.

among them. Angiogenesis inhibitors can fall into two categories. The first class, also known as the direct angiogenesis inhibitors, refers to those inhibitors which are relatively sensitive for endothelial cells than tumor cells. The additional class, on the other hand, is the indirect inhibitors, which may have no direct effects on endothelial cells, but may regulate angiogenesis via downregulating an angiogenesis stimulator [42]. Curcumin is a direct inhibitor of angiogenesis; in the meantime, it can also downregulate several proangiogenesis factors [43]. Curcumin affects the whole process of angiogenesis through downregulating transcription factors such as NF-κB and proangiogenesis factors such as VEGF, bFGF, and MMPs [43], all of which are closely and directly linked with tumorigenesis, involving in the complicated regulating process of curcumin.

5.1.1. Fibroblast Growth Factor. bFGF was isolated from bovine pituitary known as highly angiogenic and widely expressed in normal and malignant tissues. bFGF induces angiogenesis as a result of its effects on smooth muscle cells and endothelial cells, as well as its role as a chemoattractant and aid in the proliferation of fibroblasts and epithelial cells. bFGF is expressed in vascular endothelium during tumor neovascularization and antiproliferative diseases. Besides their angiogenic activity, the FGFs are critical for wound healing [44]. Because bFGF is essential preconditions for initiation angiogenesis process, researches focusing on regulation of curcumin on bFGF have been carried out. Results showed that curcumin could inhibit bFGF and FGF-induced angiogenesis in vivo [42, 45]. In an investigation, it was reported that curcumin and its derivatives significantly inhibit corneal neovascularization induced by basic fibroblast growth factor [42]. And a previous study revealed that curcumin could inhibit FGF-induced neovascularization [46], indicating FGFs play an important role in inhibiting angiogenesis by curcumin.

5.1.2. Matrix Metalloproteinases. MMPs have an expanded role in angiogenesis, as they are essential for the creation and maintenance of supporting growth and angiogenesis of tumor [47]. MMPs released by endothelial cells represent a key process in neovascularization. Within all MMPs, MMP-9 plays a regulatory role in angiogenesis not only through proteolytic activity, but also through other downstream angiogenesis factors; study revealed that MMP-9 participated in the angiogenesis of tumors by increasing the effectiveness of VEGF, an important angiogenesis inducer in malignant tumor, indicating that the MMP-9 is a part of the angiogenic regulation [48].

Curcumin shows antiangiogenesis effect via meditating MMP level. A significant decrease of MMP-2 and MMP-9 levels has been identified in the prostate and breast cancer cells treated with curcumin [49]. Experiments concerning curcumin inhibit angiogenesis in glioblastoma xenografts have been carried out and the results showed that the antiangiogenesis activity of curcumin is at least partly via MMP-9 both *in vivo* and *vitro* [50]. These results demonstrated that the inhibition of MMP-9 is one of the major causes of angiogenesis inhibition by demethoxycurcumin [51]. It was observed that curcumin and its synthetic analogs downregulate the expression of genes responsible for angiogenesis and other angiogenesis factors such as VEGF and MMP-9 [52]

5.1.3. Vascular Endothelial Growth Factor. VEGF as the best known angiogenesis factor present was first discovered in 1986 by Senger and his colleagues [53], has been taken as the most critical factor in angiogenesis regulation processes, and is known to be required for normal as well as pathological angiogenesis in many tissues, having a key role in cancer biology and being involved in neovascularization [54]. There are three known VEGF receptors that are VEGFR-1 and VEGFR-2, expressed on vascular endothelial cells and as well as VEGFR-3; VEGF directly initiate an angiogenesis process via binding to its receptors on vascular endothelial cells [55, 56].

Curcumin shows antiangiogenesis effect primarily in tumor both *in vitro* and *in vivo*. Curcumin could reduce the suppression of VEGF in an *in vitro* model of endometriosis [57] and block angiogenesis induced by hypoxia *in vitro* and downregulated VEGF expression [58]. *In vivo*, study found that curcumin inhibited angiogenesis through reducing microvessel density in Ehrlich ascites carcinoma-bearing mice; possible mechanism was proved to be inhibition of VEGF and VEGFR2 [59] and is able to inhibit tumor angiogenesis by the reduction of proangiogenesis factor VEGF in the Xenograft model of breast cancer [60]. Other than cancer, curcumin is seen as an angiogenesis inhibitor by downregulating VEGF in corneal diseases, diabetic retinopathy, diabetic nephropathy, and ectopic endometrium [61–65]. Other than tumor, curcumin effectively prevented the angiogenesis response in aortic ring models in both the diabetic and nondiabetic environment where VEGF level decreased [66]. A previous clinical trial demonstrated that curcumin could reduce VEGF level where VEGF overexpression and subsequent vasculogenesis and angiogenesis are implicated in the development of several pathological processes [67]. Another phase I trial revealed that curcumin/docetaxel combination could significantly decrease VEGF levels after three cycles of

treatment [68]. Expect for curcumin, liposome curcumin and curcumin nanoparticle also showed antiangiogenesis effect by inhibiting VEGF [69, 70]

5.1.4. VEGF-Related Mediating Factors. COX-2 is an inducible enzyme that is upregulated responsing growth factors stimuli as VEGF [71]. Numerous reports showed that one of the mechanisms of COX-2 participates in tumorigenesis is to induce angiogenesis [72]. Finding brought us the idea that the overexpression of COX-2 may be functionally significant for the early stage of tumor angiogenesis. The effects of COX-2 on tumor angiogenesis might be mediated by the upregulation of angiogenesis factors like VEGF expression. Other results showed the significant correlation between VEGF expression, COX-2 expression, and mast cell density (MCD), indicating COX-2 and MCD may contribute to tumor angiogenesis by regulating the production of VEGF [73]. All together showed that COX-2 induce angiogenesis is closely related to VEGF. *In vitro*, curcumin could inhibit hepatocellular carcinoma cells angiogenesis through reducing the expression of COX-2 and VEGF [74]. Besides, curcumin inhibits angiogenesis in microvascular endothelial cell via suppressing COX-2 expression [75]. Curcumin analogs EF31 and UBS109 also induced the downregulation of COX-2 and VEGF in pancreatic cancer [76]. These findings indicated that COX-2 plays an important in inhibiting angiogenesis by curcumin.

NF-κB could affect the angiogenesis through regulating angiogenesis factors including MMPs and VEGF, and the production of these angiogenesis factors is regulated by NF-κB activation [77]. Activation of NF-κB and its gene products (e.g., VEGF, MMP-2, MMP-9, and COX-2) can be inhibited by curcumin both *in vitro* and *in vivo*, which has a significant role in angiogenesis [78, 79]; these findings might help in the curcumin inhibiting angiogenesis in ovarian carcinoma *in vitro* and *vivo*; results showed decreasing of microvessel density, which is regulated by targeting the nuclear factor-κB pathway [80]. Curcumin nanoparticle could also prevent corneal neovascularization by inhibiting NF-κB in corneal cells induced by lipopolysaccharide [69]. These studies further emphasize NF-κB activation in mediating angiogenesis and curcumin could downregulate NF-κB to inhibit angiogenesis.

5.2. Proangiogenesis Effects of Curcumin. Despite the antiangiogenesis of curcumin has been discussed a lot; it is found that curcumin possess a proangiogenesis effect. Study found out that curcumin pretreatment augmented adipose derived stem cells production of VEGF, which contributed to neovessels formation and improving cells survival [81]. A previous study found that curcumin could increase MMP-2, transforming growth factor (TGF)-beta, and VEGF expression, which are proangiogenesis factors and accelerate angiogenesis in an indomethacin-induced model [82]. Curcumin enhanced endothelial progenitor cells (EPCs) function, namely, angiogenesis, migration, and proliferation ability, and upregulated the angiogenesis factors including VEGF-A and Ang-1 [83]. Curcumin may promote both neovascularization and small capillary formation in a rat model of nasal mucosal trauma [84] and improved neovascularization in diabetic model of streptozotocin and gene induced [85].

Meanwhile, neovascularization represents an important part in wound healing; angiogenesis could affect the whole process of wound healing from the very beginning after skin injury until the end of the wound remodeling [86]; curcumin has been proven as an effective natural product in wound healing, which is used as a household therapy in Indian subcontinent for management of skin diseases, wound, insect bites, and other inflammatory diseases from ancient time; relevant researches have been done to explore its proangiogenesis effect in wound healing; anti-inflammatory activity may be the main mechanism by which curcumin improves wound healing [87]. Curcumin has been shown to be a promising proangiogenesis agent in wound healing by inducing TGF-beta, which could induce both angiogenesis and accumulation of extracellular matrix through the entire remodeling phase of wound repair [88]. Ken V and his colleagues found that curcumin can enhance the neo vasculogenesis and accelerate the wound healing in diabetic rats by increasing the expressions of various factors, for example, VEGF and TGF-beta1, leading to well-formed blood vessels with increased microvessel density, which indicated that curcumin could promote angiogenesis [89]. The *in vivo* effects of curcumin on wound healing in rats and guinea pigs has been studied showing that extensive neovascularization and molecular biology analysis also showed an increase in the mRNA transcripts of TGF-beta1 in curcumin-treated wounds [90]. These results revealed the proangiogenesis effect of curcumin.

Expect for curcumin itself, ethosomal curcumin also showed the effect of promoting neovascularization in the second degree burns in rat [91] and curcumin cross-linked collagen aerogels also possesses proangiogenesis efficacy [92]. Oil of *Curcuma longa* also showed significant proangiogenesis activity [93]. All together are showing the effect of curcumin on promoting angiogenesis by regulating proangiogenesis factors.

5.3. Dual Effects of Curcumin on Angiogenesis. As discussed before, it is found that curcumin shows a dual effect on angiogenesis (Figure 4); studies have confirmed this idea that curcumin shows different effects in different microenvironment. To be specific, when cells are in a microenvironment that lack of exogenous stimuli and exposed to growth factors such as FGF, curcumin may present an antiangiogenesis effect, while proangiogenesis effect of curcumin is mediated through VEGF and PI3K-Akt pathway in different microenvironment [94], which explained the underlying mechanism of opposite effect of curcumin on angiogenesis. Meanwhile, *in vitro* study showed that curcumin reveals opposite angiogenesis effects on human umbilical vein endothelial cells and chicken chorioallantoic membrane as a function of dose [95]. Besides, the dosage of curcumin may be another factor to explain why curcumin possesses both proangiogenesis and antiangiogenesis activity; curcumin could be taken to

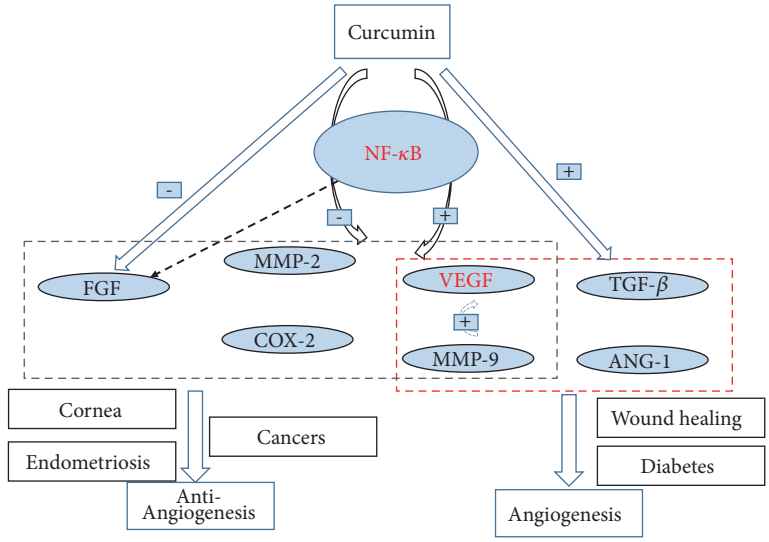

Figure 4: Possible mechanism on dual effect of curcumin on angiogenesis.

treat different medical conditions based on the dosage used to show either proangiogenesis or antiangiogenesis effect [82]. Proangiogenesis effects of curcumin were observed at a lower dose while antiangiogenesis effects were found at higher doses [19]. It was discovered that curcumin showed a proangiogenesis effect at a low dose (20 mg/kg/day) [96], while inhibited tumor progression at a high dose (100 to 300 mg/kg/day) in C57BL/6 mice [97], indicating that the dual effect of curcumin is dose-meditated.

The inhibition of angiogenesis differentiation by curcumin depends on the serum concentration present in the incubation medium. The effective concentration required to inhibit angiogenesis in the presence of 10% serum is much higher than that required to do so in the presence of 2% serum [98].

6. Discussion

As reviewed in this article, it can be seen that curcumin has dual effects on angiogenesis; curcumin can not only inhibit angiogenesis in tumor and other pathological conditions, but also promote angiogenesis in fresh wound and diabetic rats, which has broadened the clinical use, pharmaceutical significance, and therapeutic applicability of curcumin, providing a new research direction on curcumin.

Even though the dual effect of curcumin has been found during years of hard work, the molecular mechanism of its dual effects has been studied in some details but the underlying mechanism of this association between angiogenesis and the dual effect of curcumin is still not crystal clear. Some researches proposed the idea that the dual effect of curcumin is dose-based or depending on the microenvironment, there is other hypothesis that chemistry structure of curcumin may contribute to it, but no solid conclusion has been drawn; further researches based on chemical genomics approach and other methods are still needed.

Such bidirectional actions of curcumin are not uncommon. Curcumin has radioprotective effects on normal tissues and radiosensitization of tumor cells [99–101], which is regulated via NF-κB pathway. While curcumin shows a two-way prooxidant and antioxidant effects regulated by concentration [102–104], these findings indicated that bidirectional actions of curcumin are not uncommon and mechanisms of these bidirectional actions are different. In this way, the pro- and antiangiogenesis effects of curcumin are closely related to the concentration, and NF-κB pathway plays an important role as well, indicating that the underlying mechanisms of bidirectional actions of curcumin on angiogenesis are more complicated.

There is study which showed microRNAs as a part of cellular communication [105]. Research has found that curcumin alone upregulated expression of miR-122 and downregulated miR-221 expression; in the same time, curcumin affected microvessel count, expression of angiogenesis, and microRNAs [106]. In addition, another study showed that curcumin may exert its antitumor effects via inhibiting angiogenesis through modulation of VEGF signal regulatory miRNAs [107]. As for proangiogenesis effects of curcumin, curcumin had an active role in nondiabetic peripheral arterial disease by improving angiogenesis, which may be partially achieved by promoting miR-93 expression [108]. All these findings indicated that micro-RNAs may be the principal regulator of curcumin insides the cells.

Recent researches focus mostly on the unilateral role of curcumin on angiogenesis; studies focused on antiangiogenesis effect of curcumin showed that curcumin has great potential in anticancer treatment, as a natural product with great safety and low toxicity; more preclinical and clinical studies should be conducted to dig the anticancer effect of curcumin through inhibiting angiogenesis and promote new drug research and development. Novel delivery systems of curcumin have been investigated extensively to improve the bioavailability *in vitro* and *in vivo*, and curcumin has been

used in traditional medicine for many years with accurate effects and has tremendous potential in treating difficult disease; it still needs deeper researches, both evidence-based preclinical and clinical researches for evaluating its pharmaceutical potentialities and better understanding of its pharmacological mechanisms, and puts studies of curcumin translate from lab to clinical. However there are limitations to this research; there are still many deficiencies in the thesis. It is our hope that more people see the value in this natural compound and provide evidence needed to help prove its mechanisms.

Abbreviations

bFGF: Basic fibroblast growth factor
COX-2: Cyclooxygenase-2
EGF: Epidermal growth factor
EPCs: Endothelial progenitor cells
FGF: Fibroblast growth factors
HUVEC: Human umbilical vein endothelial cells
MMPs: Matrix metalloproteinases
MCD: Mast cell density
NF-κB: Nuclear factor-kappaB
TNF: Tumor necrosis factor
TGF: Transforming growth factors
VEGF: Vascular endothelial growth factor.

Data Availability

Readers can access the data underlying the findings of the study by contacting authors via e-mails.

Conflicts of Interest

The authors declare that there are no conflicts of interest regarding the publication of this paper.

Acknowledgments

This work was supported by National Natural Science Foundation of China (no. 81630104).

References

[1] F. Payton, P. Sandusky, and W. L. Alworth, "NMR study of the solution structure of curcumin," *Journal of Natural Products*, vol. 70, no. 2, pp. 143–146, 2007.

[2] B. B. Aggarwal, A. Kumar, and A. C. Bharti, "Anticancer potential of curcumin: preclinical and clinical studies," *Anticancer Reseach*, vol. 23, no. 1A, pp. 363–398, 2003.

[3] J. Miłobędzka, S. v. Kostanecki, and V. Lampe, "Zur kenntnis des curcumins," *Berichte der Deutschen Chemischen Gesellschaft*, vol. 43, no. 2, pp. 2163–2170, 1910.

[4] J. Milobedeska, V. Kostanecki, and V. Lampe, "Structure of curcumin," *Berichte der Deutschen Chemischen Gesellschaft*, vol. 43, pp. 2163–2170, 1910.

[5] A. Oppenheimer, "Turmeric (curcumin) in biliary diseases," *The Lancet*, vol. 229, no. 5924, pp. 619–621, 1937.

[6] A. Niranjan and D. Prakash, "Chemical constituents and biological activities of turmeric (Curcuma longa L.) -A review," *Journal of Food Science and Technology*, vol. 45, no. 2, pp. 109–116, 2008.

[7] Y. Panahi, M. S. Hosseini, N. Khalili, E. Naimi, M. Majeed, and A. Sahebkar, "Antioxidant and anti-inflammatory effects of curcuminoid-piperine combination in subjects with metabolic syndrome: A randomized controlled trial and an updated meta-analysis," *Clinical Nutrition*, vol. 34, no. 6, pp. 1101–1108, 2015.

[8] G. G. L. Yue, B. C. L. Chan, P.-M. Hon et al., "Evaluation of in vitro anti-proliferative and immunomodulatory activities of compounds isolated from Curcuma longa," *Food and Chemical Toxicology*, vol. 48, no. 8-9, pp. 2011–2020, 2010.

[9] S. Hu, P. Maiti, Q. Ma et al., "Clinical development of curcumin in neurodegenerative disease," *Expert Review of Neurotherapeutics*, vol. 15, no. 6, pp. 629–637, 2015.

[10] R. Srivastava, M. Dikshit, R. C. Srimal, and B. N. Dhawan, "Anti-thrombotic effect of curcumin," *Thrombosis Research*, vol. 40, no. 3, pp. 413–417, 1985.

[11] D.-W. Zhang, M. Fu, S.-H. Gao, and J.-L. Liu, "Curcumin and diabetes: a systematic review," *Evidence-Based Complementary and Alternative Medicine*, vol. 2013, Article ID 636053, 16 pages, 2013.

[12] S. Shishodia, "Molecular mechanisms of curcumin action: gene expression," *BioFactors*, vol. 39, no. 1, pp. 37–55, 2013.

[13] L. Yadav, N. Puri, V. Rastogi, P. Satpute, and V. Sharma, "Tumour angiogenesis and angiogenic inhibitors: A review," *Journal of Clinical and Diagnostic Research*, vol. 9, no. 6, pp. XE01–XE05, 2015.

[14] J. Folkman, "Tumor angiogenesis: therapeutic implications.," *The New England Journal of Medicine*, vol. 285, no. 21, pp. 1182–1186, 1971.

[15] J. Folkman, "Clinical applications of research on angiogenesis," *The New England Journal of Medicine*, vol. 333, no. 26, pp. 1757–1763, 1995.

[16] D. M. Hossain, S. Bhattacharyya, T. Das, and G. Sa, "Curcumin: the multi-targeted therapy for cancer regression," *Front Biosci*, vol. 4, pp. 335–355, 2012.

[17] M. K. Shanmugam, S. Warrier, A. Kumar, G. Sethi, and F. Arfuso, "Potential role of natural compounds as anti-angiogenic agents in cancer," *Current Vascular Pharmacology*, vol. 15, no. 6, 2017.

[18] P. D. Kasi, R. Tamilselvam, K. Skalicka-Woźniak et al., "Molecular targets of curcumin for cancer therapy: An updated review," *Tumor Biology*, vol. 37, no. 10, pp. 13017–13028, 2016.

[19] R. K. Maheshwari, A. K. Singh, J. Gaddipati, and R. C. Srimal, "Multiple biological activities of curcumin: a short review," *Life Sciences*, vol. 78, no. 18, pp. 2081–2087, 2006.

[20] J. R. Sharpe and Y. Martin, "Strategies demonstrating efficacy in reducing wound contraction *In Vivo*," *Advances in Wound Care*, vol. 2, no. 4, pp. 167–175, 2013.

[21] R. Kuttan, P. Bhanumathy, K. Nirmala, and M. C. George, "Potential anticancer activity of turmeric (*Curcuma longa*)," *Cancer Letters*, vol. 29, no. 2, pp. 197–202, 1985.

[22] I. Rahman, S. K. Biswas, and P. A. Kirkham, "Regulation of inflammation and redox signaling by dietary polyphenols," *Biochemical Pharmacology*, vol. 72, no. 11, pp. 1439–1452, 2006.

[23] N. Tirkey, G. Kaur, G. Vij, and K. Chopra, "Curcumin, a diferuloylmethane, attenuates cyclosporine-induced renal dysfunction and oxidative stress in rat kidneys," *BMC Pharmacology*, vol. 5, p. 15, 2005.

[24] K. M. Nelson et al., "The essential medicinal chemistry of curcumin," *Journal of Medicinal Chemistry*, 2017.

[25] A. Shehzad, R. Shahzad, and Y. S. Lee, "Curcumin: a potent modulator of multiple enzymes in multiple cancers," *Enzymes*, vol. 36, pp. 149–174, 2014.

[26] S. K. Sandur, M. K. Pandey, B. Sung et al., "Curcumin, demethoxycurcumin, bisdemethoxycurcumin, tetrahydrocurcumin and turmerones differentially regulate anti-inflammatory and anti-proliferative responses through a ROS-independent mechanism," *Carcinogenesis*, vol. 28, no. 8, pp. 1765–1773, 2007.

[27] K. I. Priyadarsini, D. K. Maity, G. H. Naik et al., "Role of phenolic O-H and methylene hydrogen on the free radical reactions and antioxidant activity of curcumin," *Free Radical Biology Medicine*, vol. 35, no. 5, pp. 475–484, 2003.

[28] P. Venkatesan, M. K. Unnikrishnan, M. Sudheer Kumar, and M. N. A. Rao, "Effect of curcumin analogues on oxidation of haemoglobin and lysis of erythrocytes," *Current Science*, vol. 84, no. 1, pp. 74–78, 2003.

[29] P. Anand, A. B. Kunnumakkara, R. A. Newman, and B. B. Aggarwal, "Bioavailability of curcumin: problems and promises," *Molecular Pharmaceutics*, vol. 4, no. 6, pp. 807–818, 2007.

[30] V. Ravindranath and N. Chandrasekhara, "Metabolism of curcumn-studies with [3H]curcumin," *Toxicology*, vol. 22, no. 4, pp. 337–344, 1982.

[31] J. Hrkach, D. von Hoff, M. M. Ali et al., "Preclinical development and clinical translation of a PSMA-targeted docetaxel nanoparticle with a differentiated pharmacological profile," *Science Translational Medicine*, vol. 4, no. 128, Article ID 128ra39, 2012.

[32] S. Svenson, "Clinical translation of nanomedicines," *Current Opinion in Solid State & Materials Science*, vol. 16, no. 6, pp. 287–294, 2012.

[33] R. Tong, N. P. Gabrielson, T. M. Fan, and J. Cheng, "Polymeric nanomedicines based on poly(lactide) and poly(lactide-co-glycolide)," *Current Opinion in Solid State & Materials Science*, vol. 16, no. 6, pp. 323–332, 2012.

[34] Z. Tahergorabi and M. Khazaei, "A review on angiogenesis and its assays," *Iranian Journal of Basic Medical Sciences*, vol. 15, no. 6, pp. 1110–1126, 2012.

[35] M. Zygmunt, F. Herr, K. Munstedt, U. Lang, and O. D. Liang, "Angiogenesis and vasculogenesis in pregnancy," *European Journal of Obstetrics & Gynecology and Reproductive Biology*, vol. 110, supplement 1, pp. S10–S18, 2003.

[36] A. F. Karamysheva, "Mechanisms of angiogenesis," *Biochemistry (Moscow)*, vol. 73, no. 7, pp. 751–762, 2008.

[37] H. Gerhardt, M. Golding, M. Fruttiger et al., "VEGF guides angiogenic sprouting utilizing endothelial tip cell filopodia," *The Journal of Cell Biology*, vol. 161, no. 6, pp. 1163–1177, 2003.

[38] R. K. Jain, "Molecular regulation of vessel maturation," *Nature Medicine*, vol. 9, no. 6, pp. 685–693, 2003.

[39] O. Cleaver and D. A. Melton, "Endothelial signaling during development," *Nature Medicine*, vol. 9, no. 6, pp. 661–668, 2003.

[40] Y. Cao and Q. Liu, "Therapeutic targets of multiple angiogenic factors for the treatment of cancer and metastasis," *Advances in Cancer Research*, vol. 97, pp. 203–224, 2007.

[41] P. Carmeliet and R. K. Jain, "Angiogenesis in cancer and other diseases," *Nature*, vol. 407, no. 6801, pp. 249–257, 2000.

[42] J. L. Arbiser, N. Klauber, R. Rohan et al., "Curcumin is an in vivo inhibitor of angiogenesis," *Molecular Medicine*, vol. 4, no. 6, pp. 376–383, 1998.

[43] S. S. Bhandarkar and J. L. Arbiser, "Curcumin as an inhibitor of angiogenesis," *Advances in Experimental Medicine and Biology*, vol. 595, pp. 185–195, 2007.

[44] A. Bikfalvi, S. Klein, G. Pintucci, and D. B. Rifkin, "Biological roles of fibroblast growth factor-2," *Endocrine Reviews*, vol. 18, no. 1, pp. 26–45, 1997.

[45] D. Hanahan and R. A. Weinberg, "The hallmarks of cancer," *Cell*, vol. 100, no. 1, pp. 57–70, 2000.

[46] H. Hatcher, R. Planalp, J. Cho, F. M. Torti, and S. V. Torti, "Curcumin: from ancient medicine to current clinical trials," *Cellular and Molecular Life Sciences*, vol. 65, no. 11, pp. 1631–1652, 2008.

[47] A. R. Nelson, B. Fingleton, M. L. Rothenberg, and L. M. Matrisian, "Matrix metalloproteinases: biologic activity and clinical implications," *Journal of Clinical Oncology*, vol. 18, no. 5, pp. 1135–1149, 2000.

[48] G. Bergers, R. Brekken, G. McMahon et al., "Matrix metalloproteinase-9 triggers the angiogenic switch during carcinogenesis," *Nature Cell Biology*, vol. 2, no. 10, pp. 737–744, 2000.

[49] E. Creţu, A. Trifan, A. Vasincu, and A. Miron, "Plant-derived anticancer agents - curcumin in cancer prevention and treatment," *Revista Medico-Chirurgicala A Societatii De Medici Si Naturalisti Din Iasi*, vol. 116, no. 4, pp. 1223–1229, 2012.

[50] M.-C. Perry, M. Demeule, A. Régina, R. Moumdjian, and R. Béliveau, "Curcumin inhibits tumor growth and angiogenesis in glioblastoma xenografts," *Molecular Nutrition & Food Research*, vol. 54, no. 8, pp. 1192–1201, 2010.

[51] J. H. Kim, J. S. Shim, S.-K. Lee et al., "Microarray-based analysis of anti-angiogenic activity of demethoxycurcumin on human umbilical vein endothelial cells: crucial involvement of the down-regulation of matrix metalloproteinase," *Japanese Journal of Cancer Research*, vol. 93, no. 12, pp. 1378–1385, 2002.

[52] E.-R. Hahm, Y. S. Gho, S. Park, C. Park, K.-W. Kim, and C.-H. Yang, "Synthetic curcumin analogs inhibit activator protein-1 transcription and tumor-induced angiogenesis," *Biochemical and Biophysical Research Communications*, vol. 321, no. 2, pp. 337–344, 2004.

[53] D. R. Senger, C. A. Perruzzi, J. Feder, and H. F. Dvorak, "A highly conserved vascular permeability factor secreted by a variety of human and rodent tumor cell lines," *Cancer Research*, vol. 46, no. 11, pp. 5629–5632, 1986.

[54] N. Ferrara, "Molecular and biological properties of vascular endothelial growth factor," *Journal of Molecular Medicine*, vol. 77, no. 7, pp. 527–543, 1999.

[55] C. J. Robinson and S. E. Stringer, "The splice variants of vascular endothelial growth factor (VEGF) and their receptors," *Journal of Cell Science*, vol. 114, no. 5, pp. 853–865, 2001.

[56] S. Takahashi, "Vascular endothelial growth factor (VEGF), VEGF receptors and their inhibitors for antiangiogenic tumor therapy," *Biological & Pharmaceutical Bulletin*, vol. 34, no. 12, pp. 1785–1788, 2011.

[57] F. Wieser, J. Yu, J. Park, N. Sidell, and R. N. Taylor, "Curcumin suppresses angiogenesis, cell proliferation and induces apoptosis in an in vitro model of endometriosis," *Fertility & Sterility*, vol. 88, no. 3, pp. S204–S205, 2007.

[58] M. Bae, S. Kim, J. Jeong et al., "Curcumin inhibits hypoxia-induced angiogenesis via down-regulation of HIF-1," *Oncology Reports*, vol. 15, no. 6, pp. 1557–1562, 2006.

[59] M. El-Azab, H. Hishe, Y. Moustafa, and E.-S. El-Awady, "Anti-angiogenic effect of resveratrol or curcumin in Ehrlich ascites carcinoma-bearing mice," *European Journal of Pharmacology*, vol. 652, no. 1–3, pp. 7–14, 2011.

[60] L. C. Ferreira, A. S. Arbab, B. V. Jardim-Perassi et al., "Effect of curcumin on pro-angiogenic factors in the xenograft model of

breast cancer," *Anti-Cancer Agents in Medicinal Chemistry*, vol. 15, no. 10, pp. 1285–1296, 2015.

[61] T. Sawatpanich, H. Petpiboolthai, B. Punyarachun, and V. Anupunpisit, "Effect of curcumin on vascular endothelial growth factor expression in diabetic mice kidney induced by streptozotocin," *Journal of the Medical Association of Thailand*, vol. 93, supplement 2, pp. S1–S8, 2010.

[62] Y. Zhang, H. Cao, Y.-Y. Hu, H. Wang, and C.-J. Zhang, "Inhibitory effect of curcumin on angiogenesis in ectopic endometrium of rats with experimental endometriosis," *International Journal of Molecular Medicine*, vol. 27, no. 1, pp. 87–94, 2011.

[63] J. S. Kim, J. S. Choi, and S. K. Chung, "The effect of curcumin on corneal neovascularization in rabbit eyes," *Current Eye Research*, vol. 35, no. 4, pp. 274–280, 2010.

[64] F. Bian, M.-C. Zhang, and Y. Zhu, "Inhibitory effect of curcumin on corneal neovascularization in vitro and in vivo," *Ophthalmologica*, vol. 222, no. 3, pp. 178–186, 2008.

[65] T. Mrudula, P. Suryanarayana, P. N. B. S. Srinivas, and G. B. Reddy, "Effect of curcumin on hyperglycemia-induced vascular endothelial growth factor expression in streptozotocin-induced diabetic rat retina," *Biochemical and Biophysical Research Communications*, vol. 361, no. 2, pp. 528–532, 2007.

[66] M. H. Dehghan, H. Mirmiranpour, S. Faghihi-Kashani et al., "Inhibitory effect of curcumin on angiogenesis in a streptozotocin-induced diabetic rat model: An aortic ring assay," *Journal of Traditional and Complementary Medicine*, vol. 6, no. 4, pp. 437–441, 2016.

[67] S. Ganjali, A. Sahebkar, E. Mahdipour et al., "Investigation of the effects of curcumin on serum cytokines in obese individuals: a randomized controlled trial," *The Scientific World Journal*, vol. 2014, Article ID 898361, 6 pages, 2014.

[68] M. Bayet-Robert, F. Kwiatowski, M. Leheurteur et al., "Phase I dose escalation trial of docetaxel plus curcumin in patients with advanced and metastatic breast cancer," *Cancer Biology & Therapy*, vol. 9, no. 1, pp. 8–14, 2010.

[69] N. Pradhan, R. Guha, S. Chowdhury, S. Nandi, A. Konar, and S. Hazra, "Curcumin nanoparticles inhibit corneal neovascularization," *Journal of Molecular Medicine*, vol. 93, no. 10, pp. 1095–1106, 2015.

[70] L. Li, B. Ahmed, K. Mehta, and R. Kurzrock, "Liposomal curcumin with and without oxaliplatin: effects on cell growth, apoptosis, and angiogenesis in colorectal cancer," *Molecular Cancer Therapeutics*, vol. 6, no. 4, pp. 1276–1282, 2007.

[71] B. Xiong, T.-J. Sun, H.-Y. Yuan, M.-B. Hu, W.-D. Hu, and F.-L. Cheng, "Cyclooxygenase-2 expression and angiogenesis in colorectal cancer," *World Journal of Gastroenterology*, vol. 9, no. 6, pp. 1237–1240, 2003.

[72] W. Dempke, C. Rie, A. Grothey, and H.-J. Schmoll, "Cyclooxygenase-2: a novel target for cancer chemotherapy?" *Journal of Cancer Research and Clinical Oncology*, vol. 127, no. 7, pp. 411–417, 2001.

[73] A. Akbarzadeh Baghban, N. Taghavi, and M. Shahla, "Combined analysis of vascular endothelial growth factor expression with cyclooxygenase-2 and mast cell density in oral squamous cell carcinoma," *Pathobiology*, vol. 84, no. 2, pp. 80–86, 2017.

[74] P. Yoysungnoen, P. Wirachwong, P. Bhattarakosol, H. Niimi, and S. Patumraj, "Effects of curcumin on tumor angiogenesis and biomarkers, COX-2 and VEGF, in hepatocellular carcinoma cell-implanted nude mice," *Clinical Hemorheology and Microcirculation*, vol. 34, no. 1-2, pp. 109–115, 2006.

[75] D. G. Binion, M. F. Otterson, and P. Rafiee, "Curcumin inhibits VEGF-mediated angiogenesis in human intestinal microvascular endothelial cells through COX-2 and MAPK inhibition," *Gut*, vol. 57, no. 11, pp. 1509–1517, 2008.

[76] G. P. Nagaraju, S. Zhu, J. E. Ko et al., "Antiangiogenic effects of a novel synthetic curcumin analogue in pancreatic cancer," *Cancer Letters*, vol. 357, no. 2, pp. 557–565, 2015.

[77] J. L. Arbiser, M. A. Moses, C. A. Fernandez et al., "Oncogenic H-ras stimulates tumor angiogenesis by two distinct pathways," *Proceedings of the National Acadamy of Sciences of the United States of America*, vol. 94, no. 3, pp. 861–866, 1997.

[78] S. Shankar, Q. Chen, K. Sarva, I. Siddiqui, and R. K. Srivastava, "Curcumin enhances the apoptosis-inducing potential of TRAIL in prostate cancer cells: Molecular mechanisms of apoptosis, migration and angiogenesis," *Journal of Molecular Signaling*, vol. 2, p. 10, 2007.

[79] S. Shankar, S. Ganapathy, Q. Chen, and R. K. Srivastava, "Curcumin sensitizes TRAIL-resistant xenografts: molecular mechanisms of apoptosis, metastasis and angiogenesis," *Molecular Cancer*, vol. 7, article 16, 2008.

[80] Y. G. Lin, A. B. Kunnumakkara, A. Nair, W. M. Merritt, L. Y. Han et al., "Curcumin inhibits tumor growth and angiogenesis in ovarian carcinoma by targeting the nuclear factor-kappaB pathway," *Clinical Cancer Research*, vol. 13, no. 11, pp. 3423–3430, 2007.

[81] J. Liu, P. Zhu, P. Song et al., "Pretreatment of adipose derived stem cells with curcumin facilitates myocardial recovery via antiapoptosis and angiogenesis," *Stem Cells International*, vol. 2015, Article ID 638153, 12 pages, 2015.

[82] A. V. Sharma, K. Ganguly, S. Paul, N. Maulik, and S. Swarnakar, "Curcumin heals indomethacin-induced gastric ulceration by stimulation of angiogenesis and restitution of collagen fibers via vegf and mmp-2 mediated signaling," *Antioxidants & Redox Signaling*, vol. 16, no. 4, pp. 351–362, 2012.

[83] J. You, J. Sun, T. Ma et al., "Curcumin induces therapeutic angiogenesis in a diabetic mouse hindlimb ischemia model via modulating the function of endothelial progenitor cells," *Stem Cell Research & Therapy*, vol. 8, no. 1, p. 182, 2017.

[84] G. Emiroglu, Z. Ozergin Coskun, Y. Kalkan et al., "The effects of curcumin on wound healing in a rat model of nasal mucosal trauma," *Evidence-Based Complementary and Alternative Medicine*, vol. 2017, Article ID 9452392, 6 pages, 2017.

[85] G. S. Sidhu, H. Mani, J. P. Gaddipati et al., "Curcumin enhances wound healing in streptozotocin induced diabetic rats and genetically diabetic mice," *Wound Repair and Regeneration*, vol. 7, no. 5, pp. 362–374, 1999.

[86] H. Sorg, D. J. Tilkorn, S. Hager, J. Hauser, and U. Mirastschijski, "Skin wound healing: an update on the current knowledge and concepts," *European Surgical Research*, vol. 58, no. 1-2, pp. 81–94, 2017.

[87] A. Shah and S. Amini-Nik, "The Role of Phytochemicals in the Inflammatory Phase of Wound Healing," *International Journal of Molecular Sciences*, vol. 18, no. 5, p. 1068, 2017.

[88] R. L. Thangapazham, A. Sharma, and R. K. Maheshwari, "Beneficial role of curcumin in skin diseases," *Advances in Experimental Medicine and Biology*, vol. 595, pp. 343–357, 2007.

[89] V. Kant, A. Gopal, D. Kumar et al., "Curcumin-induced angiogenesis hastens wound healing in diabetic rats," *Journal of Surgical Research*, vol. 193, no. 2, pp. 978–988, 2015.

[90] G. S. Sidhu, A. K. Singh, D. Thaloor et al., "Enhancement of wound healing by curcumin in animals," *Wound Repair and Regeneration*, vol. 6, no. 2, pp. 167–177, 1998.

[91] A. Partoazar, N. Kianvash, M. H. Darvishi, S. Nasoohi, S. M. Rezayat, and A. Bahador, "Ethosomal curcumin promoted wound healing and reduced bacterial flora in second degree burn in rat," *Drug Research*, vol. 66, no. 12, pp. 660–665, 2016.

[92] G. Dharunya, N. Duraipandy, R. Lakra, P. S. Korapatti, R. Jayavel, and M. S. Kiran, "Curcumin cross-linked collagen aerogels with controlled anti-proteolytic and pro-angiogenic efficacy," *Biomedical Materials*, vol. 11, no. 4, Article ID 045011, 2016.

[93] L. A. Araújo, R. G. Araújo, and F. O. Gomes, "Physicochemical/photophysical characterization and angiogenic properties of Curcuma longa essential oil," *Anais da Academia Brasileira de Ciências*, vol. 88, supplement 3, pp. 1889–1897, 2016.

[94] M. S. Kiran, V. B. Sameer Kumar, R. I. Viji, G. T. Sherin, K. N. Rajasekharan, and P. R. Sudhakaran, "Opposing effects of curcuminoids on serum stimulated and unstimulated angiogenic response," *Journal of Cellular Physiology*, vol. 215, no. 1, pp. 251–264, 2008.

[95] S. Fan, Y. Xu, X. Li, L. Tie, Y. Pan, and X. Li, "Opposite angiogenic outcome of curcumin against ischemia and Lewis lung cancer models: in silico, in vitro and in vivo studies," *Biochimica et Biophysica Acta (BBA) - Molecular Basis of Disease*, vol. 1842, no. 9, pp. 1742–1754, 2014.

[96] D. Thaloor, K. J. Miller, J. Gephart, P. O. Mitchell, and G. K. Pavlath, "Systemic administration of the NF-κB inhibitor curcumin stimulates muscle regeneration after traumatic injury," *American Journal of Physiology-Cell Physiology*, vol. 277, no. 2, pp. C320–C329, 1999.

[97] Y. Xu, J. Zhang, J. Han et al., "Curcumin inhibits tumor proliferation induced by neutrophil elastase through the upregulation of alpha1-antitrypsin in lung cancer," *Molecular Oncology*, vol. 6, no. 4, pp. 405–417, 2012.

[98] D. Thaloor, A. K. Singh, G. S. Sidhu, P. V. Prasad, H. K. Kleinman, and R. K. Maheshwari, "Inhibition of angiogenic differentiation of human umbilical vein endothelial cells by curcumin," *Cell Growth & Differentiation*, vol. 9, no. 4, pp. 305–312, 1998.

[99] D. Chendil, R. S. Ranga, D. Meigooni, S. Sathishkumar, and M. M. Ahmed, "Curcumin confers radiosensitizing effect in prostate cancer cell line PC-3," *Oncogene*, vol. 23, no. 8, pp. 1599–1607, 2004.

[100] A. B. Kunnumakkara, P. Diagaradjane, S. Guha et al., "Curcumin sensitizes human colorectal cancer xenografts in nude mice to γ-radiation by targeting nuclear factor-κB-regulated gene products," *Clinical Cancer Research*, vol. 14, no. 7, pp. 2128–2136, 2008.

[101] A. Kunwar, H. Narang, K. I. Priyadarsini, M. Krishna, R. Pandey, and K. Sainis, "Delayed activation of PKCδ and NFκB and higher radioprotection in splenic lymphocytes by copper (II)–Curcumin (1:1) complex as compared to curcumin," *Journal of Cellular Biochemistry*, vol. 102, no. 5, pp. 1214–1224, 2007.

[102] V. P. Menon and A. R. Sudheer, "Antioxidant and anti-inflammatory properties of curcumin," *Adv Exp Med Biol*, vol. 595, pp. 105–125, 2007.

[103] S. K. Sandur, H. Ichikawa, M. K. Pandey et al., "Role of pro-oxidants and antioxidants in the anti-inflammatory and apoptotic effects of curcumin (diferuloylmethane)," *Free Radical Biology & Medicine*, vol. 43, no. 4, pp. 568–580, 2007.

[104] G. Galati, O. Sabzevari, J. X. Wilson, and P. J. O'Brien, "Prooxidant activity and cellular effects of the phenoxyl radicals of dietary flavonoids and other polyphenolics," *Toxicology*, vol. 177, no. 1, pp. 91–104, 2002.

[105] A. Mohr and J. Mott, "Overview of microRNA biology," *Seminars in Liver Disease*, vol. 35, no. 01, pp. 003–011, 2015.

[106] S. Zhang, D. Tang, W. Zang et al., "Synergistic inhibitory effect of traditional Chinese medicine astragaloside IV and curcumin on tumor growth and angiogenesis in an orthotopic nude-mouse model of human hepatocellular carcinoma," *Anticancer Reseach*, vol. 37, no. 2, pp. 465–474, 2017.

[107] R. Moradi-Marjaneh, S. M. Hassanian, F. Rahmani, S. H. Aghaee-Bakhtiari, A. Avan, and M. Khazaei, "Phytosomal curcumin elicits anti-tumor properties through suppression of angiogenesis, cell proliferation and induction of oxidative stress in colorectal cancer," *Current Pharmaceutical Design*, vol. 24, no. 39, pp. 4626–4638, 2019.

[108] J. Zhang, Q. Wang, G. Rao, J. Qiu, and R. He, "Curcumin improves perfusion recovery in experimental peripheral arterial disease by upregulating microRNA-93 expression," *Experimental and Therapeutic Medicine*, vol. 17, no. 1, pp. 798–802, 2019.

Hindawi
Evidence-Based Complementary and Alternative Medicine
Volume 2019, Article ID 3648685, 10 pages
https://doi.org/10.1155/2019/3648685

Research Article

An Ancient Chinese Herbal Decoction Containing Angelicae Sinensis Radix, Astragali Radix, Jujuba Fructus, and Zingiberis Rhizoma Recens Stimulates the Browning Conversion of White Adipocyte in Cultured 3T3-L1 Cells

Guowei Gong,[1] Guangyi Han,[2] Huan He,[1] Tina T. X. Dong,[3,4] Karl W. K. Tsim,[3,4] and Yuzhong Zheng[5]

[1]*Department of Bioengineering, Zunyi Medical University, Zhuhai Campus, Zhuhai, Guangdong, 519041, China*
[2]*Gansu Institute for Drug Control, Lanzhou, Gansu, 730070, China*
[3]*Shenzhen Key Laboratory of Edible and Medicinal Bioresources, SRI, The Hong Kong University of Science and Technology, Shenzhen, 518057, China*
[4]*Division of Life Science, Center for Chinese Medicine, The Hong Kong University of Science and Technology, Clear Water Bay, Hong Kong*
[5]*Department of Biology, Hanshan Normal University, Chaozhou, Guangdong 521041, China*

Correspondence should be addressed to Karl W. K. Tsim; botsim@ust.hk and Yuzhong Zheng; zhengyuzhong@gmail.com

Received 6 March 2019; Revised 29 May 2019; Accepted 4 June 2019; Published 16 June 2019

Guest Editor: Chongshan Dai

Background. Abnormal storage of white adipocyte tissue (WAT) is the major factor causing obesity. The promising strategies for obesity treatment are building up the brown adipocyte tissue (BAT) and/or expedite fatty acid catabolism. Traditional Chinese Medicine (TCM) sheds light on preventing obesity. Ginger is one of the most effective herbs for antiobesity by accelerating browning WAT. To fortify the antiobesity effect of ginger, an ancient Chinese herbal decoction composed of four herbs, Angelicae Sinensis Radix (ASR), Astragali Radix (AR), Jujuba Fructus (JF), and Zingiberis Rhizoma Recens (ZRR; ginger), was tested here: this herbal formula was written in AD 1155, named as Danggui Buxue Tang (DBT_{1155}). Therefore, the antiobesity function of this ancient herbal decoction was revealed *in vitro* by cultured 3T3-L1 cells. *Materials and Method*. The lipid accumulation was detected by Oil Red O staining. Furthermore, the underlying working mechanisms of antiobesity functions of DBT_{1155} were confirmed in 3T3-L1 cells by confocal microscopy, western blot, and RT-PCR. *Results*. DBT_{1155} was able to actuate brown fat-specific gene activations, which included (i) expression of PPARγ, UCP1, and PCG1α and (ii) fatty acid oxidation genes, i.e., CPT1A and HSL. The increase of browning WAT, triggered by DBT_{1155}, was possibly mediated by a Ca^{2+}-AMPK signaling pathway, because the application of Ca^{2+} chelator, BAMPTA-AM, reversed the effect. *Conclusion*. These findings suggested that the herbal mixture DBT_{1155} could potentiate the antiobesity functions of ginger, which might have potential therapeutic implications.

1. Introduction

Obesity is characterized as abnormal or excessive accumulated adipose tissues, which is believed to be induced by multiple factors, including genetically and environmentally. Obesity incidence is increasing and becomes a normal phenomenon in both developing and developed countries, posting a great challenging for health care professionals. The obese persons could undergo high risks of metabolic abnormalities, diabetes, and several types of cancers diseases [1, 2]. Antiobesity therapeutic treatments have been proposed for decades. The limitation of carbohydrate intake used to be believed as the most effective strategy for antiobesity; however, this treatment has been reported to have negative impact on mental development [3, 4]. On the other hand, the side effects of popular weight loss synthetic medicines,

e.g., phentermine-topiramate and lorcaserin, are commonly ameliorating the risks of hepatorenal syndrome and resulting in reducing the patient's life quality [5].

There are two types of adipose tissues found within human body, i.e., white adipose tissues (WAT) and brown adipose tissues (BAT). The major functions of WAT are heating insulation, buffering mechanical cushion, and, finally, storing of energy. WAT is acting as fuel for energy imbalances when the intaking energy is smaller than outputting energy; therefore, WAT is considered as a crucial component in contributing obesity [6]. BAT, on the other hand, accelerates energy expenditure and finally combats obesity [7, 8]. Physical exercise is one of typical routines to lose weight and reshape the body by hastening WAT browning and stimulating fatty acid oxidation [9]. The high expression level of mitochondrial uncoupling protein 1 (UCP1) is a hallmark of browning WAT [9]. Furthermore, peroxisome proliferator-activated receptor (PPARγ) and peroxisome proliferator-activated receptor-gamma coactivator 1 (PGC1α) are two transcriptional factors in modulating adipogenous-related gene expressions, which are highly expressed in BAT [10]. On the other hand, carnitine palmitoyl transferase I A (CPT1A) and hormone-sensitive lipase (HSL) genes can enhance mitochondrial activities and stimulate fatty acid oxidation, and therefore they are classified as the signature of fatty acid oxidation [11].

There is an increasing consumption of functional foods or food supplements aiming to control weight. Traditional Chinese Medicine (TCM) has drawn attention in the market; because it has a peculiar and organized understanding of obesity according to its specific concept. The major determinant eliciting obesity is the imbalance of "Yin" and "Yang," which results in stagnation of "Qi" and "Blood" [12]. Most of synthetic medicines alter the interaction of neurological and/or hormonal signals in acting as appetite suppressants or as inducers of diarrhea, which could be damaging to psychology and physiology of our bodies [13]. Zingiberis Rhizoma Recens (ZRR, root of *Zingiber officinale* Roscoe; ginger) is one of the most popular spices utilized in the world, and its antiobesity function has been widely reported [14]. The intake of ginger extract or curcumin, one of bioactive constituents found within ginger, significantly reduced body weight, leptin, insulin, amylase, lipase plasma, and tissue lipids in rats. In parallel, the level of peroxisomal catalase in serum was enhanced in ginger- and curcumin-treated rats [15–18]. ZRR was able to activate AMPK pathway, the key signaling in modulating WAT browning [19]. On the other way, oral administration of ZRR in human could reduce hunger sensation [15]. In TCM formulation, ginger is being included commonly in many herbal formulae, and indeed the therapeutic functions of these herbal formulae are believed to enhance thermogenesis, as such to reduce obesity.

An ancient herbal mixture, written by *Chen Suan* of Song Dynasty (1155 AD) in *"Chensuan Fuke Buji"*, is known to improve "Qi" and "Blood," named as Danggui Buxue Tang (DBT_{1155}). DBT_{1155} composes four herbs: Angelicae Sinensis Radix (ASR), Astragali Radix (AR), Jujuba Fructus (JF), and Zingiberis Rhizoma Recens (ZRR) in a weight ratio of 36: 30: 15: 20. The antiobesity functions of curcumin-enriched ZRR were widely reported, and this herbal formula was shown to have antilipid accumulation in our preliminary study. Thus, the antiobesity functions of DBT_{1155} in cultured 3T3-L1 adipocytes were tested here.

2. Materials and Methods

2.1. Preparation of Herbal Extract. The raw herbs of root of *Astragali membranaceus* var. *mongholicus* (AR), root of *Angelica sinensis* (Oliv) Diels. (ASR), fruit of *Ziziphus jujuba* cv. Jinsixiaozao (JF), and rhizome of *Zingiber officinale* Roscoe (ZRR; ginger) were collected and identified in 2013. The voucher specimen of AR, ASR, JF, and ZRR was kept in Centre for Chinese Medicine of HKUST. AR, ASR, JF, and ZRR in a weight ratio of 36: 30: 15: 20 were used to prepare DBT_{1155} decoction. The mixture was boiled in 8 volumes of water for twice. Fifty grams of ZRR was also boiled in water twice, each with 8 volumes of water. This preparation was verified in previous studies [20, 21]. All samples were dried by lyophilization and resuspended in water at final concentration of 100 mg/mL, which were kept at −80°C.

2.2. HPLC Analysis and Chemical Quantifications. Chemical standardization and quantification of herbal mixture are the first step in performing biological assay [20, 22, 23]. According to China Pharmacopeia, ferulic acid was chosen as marker chemical in ASR. Calycosin and formononetin were selected as quantification markers in AR; cyclic AMP (cAMP) was reported to be the bioactive chemical found within JF; and 6-gingerol was elite as standard for ZRR (CP, 2015). The HPLC mobile phases were composed of 0.1% formic acid in water (A) and 0.1% formic acid in acetonitrile (B), respectively. An elution gradient was set up as follows: 0-2 min isocratic gradient 95% (A); 2-4 min, linear gradient 95-90% (A); 4-15 min, linear gradient 90-80% (A); 15-20 min, isocratic gradient 80% (A); 20-27 min, linear gradient 80%-70% (A); and 17-70 min, linear gradient 70-45% (A). The preequilibration period of 15 min was used between each run. The column temperature was set to 25°C. The injection volume was 10 μL. A wavelength of 254 nm was employed for detection. The flow rate was set at 1.0 mL/min. Agilent RRLC 1200 series system (Waldron, Germany) equipped with a degasser, a binary pump, an auto-sampler, a diode array detector (DAD), and a thermo-stated column compartment was adopted for establishment of fingerprint for herbal extracts. The HPLC condition was conducted on Agilent ZORBAX SB-Aq (4.6 × 250 mm, 5 μm) C18 column.

2.3. Cell Cultures. Mouse 3T3-L1 fibroblast cells (CL-173) were obtained from ATCC (Manassas, VA) and maintained at 37°C in a water-saturated incubator containing 5% CO_2 and in DMEM supplemented with 4.5 g/L glucose, 10% FBS, 100 U/mL penicillin, and 100 μg/mL streptomycin. Induction of lipogenic differentiation was detailed in a previous study [24]. Briefly, cultured cells were treated with dexamethasone (1 μM, Sigma-Aldrich, St Louis, MO), insulin (1.8 μM, Sigma-Aldrich), and dibutryl-cAMP (300 μM, Sigma-Aldrich) for 72 hours to induce lipogenesis. The cultures were set as day 0 and replaced with the culture medium containing insulin

(1.8 μM) for every two days. At day 10, about 80% of cultures were induced to contain triglyceride. Treatments including negative control (0.02% DMSO only), cocktail (1.8 μM of rosiglitazone and triiodothyronine), low concentration of DBT (DBT-L, 0.125 mg/mL), and high concentration of DBT (DBT-H, 1.0 mg/mL) were given to differentiated cultures (on day 10) for 72 hours. Unless described otherwise, all the culture reagents were purchased from Invitrogen Technologies (Waltham, MA).

2.4. Cell Viability. The cell viability was measured by MTT assay. In brief, cells were cultured in 96-well plate. After drug treatments for indicated durations, MTT solution was added into the cultures in the final concentration of 0.5 mg/mL; after incubation for 2 hours, the production of purple crystal was dissolved by DMSO solvent. The absorbance at 570 nm was measured.

2.5. Oil Red O Staining. Oil Red O at 0.2% in isopropanol was filtered. Experimental cultured cells were washed with PBS, fixed by paraformaldehyde (4% in PBS, Sigma-Aldrich) for 5 min, incubated with Oil Red O staining for 30 min, and washed twice with PBS. The stained triglyceride (TG) was resolved in isopropanol and measured at the absorbance of 490 nm [24].

2.6. Laser Confocal Fluorescence Microscopy. Fluorimetric measurements were performed on cultured 3T3 cells using an Olympus Fluoview FV1000 laser scanning confocal system (Olympus America, Manassas, VA) mounted on an inverted Olympus microscope, equipped with a 10X objective. Intracellular Ca^{2+} concentration was detected by fluorescent calcium indicator Fluo-4 AM (Sigma-Aldrich). Cultured cells were seeded on the glass coverslips and incubated for 30 min at 37°C in a normal physiological solution containing Ca^{2+}-free normal physiological solution containing 5 μM Fluo-4 AM. A23187 (Sigma-Aldrich), a calcium ionophore, was used as a positive control. The amount of Ca^{2+} was evaluated by measuring the fluorescence intensity exiting at 488 nm and emitted at 525 nm.

2.7. Western Blot Assay. The protein expressions of PPARγ, PGC1α, UCP1, and internal control GAPDH were revealed by western blot. Cultures were seeded onto 6-well plate. After drug treatment for 72 hours, including inhibitor application, the cultures were harvested in high salt lysis buffer (1 M NaCl, 10 mM HEPES, pH 7.5, 1 mM EDTA, 0.5% Triton X-100), followed by centrifugation at 16,100 rpm for 10 min at 4°C. Samples with equal amount of total protein were added with 2X lysis buffer (0.125 M HCl, pH 6.8, 4% SDS, 20% glycerol, 2% 2-mercaptoethanol and 0.02% bromophenol blue) and heated to 95°C, and the protein was subjected to SDS-PAGE analysis. After transferring, the membranes were incubated with antibodies against PPARγ, PGC1α, UCP1, and GAPDH (CST, Danvers, MA) at 1: 3,000 dilutions at cold room overnight.

The phosphorylation of AMPK was also determined by western blot assay. Differentiated cultures were serum-starved for 3 hours before the drug application. After treatment with BAMPTA-AM (10 μM) or WZ4003 (100 nM; Selleck, Munich, Germany), the cultures were collected immediately in lysis buffer (125 mM Tris–HCl, 2% SDS, 10% glycerol, 200 mM 2-mercaptoethanol, pH 6.8). The protein was subjected to SDS-PAGE analysis. After transferring the proteins to membranes, the membranes were incubated with anti-phospho-AMPK (Cell Signaling, MA) at 1: 5,000 dilution and anti-total-AMPK (Cell Signaling) at 1: 5,000 dilution at 4°C for 12 hours. Following incubation in horseradish peroxidase- (HRP-) conjugated anti-rabbit secondary antibodies in 1: 5,000 dilution for 3 hours at room temperature, the immune-complexes were visualized by the enhanced chemiluminescence (ECL) method (Amersham Biosciences, Piscataway, NJ). The band intensities in the control and agonist-stimulated samples, run on the same gel and under strictly standardized ECL conditions, were compared on an image analyzer, using in each case a calibration plot constructed from a parallel gel with serial dilutions of one of the samples.

2.8. RT-PCR Analysis. Total RNA was extracted from 3T3-L1 adipocyte cells with RNAzol reagent (Invitrogen) according to manufacturer's instructions. RNA samples with OD260/OD280 ratio higher than 2.0 were employed for PCR. One μg of total RNA was employed for the production of cDNA, using a PCR system. The oligonucleotide primer sequence was as follows: peroxisome proliferator-activated receptor (PPARγ): 5′-CCA GAG TCT GCT GAT CTG CG-3′ and 5′-GCC ACC TCT TTG CTC TGA TC-3′; peroxisome proliferator-activated receptor γ coactivator 1 (PGC1α): 5′-GAC CTG GAA ACT CGT CTC CA-3 and 5′-AAA CTT GCT AGC GGT CCT CA-3′; carnitine palmitoyl transferase I A (CPT1A): 5′-GGA CAT TAT CAC CTT GTT TGG C-3′ and 5′-GGA GCA ACA CCT ATT CAT T-3′; hormone-sensitive lipase (HSL): 5′-GCG CTG GAG GAG TGT TTT T-3′ and 5′-CGC TCT CCA GTT GAA CCA AG-3′; mitochondrial uncoupling protein 1 (UCP1): 5′-GAT GGT GAA CCC GAC AAC TT-3′ and 5′-CTG AAA CTC CGG CTG AGA AG- 3′; 18S: 5′-GTA ACC CGT TGA ACC CCA TT-3′ and 5′-CCA TCC AAT CGG TAG TAG CG-3′. Transcript levels were quantified by using $_{\Delta}$Ct value method, where the values of target genes were normalized by 18S in the same sample at first before comparison. PCR products were analyzed by gel electrophoresis and melting curve analysis, as to confirm the specific amplification.

2.9. Statistical Analysis and Other Assays. Protein concentrations were measured by Bradford's method (Herculues, CA). Statistical tests have been done by using one-way analysis of variance. Data were analyzed by t-test and expressed as Mean ± SEM. Statistically significant changes were classified as significant ($*$) where $p < 0.05$, more significant ($**$) where $p < 0.01$, and highly significant ($***$) where $p < 0.001$ as compared with control group.

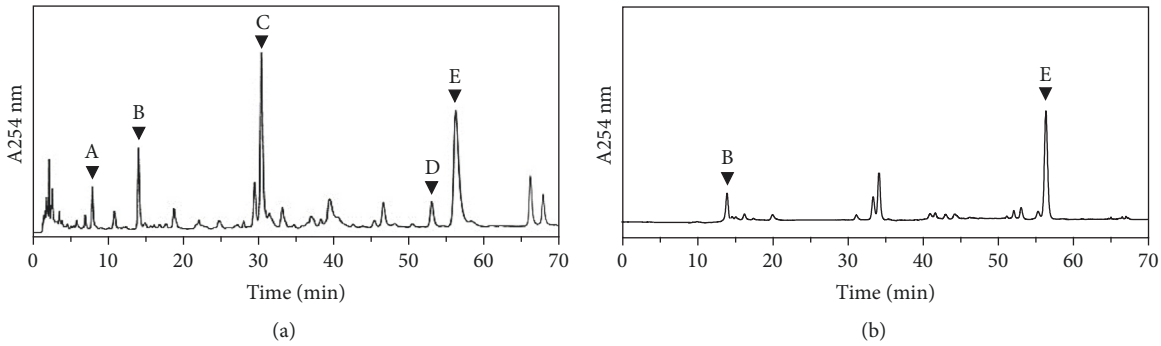

Figure 1: *Typical chromatograms of DBT$_{1155}$ and ZRR extracts*. Ten μL of 100 mg/mL of DBT$_{1155}$ decoction (a) and 100 mg/mL of ZRR extract (b) were subjected to HPLC-DAD analysis, and the chemical fingerprints were revealed at the wavelength 254 nm. The identification of ferulic acid (A), cAMP (B), calycosin (C), formononetin (D), and 6-gingerol (E) were labeled here. Representative chromatograms were shown, n = 3.

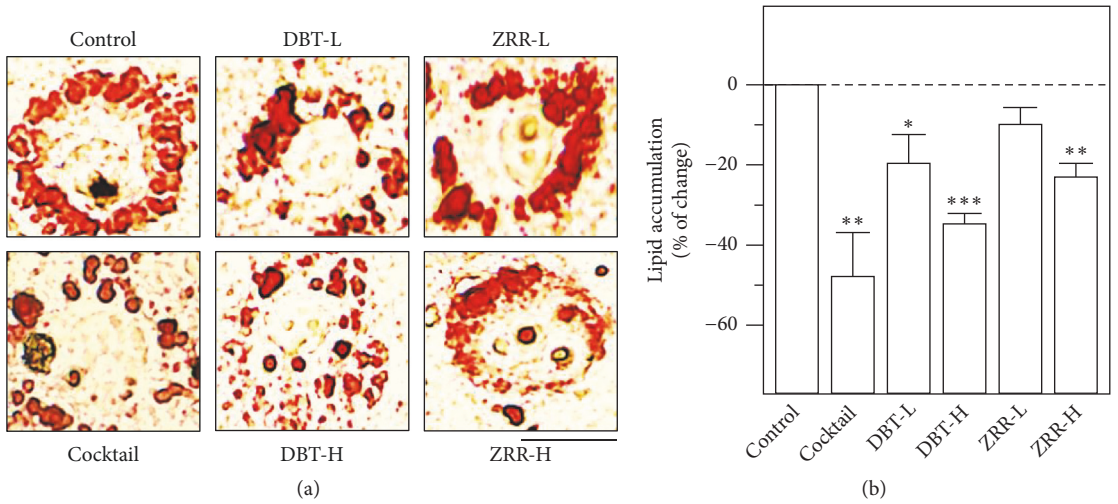

Figure 2: *DBT$_{1155}$ decreases lipid accumulation*. 3T3-L1 adipocytes were cultured to 10 days of differentiation and then applied with cocktail (1.8 μM of rosiglitazone and triiodothyronine), or different concentrations of DBT$_{1155}$ (1 mg/mL of DBT labeled as DBT-H; 0.125 mg/mL of DBT labeled as DBT-L) or ZRR (1 mg/mL of ZRR labeled as ZRR-H; 0.125 mg/mL of ZRR labeled as ZRR-L) for another 3 days. (a) Oil Red O staining was to measure lipid accumulation. Bar = 50 μm. (b) The amount of stained lipid was quantified at 490 nm absorbance. Data were expressed as mean ± SEM of the percentage of change as compared with control, where n = 3; $p < 0.05$ (∗); $p < 0.01$ (∗∗); $p < 0.001$ (∗ ∗ ∗).

3. Results

3.1. Chemical Standardization of DBT$_{1155}$. Chemical standardization is to ensure the repeatability of herbal extract in all subsequent biochemical analyses. The amounts of major components were calibrated by a calibration curve derived from HPLC, which was obtained from a series of dilutions of the chemical markers. The calibration curve of ferulic acid was y=21.134x+19.607; calycosin was y=10.189x-10.129; formononetin was y=13.602x+12.705; cAMP was y=11.218x+55.42; and 6-gingerol was y=17.311x+25.1328 (Supplementary Table 1). In quality control of herbal mixture, 1 g of dried DBT$_{1155}$ powder was proposed to contain 572.32 μg of calycosin, 205.66 μg of formononetin, 150.02 μg of ferulic acid, 102.35 μg of cAMP, and 1296.8 μg of 6-gingerol. One gram of ZRR dried extract was proposed to contain 34.63 μg of cAMP and 1203.24 μg of 6-gingerol. These chemical requirements set the minimal standards. In addition, HPLC fingerprint was developed for the standardized extracts at 254 nm wavelength (Figure 1). These chemical parameters were employed as quality control to ensure the repeatability of biochemical assays.

3.2. Browning WAT Functions. The functions of DBT$_{1155}$ and ZRR on lipid accumulation of cultured 3T3-L1 adipocytes were detected by Oil Red O. The optimized working concentration of DBT was determined by MTT assay; the highest working concentration of DBT$_{1155}$ should be 1 mg/mL, which was labeled as DBT-H. The lowest concentration should be 0.125 mg/mL which was named as DBT-L (Supplementary Figure 1). The lipid accumulation was significantly decreased under application of DBT$_{1155}$ extract, which was in a dose-dependent manner (Figures 2(a) and 2(b)). One mg/mL of DBT decoction (DBT-H) possessed ~35% decrease by

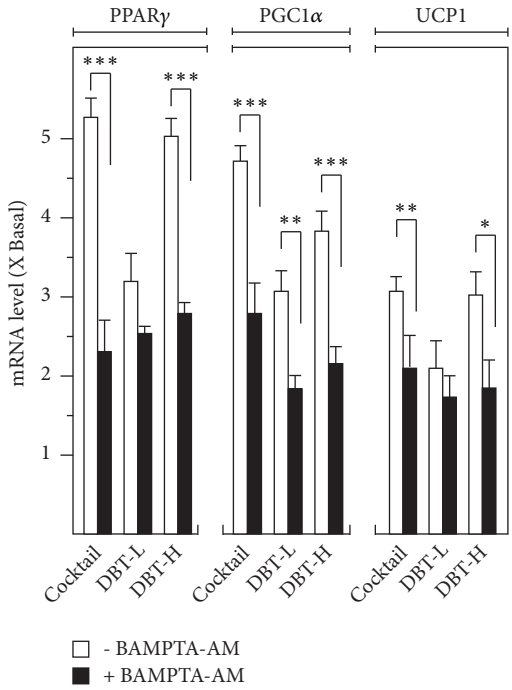

FIGURE 3: *DBT_{1155} triggers browning mRNA expressions of WAT markers*. 3T3-L1 adipocytes were cultured to 10 days of differentiation. Then, the cultures were applied with cocktail or different concentrations of DBT_{1155} (DBT-H: 1 mg/mL of DBT; DBT-L: 0.125 mg/mL) with/without cotreatment of BAMPTA-AM (10 μM) for another 3 days. Total RNAs were isolated and reverse-transcribed to cDNA for PCR analysis. The mRNA levels of PPARγ, PGC1α, and UCP1 were determined by the Ct-value method and normalized by the house keeping gene 18S rRNA. Data were expressed as mean ± SEM as compared with control, setting as 1 here, where $n = 3$; $p < 0.05$ (*); $p < 0.01$ (**); $p < 0.001$ (***).

lipid staining as compared to the negative control (Figures 2(a) and 2(b)). The antilipid accumulation effect, triggered by DBT_{1155}, was much stronger than that of ZRR alone (Figures 2(a) and 2(b)). The lipid staining results implied that other constituents within DBT_{1155} might potentiate antilipid accumulation activity of ZRR. The IC_{50} of DBT_{1155} was ~0.375 mg/mL. In the same assay, the herbal extracts of AR, ASR, and JF did not show significant antilipid effect (Supplementary Figure 2). Here, the cocktail served as a positive control suppressing lipid accumulation dramatically by ~50% decrease, as compared with a negative control (Figures 2(a) and 2(b)).

Increase levels of PPARγ, UCP1, and PCG1α are the hall markers of WAT browning [25]. Indeed, the activations of these genes have been reported in obesity and/or its related diseases [25]. The transcript levels of these BAT-specific genes were revealed by RT-PCR from total RNA deriving from DBT_{1155}-treated 3T3-L1 adipocytes. As shown in Figure 3, DBT_{1155} increased the mRNA levels of BAT markers in a dose-dependent manner. The maximal inductions of PPARγ, PCG1α, and UCP1 were revealed at ~5-fold, ~4-fold, and ~3-fold, respectively, under the application of 1 mg/mL of DBT_{1155}. Furthermore, calcium chelator, BAMPTA-AM, was employed here to identify the signaling pathway. The pretreatment of this chelator in 3T3-L1 adipocytes dramatically suppressed the BAT-specific gene transcription (Figure 3). The protein expression levels of these markers were also taken into consideration. The translational activities of these BAT-specific genes, e.g., PPARγ at ~58 kDa, PCG1α at ~100 kDa, and UCP1 at ~30 kDa, were highly expressed, from 5-to-9-fold under the challenge of 1 mg/mL of DBT_{1155} (Figure 4). On the other hand, the application of BAMPTA-AM significantly abolished the increased protein expression, triggered by this ancient herbal formula (Figure 4). Taken together, DBT_{1155} decoction possessed antiobesity functions by accelerating WAT browning.

AMPK signaling is a key player in regulating browning WAT. Application of DBT_{1155} in cultured 3T3-L1 adipocytes was capable of inducing AMPK phosphorylation, and this activation was in a time-dependent manner (Figure 5(a) right). The maximal stimulation was shown at 2 hours, as compared to control (Figure 5(a) right). Cellular Ca^{2+} level has been reported to be an indispensable factor regulating AMPK activities [26]. Here, the Ca^{2+} concentration in the treated 3T3-L1 adipocytes was detected by confocal microscopy. Fluo-4 AM, a Ca^{2+} indicator, was applied onto the cultures as to monitor the variation of Ca^{2+}-induced fluorescence signal in differentiated 3T3-L1 cells. The increased Ca^{2+} level was found after the treatment in 3T3-L1 adipocytes (Figure 5(a) left). A23187, a calcium ionophore, served as a positive control (Figure 5(a)). In line with the above BAT-specific gene expression results, the pretreatment of BAMPTA-AM markedly suppressed the Ca^{2+} influx and AMPK activation in cultured 3T3-L1 cells (Figure 5(b)). Moreover, the pretreatment with WZ4003, a specific AMPK antagonist, reduced the phosphorylation of AMPK, as shown in Figure 6. Accordingly, these data indicated that DBT_{1155} triggered WAT browning in adipocyte via an AMPK signaling.

3.3. Fatty Acid Catabolism Activities. The key function of fatty acid catabolism is to generate ATP, and thus fat oxidation is a key switch to reveal catabolism progress [11, 27]. CPT1A is recognized in precipitating mitochondrial activities and accelerating fatty acid oxidation [26]. The transcriptional activates of these marker genes were revealed here (Figure 7). Treatment with high dosage of DBT_{1155} (1 mg/mL; DBT-H) led to significant increase of mitochondrial CPT1A mRNA, indicating the accelerated fat oxidation under the challenge of herbal decoction (Figure 7). Synthesis of fatty acid is another key regulator to modulate catabolism [26]. Overexpression of HSL was observed in the DBT_{1155}-treated 3T3-L1 adipocytes. The maximal stimulation of HSL was revealed at ~2-fold, as compared with the control. The upregulation of HSL indicated that DBT_{1155} could have the possibility of suppressing fatty acid synthesis in 3T3-L1 adipocytes (Figure 7). Again, the mRNA levels of CPT1 and HSL in cultured 3T3-L1 adipocytes were downregulated upon pretreatment of BAMPTA-AM. Our data shed light on the antiobesity functions of DBT_{1155} via accelerating fatty acid oxidation and suppressing its synthesis.

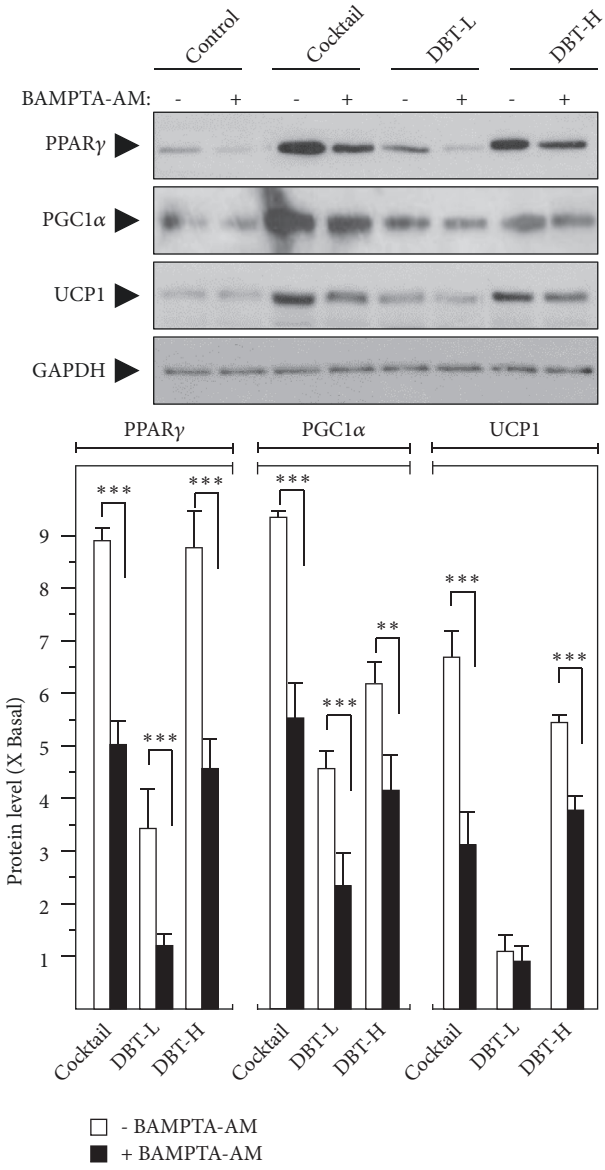

Figure 4: *DBT_{1155} triggers protein levels of browning WAT markers.* 3T3-L1 adipocytes were treated with cocktail or different concentrations of DBT_{1155} (DBT-H: 1 mg/mL of DBT; DBT-L: 0.125 mg/mL) with/without cotreatment of BAMPTA-AM (10 μM) for another 3 days after 10 days of differentiation, as in Figure 2. The translational levels of PPARγ (~58 kDa), PGC1α (~100 kDa), and UCP1 (~30 kDa) were detected by immunoblot analysis by specific antibodies. GAPDH (~38 kDa) served as an internal control. Quantification of target protein expression was calculated by a densitometer (lower panel). Data were expressed as mean ± SEM as compared with control, setting as 1 here, where $n = 3$; $p < 0.05$ (∗); $p < 0.01$ (∗∗); $p < 0.001$ (∗ ∗ ∗).

4. Discussion

During the past decade, people paid attention to the study of weight loss therapy relying on herbal medicine. However, the side-effect of TCM in weight loss is unclear, which is one of the limitations in acceptance of TCM [21, 28]. This is an urgency to search for the safe TCM that could be effective for antiobesity. DBT_{1155} is a classical herbal decoction commonly used for treatment of "Blood" and "Qi" deficiencies. "Blood" in TCM theory is to provide nutrition. "Qi" is to boost antioxidative functions and finally neutralizes "Blood." Indeed, this traditional herbal formula DBT_{1155} is comprised of 4 herbs, and each of them plays their specific responsibilities. AR is well-known for "Qi"-reinforcing, ASR is popular for "Blood-" nourishing, JF is famous for tonifying "Qi" and "Blood," and ZRR is recognized to enhance vital energy as well as improving immune system in TCM theory [28]. DBT_{1155} was shown to upregulate erythropoietic genes *in vitro* and to reverse anemia-index in rats [21]. On the other hand, DBT_{1155} has been utilized for years, and the side effect has been rarely reported. Therefore, this herbal decoction should be safe to be consumed. Furthermore, the current data shed light on inducing brown fat phenotype in cultured 3T3-L1 via elevation of PPARγ, UCP1, and PCG1α in both transcriptional and translational levels.

There are three types of bioactive constituents popular for obesity treatment. The first cluster is polysaccharide isolated from plant, acting as vital role in maintaining body health [28, 29]. In obesity animal models, the polysaccharides showed the possibilities of decreasing TG level via enhancing intestinal peristalsis, upregulating lipid absorption rate, and accelerating the transformation of exogenous cholesterol to bile acids [30]. For example, the total polysaccharide extracted from ginger had dual antiobesity functions by upregulating metabolic rate and inhibiting the absorption rate of calorie-dense dietary fats [31]. The JF-generated polysaccharide was capable of decreasing glycerol-3-phosphate dehydrogenase activity *in vitro* [32]. Flavonoid is the other bioactive group for obesity medication. Flavonoid increased thermogenesis via enhancing fatty acid transportation and reduced the triglyceride content in plasma and finally decreased lipid deposition [33]. In parallel, the *in vivo* working mechanism of flavonoids for losing weight has been well reported [34–36]. The intake of total flavonoids showed a possibility of alleviating obesity-triggered metabolic damage via suppressing inflammation [35]. Formononetin, one of isoflavones extracted from AR, as well as in DBT, was capable of stimulating AMPK pathway *in vitro*, and suppressed the development of obesity by attenuating high fat diet-induced body weight gain and visceral fat accumulation [36]. The last group of nature product for obesity treatment is believed to be polyphenols. Among them, the most famous one is curcumin [37–40]. Pan et al. demonstrated that treatment of male C57BL/6 J obese mice with curcumin significantly decreased body weight and fat mass after 2 months of observation, but enhanced insulin sensitivity in mice [37]. Moreover, oral administration of curcumin-enriched supplementation was effective in suppressing oxidative stress via modulation of antioxidation enzymes activities, i.e., superoxide dismutase (SOD) and glutathione peroxidase (GPx) in obese patients [39, 40]. The constituents of DBT_{1155} decoction, i.e., AR, ASR, and JF, showed synergistic effects to ZRR because the antilipid functions of AR, ASR, and JF were very limited. The cAMP-induced AMPK signaling is the major mechanism for antiobesity [41–44]. The DBT_{1155}-triggered AMPK signaling

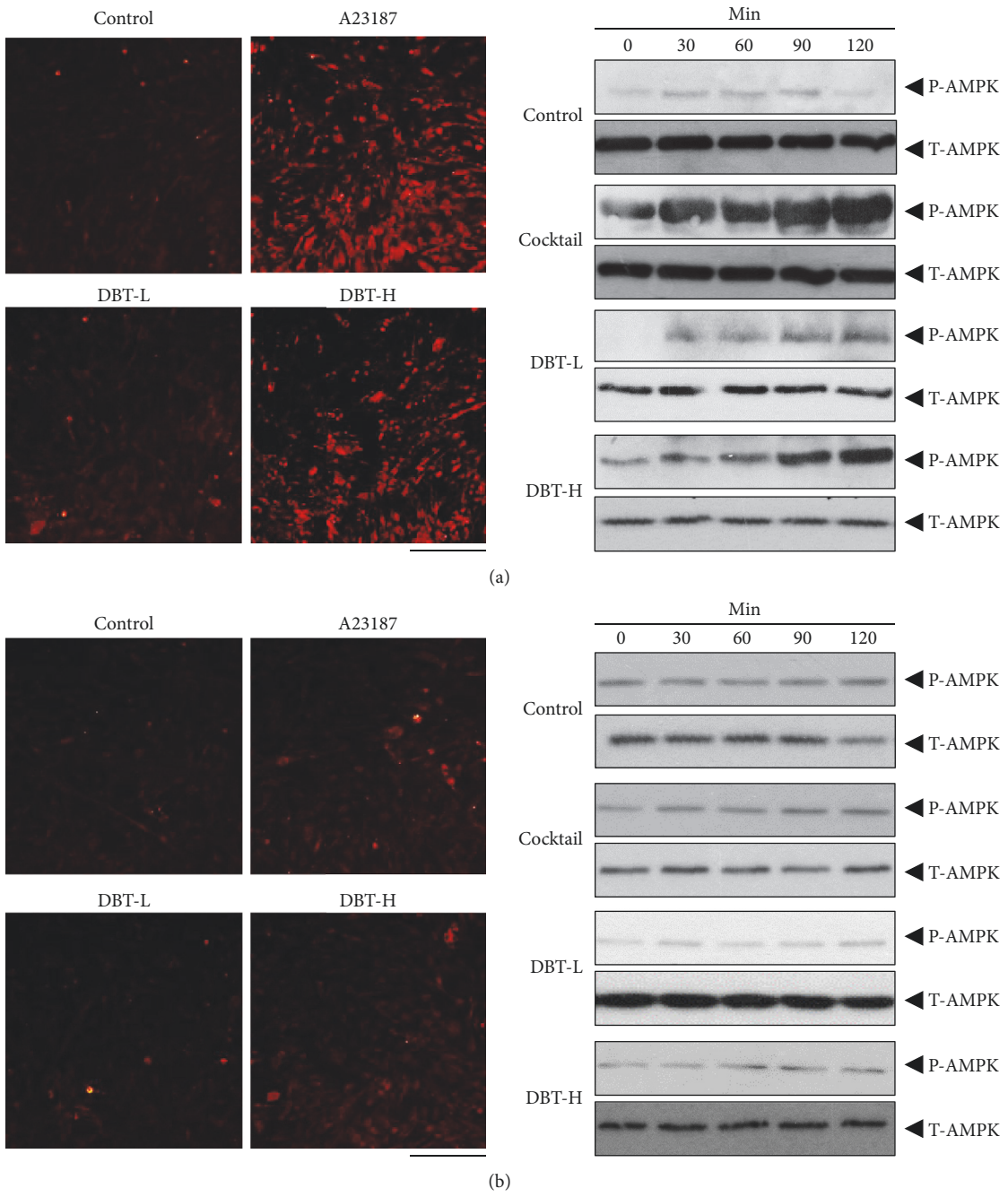

FIGURE 5: *DBT_{1155} stimulates Ca^{2+}-AMPK pathway.* 3T3-L1 adipocytes were pretreated with medium (a) or BAMPTA-AM (10 μM) (b) for 3 hours and then were labeled with fluorescent Ca^{2+} indicator Fluo-4 AM for half an hour. Fluorimetric measurement was performed after the treatment of different concentrations of DBT_{1155} decoctions, as in Figure 2. A23187 (100 nM) served as a control. The amounts of Ca^{2+} were evaluated by measuring the fluorescence intensity (left panel). Micrographs were taken by a confocal microscope; Bar = 100 μm. Differentiated cells were subjected to the phosphorylation assay. Phospho-AMPK (P-AMPK, ~ 60 kDa) and total AMPK (T-AMPK, ~ 60 kDa) were revealed by using specific antibodies (right panel). Representative photos were shown, $n = 4$.

could be significantly suppressed by the Ca^{2+} chelator; hence, the abovementioned data strongly supported that this conventional herbal formula reduced obesity by a Ca^{2+}-AMPK signaling.

Obesity posts a great challenge on body health in a variety of ways, including high blood pressure and cholesterol, cardiovascular diseases, type II diabetes, and musculoskeletal discomfort [44]. The antiobesity functions of DBT_{1155} were never reported and, therefore, we believe this could be a significant breakthrough for further study. The aim here is to reveal TCM formulae that could be used for obesity treatment. Although our *in vitro* data suggest this herbal

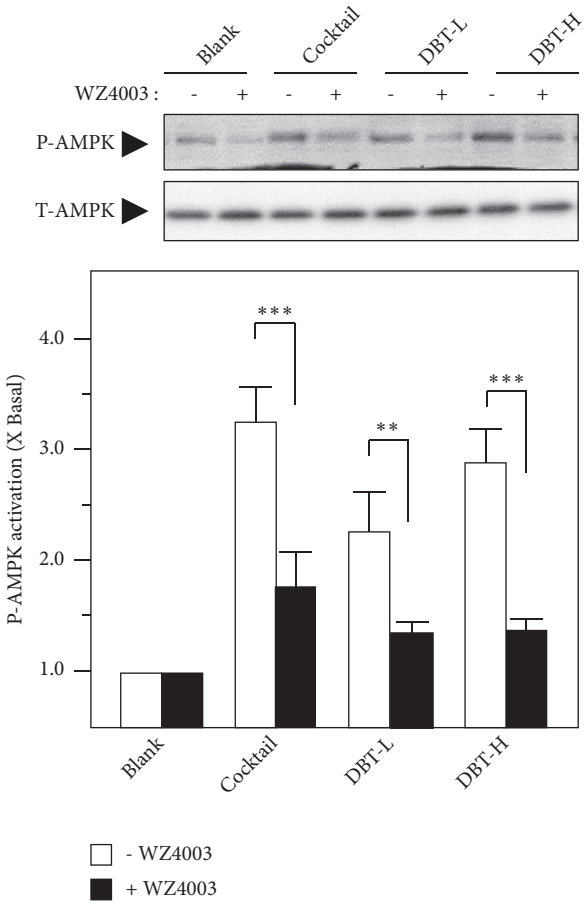

Figure 6: *WZ4003 suppresses AMPK phosphorylation*. 3T3-L1 adipocytes were pretreated with medium or WZ4003 (100 nM) for 3 hours and then subjected to the phosphorylation assay. The treatment of different concentrations of DBT_{1155} decoctions was as in Figure 2. Phospho-AMPK (P-AMPK, ~ 60 kDa) and total AMPK (T-AMPK, ~ 60 kDa) were revealed by using specific antibodies (upper panel). Quantification of protein expression was calculated by a densitometer (lower panel). Data were expressed as mean ± SEM as compared with control, setting as 1 here, where $n = 3$; $p < 0.05$ (∗); $p < 0.01$ (∗∗); $p < 0.001$ (∗ ∗ ∗).

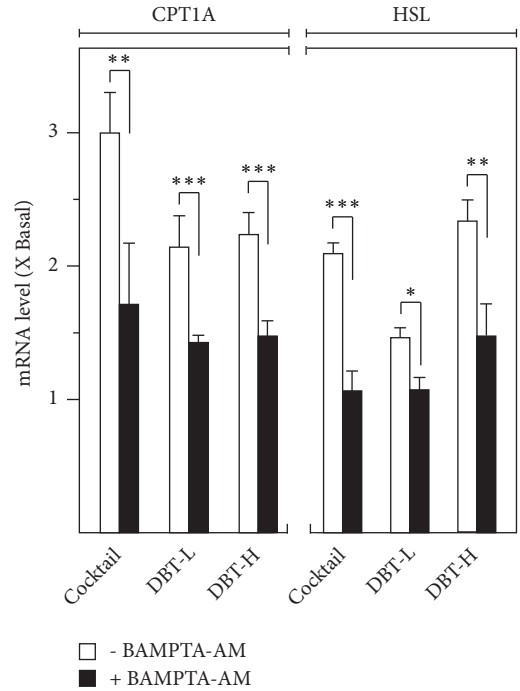

Figure 7: *DBT enhances fatty acid catabolism*. 3T3-L1 adipocytes were cultured for 10 days of differentiation. Then cocktail or different concentrations of DBT_{1155} with/without cotreatment of BAMPTA-AM (10 μM) were applied for another 3 days, as in Figure 2. Total RNAs were isolated and reverse-transcribed to cDNA for PCR analysis. The transcriptional levels of CPT1A and HSL were determined by the Ct-value method and normalized by 18S rRNA. Data were expressed as mean ± SEM as compared with control, setting as 1 here, where $n = 3$; $p < 0.05$ (∗); $p < 0.01$ (∗∗); $p < 0.001$ (∗ ∗ ∗).

formula possesses antiobesity functions via accelerating WAT browning and lipid catabolism, the *in vivo* experiments are indispensable as to further confirm the functions.

Data Availability

The data used to support the findings of this study are included within the article.

Conflicts of Interest

The authors declare that there is no conflict of interests regarding the publication of this paper.

Acknowledgments

This study is supported by Research Fund of Zunyi Medical University for the Doctoral Program (F-937), NNSF of Guangdong (2018A030307074), Science and Technology Planning Project of Guangdong (2014A020221058), China, and Shenzhen Science and Technology Committee Research Grant (ZDSYS201707281432317; JCYJ20180214151016621; JCYJ20170413173747440; JCYJ 20160229205812004; JCYJ20160229210027564; CKFW2016082916015476).

Supplementary Materials

Supplementary Figure 1. Cell viability under the treatment of DBT1155. Supplementary Figure 2. ASR, AR, and JF show insignificant inhibition of lipid accumulation. Supplementary Table 1 Calibration curves, LOD and LOQ in HPLC analysis. *(Supplementary Materials)*

References

[1] D. W. Haslam and W. P. T. James, "Obesity," *The Lancet*, vol. 366, no. 9492, pp. 1197–1209, 2005.

[2] P. Hossain, B. Kawar, and M. El Nahas, "Obesity and diabetes in the developing world—a growing challenge," *The New England Journal of Medicine*, vol. 356, no. 3, pp. 213–215, 2007.

[3] F. Bustamante, V. O. Brunaldi, W. M. Bernardo et al., "Obesity treatment with botulinum toxin-A is not effective: a systematic review and meta-analysis," *Obesity Surgery*, vol. 27, no. 10, pp. 2716–2723, 2017.

[4] K. D. Hoerster, S. Wilson, K. M. Nelson, G. E. Reiber, and R. M. Masheb, "Diet quality is associated with mental health, social support, and neighborhood factors among Veterans," *Eating Behaviors*, vol. 23, pp. 168–173, 2016.

[5] R. Fogari and A. Zoppi, "Effect of antihypertensive agents on quality of life in the elderly," *Drugs & Aging*, vol. 21, no. 6, pp. 377–393, 2004.

[6] Y. Nishimoto and Y. Tamori, "CIDE family-mediated unique lipid droplet morphology in white adipose tissue and brown adipose tissue determines the adipocyte energy metabolism," *Journal of Atherosclerosis and Thrombosis*, vol. 24, no. 10, pp. 989–998, 2017.

[7] A. Guilherme, D. J. Pedersen, E. Henchey et al., "Adipocyte lipid synthesis coupled to neuronal control of thermogenic programming," *Molecular Metabolism*, vol. 6, no. 8, pp. 781–796, 2017.

[8] A. Ghasemi and S. Jeddi, "Anti-obesity and anti-diabetic effects of nitrate and nitrite," *Nitric Oxide: Biology and Chemistry*, vol. 70, pp. 9–24, 2017.

[9] J. Lone, J. H. Choi, S. W. Kim, and J. W. Yun, "Curcumin induces brown fat-like phenotype in 3T3-L1 and primary white adipocytes," *The Journal of Nutritional Biochemistry*, vol. 27, pp. 193–202, 2016.

[10] L. M. Acevedo, A. I. Raya, R. Ríos, E. Aguilera-Tejero, and J.-L. L. Rivero, "Obesity-induced discrepancy between contractile and metabolic phenotypes in slow- and fast-twitch skeletal muscles of female obese Zucker rats," *Journal of Applied Physiology*, vol. 123, no. 1, pp. 249–259, 2017.

[11] M. T. Nakamura, B. E. Yudell, and J. J. Loor, "Regulation of energy metabolism by long-chain fatty acids," *Progress in Lipid Research*, vol. 53, no. 1, pp. 124–144, 2014.

[12] L. Zhang, C. Virgous, and H. Si, "Ginseng and obesity: observations and understanding in cultured cells, animals and humans," *The Journal of Nutritional Biochemistry*, vol. 44, pp. 1–10, 2017.

[13] N. Sun, T. Wu, and C. Chau, "Natural dietary and herbal products in anti-obesity treatment," *Molecules*, vol. 21, no. 10, p. E1351, 2016.

[14] M. S. Mansour, Y.-M. Ni, A. L. Roberts, M. Kelleman, A. Roychoudhury, and M.-P. St-Onge, "Ginger consumption enhances the thermic effect of food and promotes feelings of satiety without affecting metabolic and hormonal parameters in overweight men: a pilot study," *Metabolism - Clinical and Experimental*, vol. 61, no. 10, pp. 1347–1352, 2012.

[15] R. H. Mahmoud and W. A. Elnour, "Comparative evaluation of the efficacy of ginger and orlistat on obesity management, pancreatic lipase and liver peroxisomal catalase enzyme in male albino rats," *European Review for Medical and Pharmacological Sciences*, vol. 17, no. 1, pp. 75–83, 2013.

[16] G. Saravanan, P. Ponmurugan, M. A. Deepa, and B. Senthilkumar, "Anti-obesity action of gingerol: effect on lipid profile, insulin, leptin, amylase and lipase in male obese rats induced by a high-fat diet," *Journal of the Science of Food and Agriculture*, vol. 94, no. 14, pp. 2972–2977, 2014.

[17] V. Ebrahimzadeh Attari, A. Malek Mahdavi, Z. Javadivala, S. Mahluji, S. Zununi Vahed, and A. Ostadrahimi, "A systematic review of the anti-obesity and weight lowering effect of ginger (Zingiber officinale Roscoe) and its mechanisms of action," *Phytotherapy Research*, vol. 32, no. 4, pp. 577–585, 2018.

[18] Y. Zhao and Z.-Y. Chen, "Roles of spicy foods and their bioactive compounds in management of hypercholesterolemia," *Journal of Agricultural and Food Chemistry*, vol. 66, no. 33, pp. 8662–8671, 2018.

[19] M. Lu, Y. Cao, J. Xiao, M. Song, and C. Ho, "Molecular mechanisms of the anti-obesity effect of bioactive ingredients in common spices: a review," *Food & Function*, vol. 9, no. 9, pp. 4569–4581, 2018.

[20] T. T. X. Dong, K. J. Zhao, Q. T. Gao et al., "Chemical and biological assessment of a Chinese herbal decoction containing Radix Astragali and Radix Angelicae Sinensis: determination of drug ratio in having optimized properties," *Journal of Agricultural and Food Chemistry*, vol. 54, no. 7, pp. 2767–2774, 2006.

[21] W. L. Zhang, K. Y.-Z. Zheng, K. Y. Zhu et al., "Chemical and biological assessment of Angelica herbal decoction: comparison of different preparations during historical applications," *Phytomedicine*, vol. 19, no. 11, pp. 1042–1048, 2012.

[22] A. G. Gong, N. Li, K. Lau et al., "Calycosin orchestrates the functions of Danggui Buxue Tang, a Chinese herbal decoction composing of Astragali Radix and Angelica Sinensis Radix: an evaluation by using calycosin-knock out herbal extract," *Journal of Ethnopharmacology*, vol. 168, pp. 150–157, 2015.

[23] C. T. Lam, P. H. Chan, P. S. Lee et al., "Chemical and biological assessment of Jujube (Ziziphus jujuba)-containing herbal decoctions: induction of erythropoietin expression in cultures," *Journal of Chromatography B*, vol. 1026, pp. 254–262, 2016.

[24] A. J. Guo, R. C. Choi, A. W. Cheung et al., "Stimulation of Apolipoprotein A-IV expression in Caco-2/TC7 enterocytes and reduction of triglyceride formation in 3T3-L1 adipocytes by potential anti-obesity Chinese herbal medicines," *Chinese Medicine*, vol. 4, no. 1, p. 5, 2009.

[25] T. C. Bargut, V. Souza-Mello, M. B. Aguila, and C. A. Mandarim-de-Lacerda, "Browning of white adipose tissue: lessons from experimental models," *Hormone Molecular Biology and Clinical Investigation*, vol. 31, no. 1, 2017.

[26] P. Walle, M. Takkunen, V. Männistö et al., "Alterations in fatty acid metabolism in response to obesity surgery combined with dietary counseling," *Nutrition & Diabetes*, vol. 7, no. 9, p. e285, 2017.

[27] S. Kim, S. Cheong, A. Chou, and R. Gonzalez, "Engineered fatty acid catabolism for fuel and chemical production," *Current Opinion in Biotechnology*, vol. 42, pp. 206–215, 2016.

[28] W.-L. Zhang, L. Zhu, and J.-G. Jiang, "Active ingredients from natural botanicals in the treatment of obesity," *Obesity Reviews*, vol. 15, no. 12, pp. 957–967, 2014.

[29] A. J. Silvester, K. R. Aseer, and J. W. Yun, "Dietary polyphenols and their roles in fat browning," *The Journal of Nutritional Biochemistry*, vol. 64, pp. 1–12, 2019.

[30] A. J. Akinyemi, G. R. Thomé, V. M. Morsch et al., "Effect of ginger and turmeric rhizomes on inflammatory cytokines levels and enzyme activities of cholinergic and purinergic systems in hypertensive rats," *Planta Medica*, vol. 82, no. 7, pp. 612–620, 2016.

[31] N. Ning and J. J. Han, "Advances in studies on active components of reducing blood lipid in traditional Chinese medicine," *Asia-Pacific Traditional Medicine*, vol. 9, pp. 76–79, 2013.

[32] G. A. Mohamed, S. R. Ibrahim, E. S. Elkhayat, and R. S. El Dine, "Natural anti-obesity agents," *Bulletin of Faculty of Pharmacy, Cairo University*, vol. 52, no. 2, pp. 269–284, 2014.

[33] H. Kubota, R. Morii, A. Kojima-Yuasa, X. Huang, Y. Yano, and I. Matsui-Yuasa, "Effect of *Zizyphus jujuba* extract on the inhibition of adipogenesis in 3T3-L1 preadipocytes," *American Journal of Chinese Medicine*, vol. 37, no. 3, pp. 597–608, 2009.

[34] X. L. Zhong, J. L. Ding, and D. S. Luo, "Progress on blood lipid regulating active ingredients from traditional Chinese medicine," *Food Drug*, vol. 11, pp. 449–451, 2010.

[35] M. Zhang, C. P. Zhu, C. L. Shi, J. X. Xiao, and S. H. Zhang, "Extraction, isolation of Lycium barbarum polysaccharide-4 and its role in weight loss obesity mice on female hypothalamus injury," *Nutrition and Health*, vol. 24, pp. 114–117, 2003.

[36] R. L. C. Hoo, J. Y. L. Wong, C. F. Qiao, A. Xu, H. X. Xu, and K. S. L. Lam, "The effective fraction isolated from Radix Astragali alleviates glucose intolerance, insulin resistance and hypertriglyceridemia in db/db diabetic mice through its anti-inflammatory activity," *Journal of Nutrition and Metabolism*, vol. 7, 2010.

[37] Y. Pan, D. Zhao, N. Yu et al., "Curcumin improves glycolipid metabolism through regulating peroxisome proliferator activated receptor γ signalling pathway in high-fat diet-induced obese mice and 3T3-L1 adipocytes," *Royal Society Open Science*, vol. 4, no. 11, p. 170917, 2017.

[38] T. Jin, Z. Song, J. Weng, and I. G. Fantus, "Curcumin and other dietary polyphenols: potential mechanisms of metabolic actions and therapy for diabetes and obesity," *American Journal of Physiology-Endocrinology and Metabolism*, vol. 314, no. 3, pp. E201–E205, 2018.

[39] A. Shehzad, M. Qureshi, M. N. Anwar, and Y. S. Lee, "Multi-functional curcumin mediate multitherapeutic effects," *Journal of Food Science*, vol. 82, no. 9, pp. 2006–2015, 2017.

[40] Y. Zhao, B. Chen, J. Shen et al., "The beneficial effects of quercetin, curcumin, and resveratrol in obesity," *Oxidative Medicine and Cellular Longevity*, vol. 2017, Article ID 1459497, 8 pages, 2017.

[41] J. Gautam, V. Khedgikar, P. Kushwaha et al., "Formononetin, an isoflavone, activates AMP-activated protein kinase β-catenin signalling to inhibit adipogenesis and rescues C57BL/6 mice from high-fat diet-induced obesity and bone loss," *British Journal of Nutrition*, vol. 117, no. 5, pp. 645–661, 2017.

[42] O. H. Kang, S. B. Kim, Y. S. Seo et al., "Curcumin decreases oleic acid-induced lipid accumulation via AMPK phosphorylation in hepatocarcinoma cells," *European Review for Medical and Pharmacological Sciences*, vol. 17, no. 19, pp. 2578–2586, 2013.

[43] S. Lv, X. Qiu, J. Li et al., "Glucagon-induced extracellular cAMP regulates hepatic lipid metabolism," *Journal of Endocrinology*, vol. 234, no. 2, pp. 73–87, 2017.

[44] N. Lv, K. M. J. Azar, L. G. Rosas, S. Wulfovich, L. Xiao, and J. Ma, "Behavioral lifestyle interventions for moderate and severe obesity: a systematic review," *Preventive Medicine*, vol. 100, pp. 180–193, 2017.

Hindawi
Evidence-Based Complementary and Alternative Medicine
Volume 2019, Article ID 9689325, 10 pages
https://doi.org/10.1155/2019/9689325

Research Article

Cynomorium songaricum Extract Alleviates Memory Impairment through Increasing CREB/BDNF via Suppression of p38MAPK/ERK Pathway in Ovariectomized Rats

Fang-ze Tian,[1] **Hong-sheng Chang**,[2] **Jian-xun Liu**,[3] **Junchao Zheng**,[2] **Dan Cheng**,[2] **and Yi Lu**[2]

[1]*Graduate School, Beijing University of Chinese Medicine, Beijing 100029, China*
[2]*School of Preclinical Medicine, Beijing University of Chinese Medicines, Beijing, China*
[3]*Xiyuan Hospital, China Academy of Chinese Medical Sciences, Haidian District, Beijing, China*

Correspondence should be addressed to Yi Lu; luyi@bucm.edu.cn

Received 5 March 2019; Revised 14 April 2019; Accepted 5 May 2019; Published 23 May 2019

Guest Editor: Keyu Zhang

Cynomorium songaricum Rupr is a very important traditional Chinese medicine for tonifying the kidney, which has a significant effect on improving estrogen level on the long term. In many studies, it can improve the learning and memory function of ovariectomized (OVX) model animals. 10 of the 50 rats received only bilateral back surgery and were harvested with the same amount of fat as the ovaries without removing the ovaries as sham group; remains underwent bilateral ovariectomy and equally randomized into five groups: sham group, with OVX as model group, estradiol valerate (EV, 0.2 mg/kg) as positive control, with 3.3 and 33 mg/kg body weight/day of ethyl acetate extract of *Cynomorium songaricum* extract (CSE) as low and high dosage groups, respectively. The orally administered CSE to ovariectomized rats exerted an ameliorative effect on learning and memory in the Morris water maze tests. All rats were sacrificed after 8 weeks of treatment, and tissue was analyzed using histopathology and electron microscopy. To comprehensively examine the mechanism, brain derived neurotrophic factor (BDNF), p-p38 mitogen-activated protein kinase (p-p38MAPK), extracellular regulated protein kinases (ERK), p-extracellular regulated protein kinases (p-ERK), and p-cAMP-response element binding protein (p-CREB) were detected by Western blotting. Using histopathology and electron microscopy, it was clearly observed that the pyramidal neurons of the hippocampal CA1 area were reduced in the OVX groups, indicating that CSE could attenuate the loss of pyramidal neurons in hippocampal CA1 and revert the synaptic morphological variations produced by ovariectomy. Mechanistically, the expressions of p-p38MAPK and p-ERK levels were significantly downregulated by CSE intervention, whereas the BDNF and p-CREB were significantly upregulated by CSE as compared to the control. Concisely, *Cynomorium songaricum Rupr* exhibited potential therapeutic effect on Neuroprotection of ovariectomized rats, and its effect was possibly exerted by p-CREB/BDNF mediated down regulation of ERK/p38MAPK.

1. Introduction

Clinical studies have demonstrated that estrogen can protect neurons [1]. Thus, estrogen treatment could be used to attenuate the prevalence of Alzheimer's disease (AD) and ameliorate learning and memory deficits [2, 3]. The cognitive dysfunction due to natural or surgical menopause is linked to the deficiency of the hormone estrogen. In general, experimental studies assessing the influence of estrogen on cognition are performed using ovariectomized (OVX) rats or mice. Menopausal hormone therapy, also called hormone replacement therapy (HRT), has been found to be effective in protecting against memory and learning dysfunction due to estrogen deficiency [4, 5]. However, currently used estrogenic treatments have several undesired effects, such as breast cancer and cardiac disorders [6, 7]. These findings argue for the need for further studies to explore new estrogenic treatments. Complementary and alternative medicines are recognized to have fewer undesired effects as well as promising therapeutic effectiveness against many chronic diseases, such as cognitive dysfunction.

Some laboratory discovered that phosphorylation of the extracellular signal-regulated kinase (ERK) was necessary for estradiol (E2) to enhance object recognition memory in ovariectomized female mice [8, 9]. They have since extended this finding to object placement (spatial memory) as well [10–13]. These findings demonstrated that the memory-enhancing effects of E2 depended on phosphorylation (i.e., activation) of a cell-signaling kinase. There is some precedence for sex differences in the mechanisms through which E2 regulates hippocampal function. In a study of neonatal rat hippocampal cultures, E2 interacted with mGluRs to increase ERK-dependent phosphorylation of cAMP response element binding (CREB) protein in females, but this phenomenon did not occur in males [14]. E2 enhances the memory consolidation of adult women as an important cause of mGluR activation [9], but E2 does not stimulate ERK-dependent CREB activation in male neonates, suggesting that E2-induced ERK activation is a gender difference. Subsequent studies have shown that E2 can increase the acetylation of the specific promoter H3 of the BDNF gene within 30 min. [12], a neurotrophin that is essential for hippocampal memory formation [15–17].

Cynomorium is an important tonic Chinese medicine. This herb is extensively distributed in Asian hilly areas, especially in China and Mongolia. *Cynomorium songaricum* is useful against symptoms of aging, ranging from mild forms of memory impairment to dementia, regulating endocrinopathy, and improving sexual function [11, 18, 19]. Moreover, pharmacological studies have revealed that various ingredients obtained from this herb have a number of activities, such as anti-HCV protease [20], antiapoptosis, anticancer [21], antiprostatic hyperplasia [22], and fertility-promoting, actions [23–25]. *Cynomorium songaricum* contains various active constituents including flavonoid, organic acids, and polysaccharides (Figure 1) [26–28], making it an important antimemory impairment herbal medicine in China.

Cynomorium songaricum extract (CSE) improves learning and memory *in vitro*, as studied through the water maze test method [20]; however, *in vivo* confirmation of this activity has not yet been confirmed. Thus, the present study was carried out to investigate the influence of CSE on spatial recognition memory in ovariectomized rats.

2. Materials and Methods

2.1. Animals. Fifty female rats were obtained from the Experimental Animal Center, The Academy of Military Medical Sciences (SD) (Certificate number: SCXK [jun] 2007-004). Their weight ranged between 180 and 200 g. Rats were housed in a room at a relative humidity of approximately 55%, 22°C temperature, and 12 h light/dark cycles. This study was approved by the University Ethical Committee on Research Practice at Beijing University of Chinese Medicines and performed in accordance with approved standards of laboratory animal care and use in experiments.

2.2. Ovariectomy. Fourty rats were ovariectomized under anesthesia induced by intraperitoneal injection of 7% chloral hydrate (250 mg/kg). For ovarian excision, approximately 5 cm incisions were made bilaterally in the dorsal-ventral region from the most posterior point of the rib cage. After the ovaries were excised, ovarian blood vessels were ligated by sterile thread. Sham-operated rats remove equal amounts of adipose tissue around the ovary. Following surgery, the rats were allowed to rest for 3 days. Water was given ad libitum. After ovariectomy, rat vaginal smears were detected by Wright's staining. If the vaginal cell smear loses its periodic changes, the white blood cells mainly last for more than 5 days, indicating that the estrogen level of the rat is decreased and entering the estrus interval.

2.3. Animal Treatment. Fourty rats were ovariectomized; six rats were assigned to sham-operation and maintained for 8 weeks. Rats were assigned to five experimental groups randomly with six animals for each group: the sham-operated (sham), ovariectomized (OVX, model), OVX + estradiol valerate (EV) treatment group, OVX + 3.3 CSE treatment group, and 33 CSE treatment group. The CSE and EV groups were treated intragastrically with CSE (33 mg/kg, 3.3mg/kg) and EV (0.2 mg/kg, Bayer, Germany) for 8 consecutive weeks starting on the third day after surgery, while rats in the sham and model groups were treated with distilled water only.

2.4. Preparation of Cynomorium songaricum Extract. *Cynomorium songaricum* Rupr was procured from the Anguo Chinese herbs market in Hebei province, People's Republic of China, authenticated as the fleshy stems by Professor Chun-Sheng Liu in Beijing University of Chinese Medicine, and the specimen was placed in university herbarium with voucher number CSE 601003042. For the preparation of CSE extract, the dried stems were crushed into small pieces and extracted using 20 kg powder with 8 volumes of 70% ethanol three times (each time for 1.5 h), followed by extraction with petroleum ether and ethyl acetate. CSE was dried at 60°C and stored at room temperature.

2.5. Morris Water Maze Test. The Morris water maze (MWM) test was used to assess spatial learning and memory of the rats. The test was conducted on day 7 after the start of drug administration. The MWM pool with a diameter of 120 cm was filled with water (22-25°C) and divided into four quadrants. An unseen platform was placed in the middle of the marked quadrant 1.5-2.0 cm under the surface of water. MWM consisted of two phases, the directional navigation period and the spatial probe test. In the former, all rats were given training 3 times per day for 4 days. First, rats were placed in platform-free quadrants. The trial ended when the rat reached the platform or after a maximum of one minute. If the rats reached the platform in less than one minute, that time was considered the escape latency. The escape latency was considered sixty seconds if the mouse could not find the platform within one minute. Then, the spatial probe test was carried out. For this test the platform was removed and the rat was permitted to swim for sixty seconds. The distance in the target area was determined. The Top View Animal Behavior Analyzing System (developed by the Institute of Materia Medica Chinese Academy of Medical Sciences, Beijing, China) was utilized to record and analyze data.

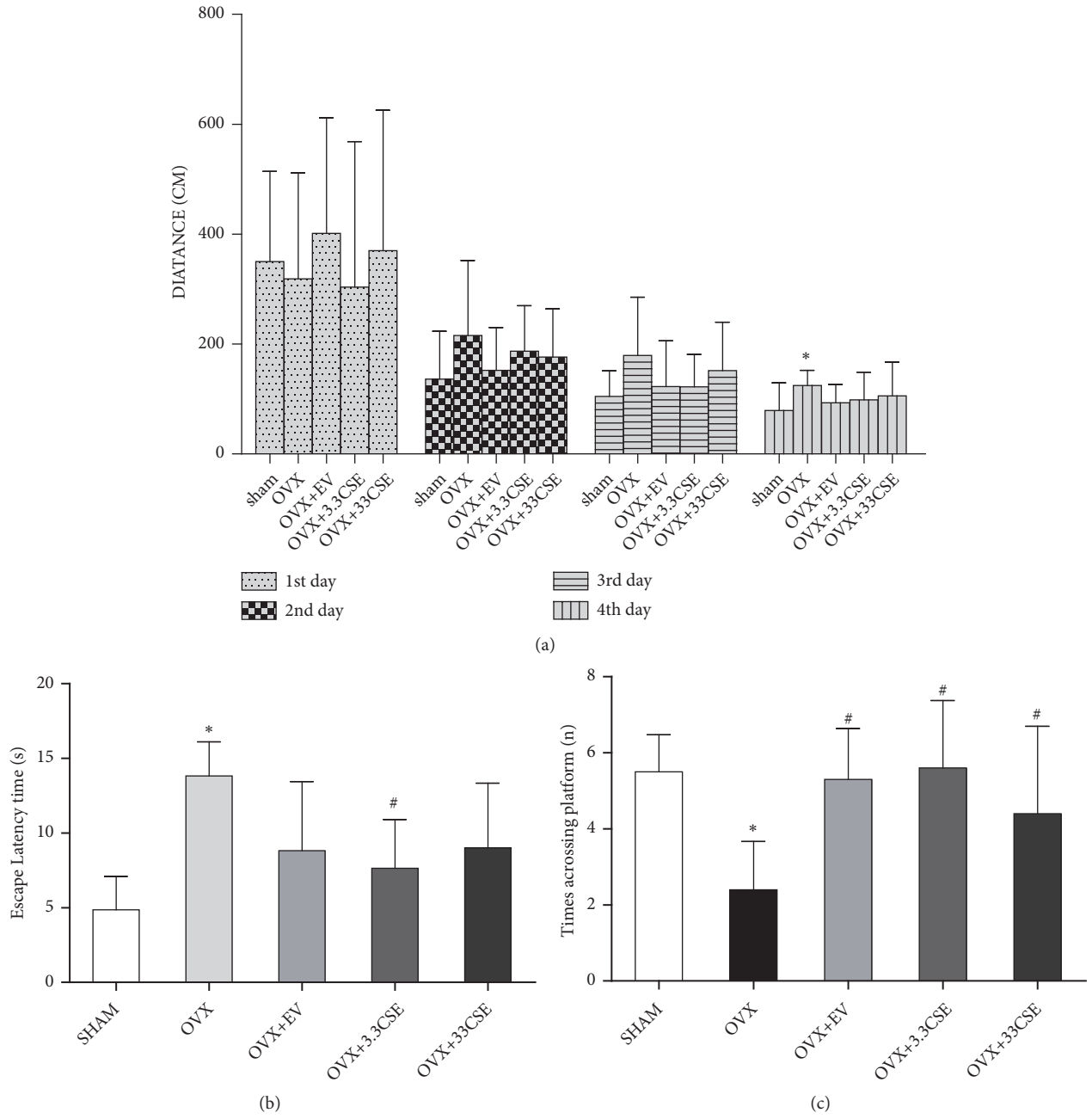

Figure 1: Effect of CSE on recognition memory in Morris water maze test. (a) The graph represents the escape latent distance in period of directional navigation of different groups. (b)-(c) Graph describes the escape latency and the times across platform in space probe test. Data were expressed as means ± SD (n = 10). $^{*}P < 0.05$ vs. sham group, $^{\#}P<0.05$ vs. OVX group.

2.6. Morphometric Analysis. For morphometric analysis (Williams and Carter, 2009), 6 randomly selected rats from each group were anesthetized with 7% chloral hydrate and perfused with PBS (phosphate buffer saline, 0.1 M, 4°C) and then with 4% paraformaldehyde through the ascending aorta until stiffening of the tail and limbs. Subsequently, the brains were removed and divided into two parts: one part was stored in 4% paraformaldehyde for 7 days and sliced into coronal sections of 4 μm thickness for hematoxylin and eosin (HE) staining, while the other part was used for fixing with 2.5% glutaraldehyde for electron microscopy.

2.7. Cell Culture. Neuro-2a cells were procured from the Cell Center, Peking Union Medical College. The culturing of these cells was carried out in 10 cm cell culture plates. The initial density was set at 5×10^4 cells/ml. Containing 10% bovine serum albumin was used to culture the cells. The cells were used 36 h or 48 h after cell passage.

2.8. Cell Viability Analysis (CCK-8 Assay). The cell viability (Studler et al., 1982) was assessed using a CCK-8 Cell Counting Kit-8. After treating cells with sequential concentrations of CSE (100 mg/L) for 22 h, 200 μM H_2O_2 was added

to each well for 2 h. Finally, the absorption at 450 nm was measured by a microplate reader (Thermo Labsystems, Helsinki, Finland).

2.9. Western Blot

2.9.1. Animals. After the MWM test, three rats from each group were sacrificed for Western blot analysis to collect the hippocampal tissue. The tissue was homogenized in RIPA lysis buffer (1:5, w/v). Protein quantification was performed using a BCA protein assay kit. Accurately weighed 27 μg of protein was used for electrophoresis. The proteins were transferred to polyvinylidene fluoride (PVDF) membranes, which were blocked with 5% fat-free milk powder in TBST buffer for a duration of one hour at room temperature, followed by incubation with primary antibody: p-p38 mitogen-activated protein kinase (1:1000), extracellular signal-regulated kinases (ERK) (1:1,000), brain-derived neurotrophic factor (BDNF) (1:2,000), p-cAMP-response element binding protein (p-CREB) (1:1,000), and p-extracellular regulated protein kinase (p-ERK) (1:2,000), acquired from Abcam, USA, for 12 h at 4°C. Subsequently, incubation of HRP-labeled goat anti-rabbit IgG (Jackson 111-035-003, 1:10,000) with the membrane was conducted for 60 minutes at room temperature. Finally, the visualization and scanning of the blots were carried out utilizing enhanced chemiluminescence (ECL) Western blot detection (Millipore WBKLS0500).

2.9.2. Cells. Neuro-2a cells were washed with ice-cold PBS three times and harvested by adding ice-cold cell lysis buffer supplemented with PMSF. The protein was quantified using a BCA protein assay kit. Then, 40 μg of protein was added to an 8% SDS-PAGE gel and transferred onto PVDF membranes. The primary antibodies p-p38 (1:1000), PSD95 (1:2000), and actin (1:2500), acquired from Abcam, USA, were incubated at 4°C overnight. The secondary antibody was incubated for 90 minutes. The bands were visualized using an ECL system (C600, Azure, USA).

Neuro-2a cells were treated with 100 mg / L CSE or 100 mg / L SB203580 for 22 hours each; 200 μM H_2O_2 was added and then incubated for 2 hours. Then, the cells were lysed, and Western blot analysis was carried out using antibodies PSD95 and p-p38 to detect the effect of CSE.

3. Results

3.1. Effect of CSE on Spatial Recognition Memory. To evaluate cognitive function, spatial learning, and memory abilities, the MWM test was performed (Figure 1). The OVX rats did not differ from the sham group in terms of escape latency to find the platform on days 1-2 of training (directional navigation period). However, the latency distance to find the platform on days 3-5 of training was longer in OVX rats than in sham groups. Compared with OVX rats, the EV and CSE rats had a significantly lower escape latency distance ($P < 0.05$) in the navigation test.

Additional analyses were conducted to determine the escape latency and traversing time after the platform was removed from the maze (Figures 1(b) and 1(c)). After 4 days of treatment, compared with OVX rats, the CSE rats had decreased escape latencies and spent significantly more time traversing the position of the virtual platform ($P < 0.05$). These results suggest that there was obvious impairment of cognitive function and spatial learning and memory ability in the ovariectomized rats.

3.2. Morphological Changes of Hippocampus Tissues

3.2.1. HE Staining. Histological changes in the neurons of the hippocampal CA1 region were obtained by HE staining in all groups (Figure 2). In the sham group, no histopathological abnormalities were observed (Figure 2(a)). However, most neurons in the CA1 region in the OVX group (Figure 2(b)) appeared to have triangulated pycnotic nuclei. Moreover, the image showed that the number of neurons was not affected in the sham group but decreased in the OVX group, while CSE treatment (Figures 2(d) and 2(e)) significantly increased the number of necrotic neurons.

3.2.2. Transmission Electron Microscopy (TEM). Under TEM, the pyramidal neurons of the hippocampal CA1 area in the sham group exhibited a clear nuclear membrane, evident nucleolus, rich organelles, and complete synaptic structure (Figure 3). The rats in the OVX group showed distorted nuclei with partial disappearance of decreased presynaptic vesicles and nuclear membrane damage (Figure 3(b)). After 8 weeks of treatment with CSE, there was a similarity in neural cells and synaptic structure of the CSE and sham groups (Figures 3(d) and 3(e)).

3.3. Effect of CES on the Protein Expressions of BDNF, p-p38, and p-CREB, ERK, and p-ERK in the Hippocampus. The results showed that CSE significantly ($^{\#\#}P < 0.01$) increased the expression of p-CREB and BDNF in the hippocampus of OVX rats and significantly ($^{\#\#}P < 0.01$) decreased the expression of p-p38 and p-ERK ($^{\#\#}P < 0.01$) (Figure 4).

3.4. CSE Attenuated Cell Loss Induced by H_2O_2 in Cultured Neuro-2a Cells. CSE was found to have protective effect against H_2O_2-induced damage of Neuro-2a cells, revealing the likely role of CSE against cognitive impairment (Figure 5).

3.5. p-p38 Pathway Was Involved in the Protection Effects of CSE. The results (Figure 6) showed that CSE had a protective effect against H_2O_2 damaged Neuro-2a cells, an improved expression of PSD95 compared with H_2O_2 group, and decreased expression of p-p38, indicating the alleviated cognition.

4. Discussion

The effects of estrogen on learning and memory are mainly dependent on the hippocampus and related nervous systems [29, 30]. Estrogen deficiency can cause a series of brain pathological changes such as memory, synaptic plasticity and neuronal morphology [31]. Estrogen replacement therapy can alleviate cognitive deficits caused by decreased estrogen after menopause, but this therapy does not produce the expected

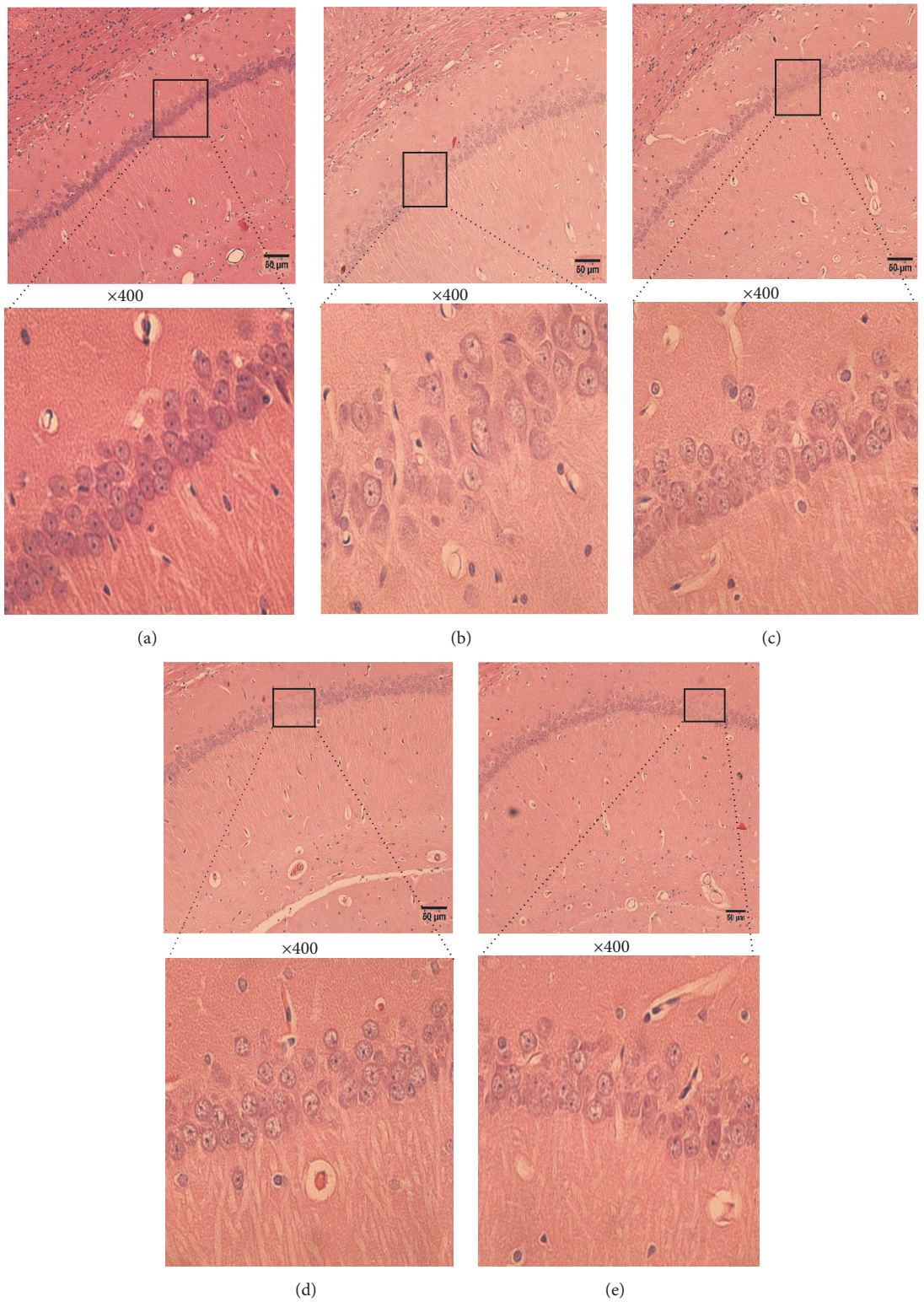

Figure 2: HE stains of hippocampal CA1 of brain after 8 w of OVX. (a) Sham group; (b) OVX group; (c) 0.2 mg/kg EV; (d) 3.3 mg/kg CSE. (e) 33 mg/kg CSE 100, 400× magnification. Scale bar: 50 μm.

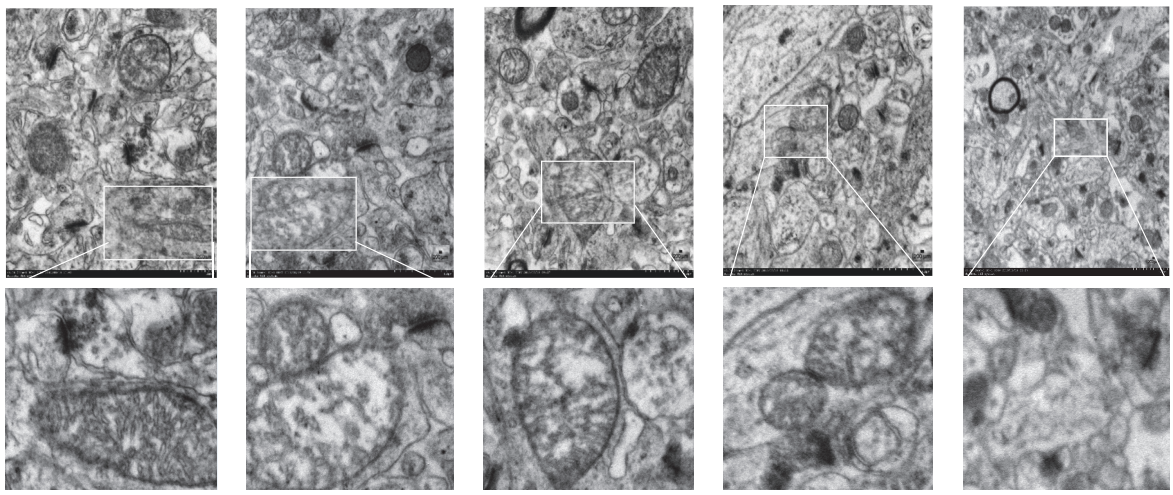

Figure 3: TEM of hippocampal CA1 of brain after 8 w of OVX. (a) Sham group; (b) OVX group; (c) 0.2 mg/kg EV; (d) 3.3 mg/kg CSE. (e) 33 mg/kg CSE, 6000×magnification. Scale bar: 200 μm.

results in reversing memory loss in older women. For example, treatment with conjugated equine estrogens does not maintain or improve cognitive function in postmenopausal women over age 65, and in fact it can be detrimental to cognitive function in this population [32, 33]. In addition, hormone replacement therapy has a small risk of developing breast cancer, heart disease, and stroke but is statistically significant [34, 35]. Traditional Chinese medicines (TCM), such as CSE, provide a new approach to treat or prevent cognitive decline and related diseases.

Interestingly, the biochemical mechanisms underlying the memory-enhancing effects of E2 may differ between the sexes [36]. The ability of E2 to enhance object recognition and object placement memory consolidation in women depends on phosphorylation of ERK in the dorsal hippocampus [8, 10]. For example, in hippocampal cultures from neonatal rats, E2 interacts with mGluRs to increase ERK-dependent phosphorylation of cAMP response element binding (CREB) protein in females, but not in males [14].

Previous studies in our laboratory have shown that CSE has a good antioxidant effect [36] against SK-N-SH and PC12 cell injury triggered by hypoxanthine/xanthine oxidase (HPX/XO) or Aβ25-35t [37, 38]. More importantly, it proves that CSE has an estrogen-like effect. CSE plays a role of estrogen-like compounds and improved learning and memory through the MAPK pathway by combining with GPR30 [39]. In the current research, we aimed to investigate the mechanism of CSE to protect OVX rats.

The MWM test employed in the present study is a hippocampus-dependent memory task. This test is commonly employed in the evaluation of cognitive status [40]. The directional navigation training trials were utilized to explore spatial or place learning and the probe trials to examine whether the animal remembers the location of the platform, which indicates memory [41]. The latency time in the MWM was significantly shorter in the OVX rats after oral treatment with CSE. At the same time, we found that the 3.3mg/kg CSE treatment group is more capable of improving learning and memory in OVX rats.

The majority of studies have shown that hippocampus-dependent learning and memory are impaired by ovariectomy [42]. This study involved the attenuation of memory function in the OVX rats in the step-through passive avoidance test, and it was demonstrated that CSE improved this memory activity. The present results are consistent with previous findings showing that CSE plays a crucial role in the prevention or improvement of the cognitive loss triggered by OVX or D-galactose [43]. In short, the enhancement of memory activity by CSE was significant in the OVX rats.

The hippocampus is a crucial structure linked with learning and memory in humans and rodents [44]. In addition, the hippocampal CA1 region is very prone to degeneration [45]. Thus, the effects of CSE on cognitive processes in the hippocampal region were observed. In the present study, the potential mechanisms by which CSE enhanced learning and memory abilities were analyzed. The results showed that CSE significantly enhanced the number of CA1 pyramidal neurons in hippocampal slices obtained from OVX rats. CSE was found to have an ameliorating effect on neuronal cell viability and a neuroprotective influence on the hippocampal part of the OVX rats. The rats treated with CSE also exhibited an improved cell density compared to that of the OVX group. These results are in agreement with the findings of the behavioral analysis in the present study that the EV group had improved learning and memory function. However, the exact mode of action by which CSE improves the abilities of learning and memory in non-OVX rats is unclear.

Published work indicates that E2 enhances memory consolidation in ovariectomized female mice by rapidly activating ERK via ERα/β-mGluR1a interactions, NMDA receptors, and activation of PI3K/Akt and PKA [10, 46, 47]. ERK phosphorylation triggers activation of mTOR signaling

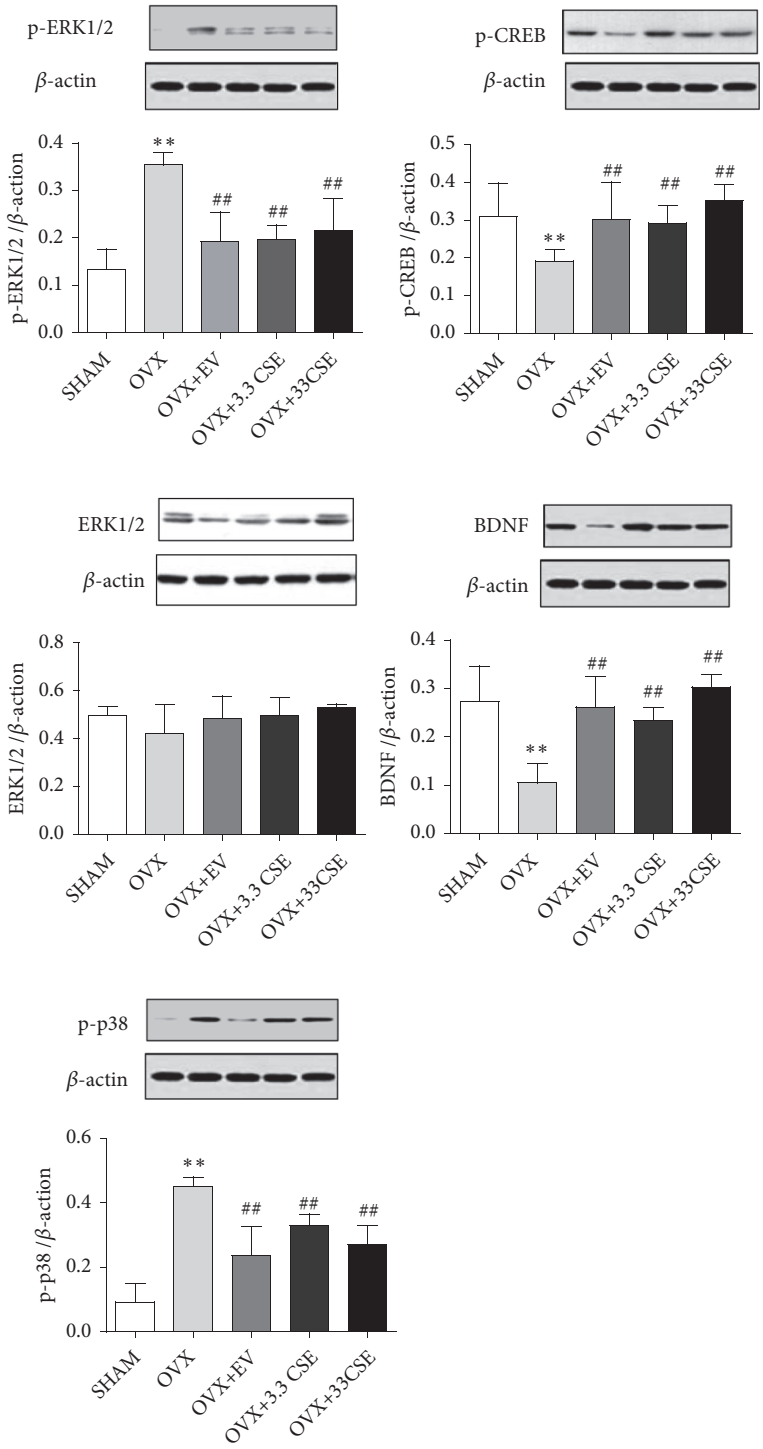

Figure 4: Western blot of hippocampal CA1 of brain after 8 w of OVX. (1) Sham group; (2) OVX group; (3) 0.2 mg/kg EV; (4) 3.3 mg/kg CSE. (5) 33mg/kg CSE. $^{**}P < 0.01$ vs. sham group, $^{\#\#}P<0.01$ vs. OVX group.

and CA1 dendritic spinogenesis [46, 48], as well as histone H3 acetylation of BDNF and transcription of multiple other genes. The p38MAPK pathway plays an important role in cell proliferation and differentiation; that is, the inhibition of the p38MAPK pathway reduces the production of inflammatory mediators and inhibits apoptosis, so p38 inhibitors are being used in the development of antineoplastic drugs [49]. The present study revealed an increase in p38MAPK protein expression in OVX rats; thus, the pathological effects of the hippocampal CA1 subfield in the sham and OVX groups were significantly different. CSE significantly reduced the phosphorylation level of p38MAPK, leading to the restricted

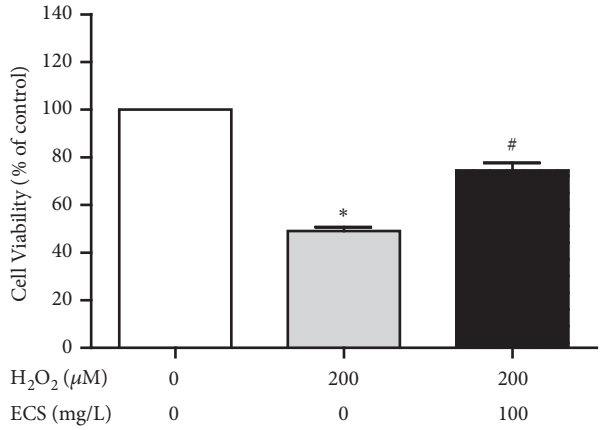

Figure 5: The effect of CSE on the viability of H_2O_2-induced Neuro 2a cells. (1) Sham group; (2) H_2O_2 group; (3) H_2O_2 + CSE group $^*P < 0.05$ vs. control group, $^\#P < 0.05$ vs. H_2O_2 group.

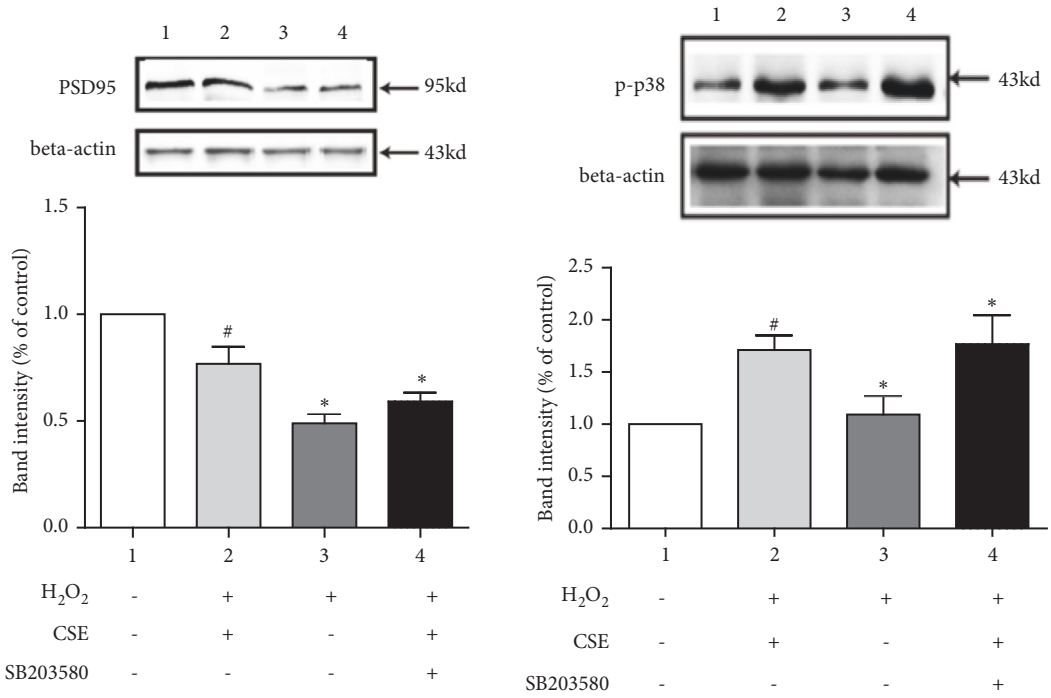

Figure 6: Western blot of PSD95 and p-p38 in H_2O_2-induced Neuro-2a cells. (1) Sham group; (2) H_2O_2 + CSE group; (3) H_2O_2 group; (4) H_2O_2 + CSE + SB203580 group. $^\#P < 0.05$ vs. sham group, $^*P<0.05$ vs. H_2O_2 group.

apoptotic effect of CSE. This result indicates that CSE inhibits OVX- induced p38 phosphorylation by GPR30.

Evidence-based studies have shown that estrogen receptors can influence phosphorylated CREB (p-CREB) to regulate synaptic plasticity in the hippocampal CA1 region of adult rats. Neuronal survival and plasticity were assessed by measuring expression of p-CREB and the level of its downstream factor BDNF [50–52]. In this study, an increase in the expression of p-CREB and BDNF proteins was observed in CSE-supplemented OVX rats.

These findings together revealed that the improved synaptic plasticity and cognition are closely associated with the ameliorated expression of p-CREB and BDNF. Therefore, BDNF could be involved in CREB-provoked regulation of synaptic plasticity and cognitive activity with CSE treatment. These findings are valuable for supporting the assumption that CSE influences cognition and synaptic plasticity in OVX rats.

4.1. Statistical Analysis. Graph Pad Prism 5 (GraphPad Software Incorporated, La Jolla, CA) was used to construct graphs. Data analysis was carried out using one-way ANOVA or Student's t-test utilizing Statistical Package for Social Sciences (SPSS) 13.0. All data were narrated as mean±standard error, while the statistical significance of difference was determined by $P < 0.05$.

Data Availability

The data used to support the findings of this study are available from the corresponding author upon request.

Conflicts of Interest

There are no conflicts of interest associated with this work.

Authors' Contributions

Fang-ze Tian and Hong-sheng Chang contributed equally to this study.

Acknowledgments

This study was financially supported by New Century Excellent Talents in University (NECT-13-0695), NSFC with Grant No. 81102623, and Beijing Municipal Natural Science Foundation (Grant number 7182095).

References

[1] C. D. Toran-Allerand, "Minireview: a plethora of estrogen receptors in the brain: where will it end?" *Endocrinology*, vol. 145, no. 3, pp. 1069–1074, 2004.

[2] S. Carranza-Lira and M. L. Valentino-Figueroa, "Estrogen therapy for depression in postmenopausal women," *International Journal of Gynecology and Obstetrics*, vol. 65, no. 1, pp. 35–38, 1999.

[3] E. S. LeBlanc, J. Janowsky, B. K. S. Chan, and H. D. Nelson, "Hormone replacement therapy and cognition: systematic review and meta-analysis," *The Journal of the American Medical Association*, vol. 285, no. 11, pp. 1489–1499, 2001.

[4] M. M. Miller, S. M. Hyder, R. Assayag, S. R. Panarella, P. Tousignant, and K. B. J. Franklin, "Estrogen modulates spontaneous alternation and the cholinergic phenotype in the basal forebrain," *Neuroscience*, vol. 91, no. 3, pp. 1143–1153, 1999.

[5] J. S. Talboom, B. J. Williams, E. R. Baxley, S. G. West, and H. A. Bimonte-Nelson, "Higher levels of estradiol replacement correlate with better spatial memory in surgically menopausal young and middle-aged rats," *Neurobiology of Learning and Memory*, vol. 90, no. 1, pp. 155–163, 2008.

[6] G. C. Panzica, C. Viglietti-Panzica, M. Sica et al., "Effects of gonadal hormones on central nitric oxide producing systems," *Neuroscience*, vol. 138, no. 3, pp. 987–995, 2006.

[7] E. F. Eriksen, "Hormone replacement therapy or SERMS in the long term treatment of osteoporosis," *Minerva Ginecologica*, vol. 64, no. 3, pp. 207–221, 2012.

[8] S. M. Fernandez, M. C. Lewis, A. S. Pechenino et al., "Estradiol-induced enhancement of object memory consolidation involves hippocampal extracellular signal-regulated kinase activation and membrane-bound estrogen receptors," *The Journal of Neuroscience*, vol. 28, no. 35, pp. 8660–8667, 2008.

[9] K. Frick M, J. Tuscher, and W. A. Koss, "Estrogenic regulation of memory consolidation: a look beyond the hippocampus, ovaries, and females," *Physiology & Behavior*, vol. 187, pp. 57–66, 2017.

[10] M. I. Boulware, J. D. Heisler, and K. M. Frick, "The memory-enhancing effects of hippocampal estrogen receptor activation involve metabotropic glutamate receptor signaling," *The Journal of Neuroscience*, vol. 33, no. 38, pp. 15184–15194, 2013.

[11] J. J. Tuscher, J. S. Szinte, J. R. Starrett et al., "Inhibition of local estrogen synthesis in the hippocampus impairs hippocampal memory consolidation in ovariectomized female mice," *Hormones and Behavior*, vol. 83, pp. 60–67, 2016.

[12] A. M. Fortress, J. Kim, R. L. Poole, T. J. Gould, and K. M. Frick, "17β-estradiol regulates histone alterations associated with memory consolidation and increases Bdnf promoter acetylation in middle-aged female mice," *Learning & Memory*, vol. 21, no. 9, pp. 457–467, 2014.

[13] J. Kim, J. S. Szinte, M. I. Boulware, and K. M. Frick, "17β-Estradiol and agonism of g-protein-coupled estrogen receptor enhance hippocampal memory via different cell-signaling mechanisms," *The Journal of Neuroscience*, vol. 36, no. 11, pp. 3309–3321, 2016.

[14] M. I. Boulware, J. P. Weick, B. R. Becklund, S. P. Kuo, R. D. Groth, and P. G. Mermelstein, "Estradiol activates group I and II metabotropic glutamate receptor signaling, leading to opposing influences on cAMP response element-binding protein," *The Journal of Neuroscience*, vol. 25, no. 20, pp. 5066–5078, 2005.

[15] S. A. Heldt, L. Stanek, J. P. Chhatwal, and K. J. Ressler, "Hippocampus-specific deletion of BDNF in adult mice impairs spatial memory and extinction of aversive memories," *Molecular Psychiatry*, vol. 12, no. 7, pp. 656–670, 2007.

[16] H. E. Scharfman, T. C. Mercurio, J. H. Goodman, M. A. Wilson, and N. J. MacLusky, "Hippocampal excitability increases during the estrous cycle in the rat: a potential role for brain-derived neurotrophic factor," *The Journal of Neuroscience*, vol. 23, no. 37, pp. 11641–11652, 2003.

[17] R. B. Gibbs, "Erratum: levels of trkA and BDNF mRNA, but not NGF mRNA, fluctuate across the estrous cycle and increase in response to acute hormone replacement," *Brain Research*, vol. 810, no. 1-2, p. 294, 1998.

[18] H.-C. Meng, S. Wang, Y. Li, Y.-Y. Kuang, and C.-M. Ma, "Chemical constituents and pharmacologic actions of cynomorium plants," *Chinese Journal of Natural Medicines*, vol. 11, no. 4, pp. 321–329, 2013.

[19] X. Ma, J. Liu, L. Yang, B. Zhang, Y. Dong, and Q. Zhao, "Cynomorium songaricum prevents bone resorption in ovariectomized rats through RANKL/RANK/TRAF6 mediated suppression of PI3K/AKT and NF-κB pathways," *Life Sciences*, vol. 209, pp. 140–148, 2018.

[20] C.-M. Ma, Y. Wei, Z.-G. Wang, and M. Hattori, "Triterpenes from Cynomorium songaricium - Analysis of HCV protease inhibitory activity, quantification, and content change under the influence of heating," *Journal of Natural Medicines*, vol. 63, no. 1, pp. 9–14, 2009.

[21] M. Sdiri, X. Li, W. Du et al., "Anticancer activity of Cynomorium coccineum," *Cancers*, vol. 10, no. 10, 2018.

[22] R. Tao, L. Miao, X. Yu et al., "Cynomorium songaricum Rupr demonstrates phytoestrogenic or phytoandrogenic like activities that attenuates benign prostatic hyperplasia via regulating steroid 5-α-reductase," *Journal of Ethnopharmacology*, vol. 235, pp. 65–74, 2019.

[23] L. Zhang, Y. Zhao, Z. A. Wang et al., "The genus boschniakia in china: an ethnopharmacological and phytochemical review," *Journal of Ethnopharmacology*, vol. 194, pp. 987–1004, 2016.

[24] J. Chen and K. M. Ko, "Ursolic-acid-enriched herba cynomorii extract protects against oxidant injury in H9c2 cells and rat myocardium by increasing mitochondrial ATP generation

capacity and enhancing cellular glutathione redox cycling, possibly through mitochondrial uncoupling," *Evidence-Based Complementary and Alternative Medicine*, vol. 2013, Article ID 924128, 14 pages, 2013.

[25] F. Yu, Y. Liu, Y. Cui et al., "Effects of a flavonoid extract from Cynomorium songaricum on the swimming endurance of rats," *American Journal of Chinese Medicine*, vol. 38, no. 1, pp. 65–73, 2010.

[26] Z.-H. Jiang, T. Tanaka, M. Sakamoto, T. Jiang, and I. Kouno, "Studies on a medicinal parasitic plant: lignans from the stems of Cynomorium songaricum," *Chemical & Pharmaceutical Bulletin*, vol. 49, no. 8, pp. 1036–1038, 2001.

[27] Q. Chu, X. Tian, M. Lin, and J. Ye, "Electromigration profiles of Cynomorium songaricum based on capillary electrophoresis with amperometric detection," *Journal of Agricultural and Food Chemistry*, vol. 54, no. 21, pp. 7979–7983, 2006.

[28] X. Wang, R. Tao, J. Yang et al., "Compounds from Cynomorium songaricum with estrogenic and androgenic activities suppress the oestrogen/androgen-induced BPH process," *Evidence-Based Complementary and Alternative Medicine*, vol. 2017, Article ID 6438013, 12 pages, 2017.

[29] D. P. Srivastava and P. Penzes, "Rapid estradiol modulation of neuronal connectivity and its implications for disease," *Frontiers in Endocrinology*, vol. 2, article no. 77, 2011.

[30] A. Pompili, B. Arnone, and A. Gasbarri, "Estrogens and memory in physiological and neuropathological conditions," *Psychoneuroendocrinology*, vol. 37, no. 9, pp. 1379–1396, 2012.

[31] S. M. Bonomo, A. E. Rigamonti, M. Giunta et al., "Menopausal transition: a possible risk factor for brain pathologic events," *Neurobiology of Aging*, vol. 30, no. 1, pp. 71–80, 2009.

[32] M. A. Espeland, "Conjugated equine estrogens and global cognitive function in postmenopausal women: women's health initiative memory study," *JAMA*, vol. 291, no. 24, pp. 2959–2968, 2004.

[33] Y. Hasegawa, Y. Hojo, H. Kojima et al., "Estradiol rapidly modulates synaptic plasticity of hippocampal neurons: involvement of kinase networks," *Brain Research*, vol. 1621, pp. 147–161, 2015.

[34] K. Mori and M. Takeda, "Hormone replacement Up-to-date. Hormone replacement therapy and brain function," *Clinical Calcium*, vol. 17, no. 9, pp. 1349–1354, 2007.

[35] J. E. Rossouw, G. L. Anderson, and R. L. Prentice, "Risks and benefits of estrogen plus progestin in healthy postmenopausal women: principal results from the Women's Health Initiative randomized controlled trial," *JAMA*, vol. 288, no. 3, pp. 321–333, 2002.

[36] W. Wang, A. A. Le, B. Hou et al., "Memory-related synaptic plasticity is sexually dimorphic in rodent hippocampus," *The Journal of Neuroscience*, vol. 38, no. 37, pp. 7935–7951, 2018.

[37] C. Junyan, H. Ruilan, G. Junying et al., "The effect of Cynomorium ethyl acetate extract containing serum on the Injured PC12 Cells Induced by Aβ_(25-35)," *Pharmacology and Clinics of Chinese Materia Medica*, 2018.

[38] L. Yi and X. Q. Wang, "Antioxidant activities of different extracts of cynomorium songarium and their protective effects against hypoxanthine/ xanthine oxidase- induced cell injury: a comparative study," *Journal of Anhui Traditional Chinese Medical College*.

[39] S. Jun-chao Zheng and Y. Xue, "Estrogen-like effect of ethyl acetate extract of cynomorium songarium rupr," *Natural Product Research and Development*.

[40] R. D'Hooge and P. P. De Deyn, "Applications of the Morris water maze in the study of learning and memory," *Brain Research Reviews*, vol. 36, no. 1, pp. 60–90, 2001.

[41] C. V. Vorhees and M. T. Williams, "Morris water maze: procedures for assessing spatial and related forms of learning and memory," *Nature Protocols*, vol. 1, no. 2, pp. 848–858, 2006.

[42] Z. Cai, C. Wang, X. Gu et al., "Tenuigenin ameliorates learning and memory impairments induced by ovariectomy," *Physiology & Behavior*, vol. 118, pp. 112–117, 2013.

[43] L. Ma, G. Chen, L. Nie, and M. Ai, "Effect of Cynomorium songaricum polysaccharide on telomere length in blood and brain of D-galactose-induced senescence mice," *Zhongguo Zhongyao Zazhi*, vol. 34, no. 10, pp. 1257–1260, 2009.

[44] J. M. Daniel and G. P. Dohanich, "Acetylcholine mediates the estrogen-induced increase in NMDA receptor binding in CA1 of the hippocampus and the associated improvement in working memory," *The Journal of Neuroscience*, vol. 21, no. 17, pp. 6949–6956, 2001.

[45] H. Hydén, P. W. Lange, L. J. Mihailović, and B. Petrović-Minić, "Changes of RNA base composition in nerve cells of monkeys subjected to visual discrimination and delayed alternation performance," *Brain Research*, vol. 65, no. 2, pp. 215–230, 1974.

[46] A. M. Fortress, F. Lu, P. T. Orr, Z. Zhao, and K. M. Frick, "Estradiol-induced object recognition memory consolidation is dependent on activation of mTOR signaling in the dorsal hippocampus," *Learning & Memory*, vol. 20, no. 3, pp. 147–155, 2013.

[47] M. C. Lewis, K. M. Kerr, P. T. Orr, and K. M. Frick, "Estradiol-induced enhancement of object memory consolidation involves NMDA receptors and protein kinase A in the dorsal hippocampus of female C57BL/6 mice," *Behavioral Neuroscience*, vol. 122, no. 3, pp. 716–721, 2008.

[48] J. J. Tuscher, V. Luine, M. Frankfurt, and K. M. Frick, "Estradiol-mediated spine changes in the dorsal hippocampus and medial prefrontal cortex of ovariectomized female mice depend on ERK and mTOR activation in the dorsal hippocampus," *The Journal of Neuroscience*, vol. 36, no. 5, pp. 1483–1489, 2016.

[49] G. L. Schieven, "The p38alpha kinase plays a central role in inflammation," *Current Topics in Medicinal Chemistry*, vol. 9, no. 11, pp. 1038–1048, 2009.

[50] S. K. Mohamed, A. A. Ahmed, E. M. El Morsy, and S. Nofal, "The protective effect of zeranol in cerebral ischemia reperfusion via p-CREB overexpression," *Life Sciences*, vol. 217, pp. 212–221, 2019.

[51] S. Duan, T. Wang, J. Zhang et al., "Huatuo Zaizao pill promotes functional recovery and neurogenesis after cerebral ischemia-reperfusion in rats," *BMC Complementary and Alternative Medicine*, vol. 17, no. 1, article no. 19, 2017.

[52] D.-J. Yu and H.-Y. Gao, "Effect of propofol on mitochondrial ATP content and ATPase activity in hippocampus of rats with cerebral ischemia-reperfusion injury," *Saudi Journal of Biological Sciences*, vol. 24, no. 2, pp. 246–250, 2017.

Hindawi
Evidence-Based Complementary and Alternative Medicine
Volume 2019, Article ID 2682748, 7 pages
https://doi.org/10.1155/2019/2682748

Review Article

Role of Gut Microbiota in the Pharmacological Effects of Natural Products

Chuyue Pan, Qinglong Guo, and Na Lu

State Key Laboratory of Natural Medicines, Jiangsu Key Laboratory of Carcinogenesis and Intervention, Department of Basic Medicine, School of Basic Medicine and Clinical Pharmacy, China Pharmaceutical University, 24 Tongjiaxiang, Nanjing 210009, China

Correspondence should be addressed to Qinglong Guo; qinglongguo@hotmail.com and Na Lu; nalu@cpu.edu.cn

Received 6 February 2019; Revised 31 March 2019; Accepted 9 April 2019; Published 15 April 2019

Guest Editor: Chongshan Dai

Increasing evidence has demonstrated that natural products derived from traditional Chinese medicine, such as ginseng, berberine, and curcumin, possess a wide variety of biological activities on gut microbiota, which may cause changes in the composition of intestinal microbiota, microbial metabolites, intestinal tight junction structure, and mucosal immunology. These changes will eventually result in the exertion of the pharmacological effects by treatment with these natural products. In this review, we will discuss how gut microbiota is influenced by commonly used natural products. Furthermore, our findings are expected to provide novel insight into how these untargeted natural products function via gut microbiota.

1. Introduction

The relationship between gut microbiota and human diseases has been a major topic of interest for many studies. Increasing evidence has suggested that gut microbiota plays an important role in diseases, including obesity [1], type 2 diabetes mellitus (T2DM), cardiovascular diseases [2], and cancer [3, 4]. In many studies, bacteria-deficient mice have been reported to consume more calories than normal mice [5], and it was more difficult for these mice to become obese [6]. Studies in germ-free mice have indicated that gut microbiota was associated with weight gain, lipid synthesis, and fat storage. In addition, high-fat diet- (HFD-) induced obesity is usually accompanied with diabetes [7], cardiovascular diseases, and liver diseases such as nonalcoholic fatty liver disease (NAFLD). Besides, gut microbiota, which can be part of the tumor microenvironment, communicates with tumor cells, and some immune cells [8], and may be the key factor in the process of HFD-induced cancer progression [9].

In recent years, interest in the pharmacological activities of natural products has significantly increased. *In vitro* studies and clinical data have demonstrated positive effects of natural products on many diseases [10, 11]. The aim of this study was to discuss the effects of natural products on the composition of gut microbiota, metabolites, intestinal tight junction proteins, and mucosal immunity and to provide novel insight into future therapies.

2. Effect of Natural Products on Composition of Gut Microbiota

The gut microbiota is hypothesized to play a critical role in metabolic diseases, such as obesity and T2DM. An increasing number of studies have shown that natural products exert antiobesity activities by modulating the composition of gut microbiota. For example, MDG-1, a water-soluble polysaccharide extracted from the root of *Ophiopogon japonicus* Ker Gawl has been reported to regulate body metabolism, including weight loss, antiobesity, and antidiabetes. Shi et al. [12] demonstrated that, in HFD-induced obese mice that were treated with MDG-1 at a high dose of 300 mg/kg for 12 weeks, the ratio of Firmicutes/Bacteroidetes (F/B) decreased to normal levels. In addition, it was found that, in a HFD-induced diabetic mouse model, MDG-1 decreased the number of pathogenic bacteria (*Escherichia coli* and *Streptococcus*) [13]. Green tea, commonly consumed in Asia, has also been reported to have an antiobesity activity [14], and the alteration of gut microbiota composition has been presumed as one of its mechanisms of action. When sundried green tea was

fermented, it restored the increased Bacteroides/Prevotella (B/P) ratio [15] and significantly decreased the F/B ratio in HFD mice after 8 weeks of treatment. Epigallocatechin gallate (EGCG), the main type of catechin in green tea, could inhibit the formation of rat abdominal adipose tissue after a 4-week treatment regimen. In their study, it was revealed that EGCG-treated rats showed a dramatic decrease of *Clostridium* spp. and an increase of Bacteroides in feces [16]. Moreover, Chang et al. [17] reported that a water extract of *Ganoderma lucidum* (Curtis) P. Karst. (WEGL) prevented weight gain and fat accumulation in HFD-induced obese mice. Furthermore, endotoxemia and insulin resistance were found to be improved by WEGL for the modification of gut dysbiosis. The F/B ratio and levels of endotoxin-bearing Proteobacteria were also restored to normal levels. However, several bacteria increased (*Parabacteroides goldsteinii, Bacteroides* spp., *Anaerotruncus colihominis, Roseburia hominis, and Clostridium*), which negatively correlated with obesity. The authors suggested that WEGL or polysaccharides could be used as prebiotic agents for the treatment of obesity and modulating obesity-related metabolic disorders [17].

Lonicerae japonicae flos is famous for its anti-inflammatory activity and has widely been used in Asia for years. In animal studies using HFD-fed animals, administration of unfermented *Flos Lonicera* (UFL) or fermented *Flos Lonicera* (FFL) significantly reduced body weight (BW) and adipose tissue weight and decreased lipid accumulation in the liver with ameliorated serum total cholesterol, HDL, and triglyceride levels. As suggested by the authors, alterations in the relative abundance of *Lactobacillus* spp., *Bifidobacterium* spp., and B/F ratio in the intestinal tract were supposed to be one of the mechanisms of UFL or FFL [18]. In addition, the amount of *Bifidobacterium* spp. in the cecal pool of HFD-induced mice was increased by pomegranate peel extract (PPE), which is known for its beneficial effects, including anti-inflammatory and antimicrobial activities [19].

Berberine, the main active ingredient of Chinese herb Coptis chinensis, is known as an antidiabetes drug and can regulate blood glucose [20, 21]. Berberine has been shown to be beneficial for HFD-induced insulin resistance, as it improves insulin sensitivity and reduces the homeostasis assessment of the insulin resistance (HOMA-IR) value. As reported by Sun *et al*., administration of berberine reduced the ratio of F/B and partly recovered the composition of gut microbiota changed by HFD feeding. Furthermore, it also showed that both the diversity and richness of gut microbiota were significantly decreased after berberine administration [22]. These findings were supported by Zhang *et al*., who showed that the partial least squares (PLS) regression model predicted the relationship between the changes in composition of gut microbiota and host phenotype [23].

In addition to animal studies, several studies of natural products have been performed on human gut microbiota. Xu *et al.* reported that Gegen Qinlian Decoction (GQD), a traditional Chinese herbal formula, reshaped the gut microbiota in a clinical study in which 187 T2D patients were enrolled. The data showed that the symptoms of T2D, such as fasting blood glucose levels and hemoglobin A1c (HbA1c) levels, were ameliorated in GQD-treated patients, with increased amounts of beneficial bacteria, including *Faecalibacterium*, *Gemmiger*, *Bifidobacterium,* and *Escherichia* [11]. Another clinical study involving ten obese Korean women was conducted to investigate the antiobesity activity of the water extract of Ephedra sinica Stapf, which revealed that, in seven of the ten obese women, BW and body mass index (BMI) were decreased after administration of this herb. Interestingly, the antiobesity effect of ginseng varied when the composition of gut microbiota was altered. The abundance of *Subdoligranulum*, *Oscillibacter*, and *Akkermansia* in the gut associated with changes in BW and BMI, whereas *Lactobacillus* was linked to body fat percentage [10].

Natural products also play an important role in the improvement of gastrointestinal tract function. Several Chinese medicine products such as Red Ginseng and Semen Coicis were found to relieve the symptoms of ulcerative colitis (UC) [24, 25]. After Red Ginseng and Semen Coicis treatment in rats, the structure of gut microbiota was altered, which may be beneficial for promoting the growth of probiotics, such as *Bifidobacterium* and *Lactobacillus*, and for inhibiting the growth of pathogenic bacteria [25]. In a double-blind, randomized clinical trial containing 54 patients, it was revealed that the combination of herbal medicine (*Gwakhyangjeonggisan*, GJS) and probiotics (Duolac7S, DUO) alleviated the symptoms of diarrhea-predominant irritable bowel syndrome (D-IBS) by changing the composition of gut microbiota. Beneficial intestinal microbe counts, including *Bifidobacterium brevis*, *Bifidobacterium lactis*, *Streptococcus thermophilus*, *Lactobacillus rhamnosus*, *Lactobacillus plantarum, and Lactobacillus acidophilus,* were synergistically enhanced by GJS combined with DUO, suggesting that a combined treatment of herbal medicine and probiotics might provide a promising implication for clinical treatment of D-IBS [26, 27].

3. Effect of Natural Products on Metabolites of Gut Microbiota

In the human intestine, microbes are vital contributors to the host metabolism, considering that numerous important components, such as vitamin K, folate, indoles, gamma amino butyric acid, and short-chained fatty acids (SCFAs), are produced by microbiota [28–30]. In general, these metabolites are involved in many physiological and pathophysiological processes, which may be related to several diseases, including cardiovascular diseases [29], allergic reactions [30], T2DM [31], and various types of cancers [8, 32]. By changing the bacterial structure, natural products may regulate the metabolism of the microbiome, Zhao *et al*. found that the abundance of genes encoding SCFA production and the fecal butyric acid concentration were notably increased by a high fiber diet from traditional Chinese medicinal food plants, and several T2DM parameters were found to be improved after treatment, and they identified 15 positive responders of SCFA which played an important role in maintaining intestinal homeostasis [31]. When total saponins and polysaccharides (active constituents of *P. kingianum*) were administrated to diabetic rats, the abundance of the content of certain bacterial

taxa and fecal SCFAs in rats was upregulated, while the lipopolysaccharide (LPS) concentration was downregulated [33]. These results suggested that natural products might be the treat levels of protective metabolites and that detrimental metabolites can contribute to metabolic diseases. Chen *et al*. reported that sulfate-reducing bacteria were significantly decreased after *Gynostemma pentaphyllum* (GpS) treatment in $Apc^{Min/+}$ mice. As a result, the level of harmful molecular hydrogen sulfide produced by sulfate-reducing bacteria was also reduced [34].

Gut microbiota can also impact the metabolism of natural products and therefore influence their treatment effects. It has been demonstrated that commensal bacteria regulate countless genes involved in drug metabolism and hepatic expression of drug-metabolizing enzymes [35–37]. Therefore, the microbial activity in metabolic phenotype development is important, especially for pharmacokinetics [35], because treatment effects of components of traditional Chinese herbs may be enhanced by biotransformation. For instance, many glycoside compounds are hydrolyzed by gut flora when administered orally, and thereby, the solubility is improved to allow for easy absorption. Ginsensoide Rb1 [37] and aglycone of baicalin [38] are biotransformed to a more active form, aglycone. After transformation, they harbor a much better bioavailability. On the contrary, the activity of several molecules can be transformed to an inactive form and reduce their bioactivities. Ru *et al*. found that berberine is metabolized to dihydroberberine (dhBBR), which is easier to absorb but has less active properties, although in the blood it can be oxidized to berberine [39]. Several herbs are toxic and their harmful metabolites can also be more or less toxic [40, 41]. Human intestinal microbiota can metabolize aconitine, an alkaloid that can induce systemic acute toxicity, to be less harmful to the body through acetylation and esterification [40]. However, aristolochic acid in *Radix Aristolochiae Fangchi* can cause acute renal injury, and long term administration can increase the risk of cancer. Its main microbial metabolite aristolochic acid I, the most toxic component of the Aristolochia herbs, is particularly cytotoxic in the kidney [42].

From another point of view, gut microbiota has played an important role on the pharmacokinetics and pharmacodynamics of natural products. The loss of gut microbiota or dysbiosis may reduce the efficacy of traditional Chinese medicine. Liu et *al.* reported that rats treated with broad-spectrum antibiotics show a different pharmacological response to Shaoyao-Gancao decoction (SGD) when compared with control mice. The antibiotics inhibited the absorption of SGD and reduced biotransformation of SGD in the colon. Two constituents of SGD have significantly reduced $AUC_{0\text{-}24h}$ after antibiotics treatment, but the half-lives ($T_{1/2}$) and mean retention times (MRT) did not remarkably change [43]. It seems that gut microbiota mainly affects the blood concentration and AUC of herb medicines. Furthermore, Shen *et al.* used 5% dextran sulfate sodium (DSS) to disturb gut microbial homeostasis and observed a quicker absorption (less T_{max}) and a lower max concentration (C_{max}) of ginsenoside Rb1 in DSS-treated mice. Once given drugs to restore the balance, these changes recovered, which indicated the importance of the intestinal flora in drug metabolism [44]. Thus, it is of importance to consider the influence of gut microbiota in clinical medicine. Digoxin is an example of a drug that decreases drug efficacy when it metabolized by microbiota. It has been reported that gut microbiota can degrade digoxin to its inactive form, such as dihydrodigoxin and dihydrodigoxigenin [45], which hardly bind Na^+-K^+-ATPase of cardiac cells [46]. Conversely, some new effects can be functioned during the interaction between drugs and gut microbiota. In a study by Ru et al., the mechanism of antihyperlipidemia function and pharmacokinetics in beagle dogs was determined. Different from effects such as anti-inflammatory and antidiabetes activities, berberine induced the production of butyrate by upregulating butyrate-producing microbiota [47]. All studies involving novel effects or mechanism may have direct applications to clinical medicines.

In conclusion, natural products can affect the metabolism of gut microbes, and the microbiome can change the metabolic process of natural components.

4. Effect of Natural Products on Improving Gut Tight Junction through Regulating Intestinal Microbes

In intestinal epithelial cells, tight junctions usually function as a barrier to defense against bacterial endotoxin. In addition, LPS-induced disruption of tight junctions can lead to dysregulation of intestinal epithelial cells, as well as of the immune system [48]. A HFD could increase LPS release induced by gut microbiota, thereby impairing the expression of tight junction proteins leading to the increase of intestinal permeability [49]. Furthermore, HFD elevated the LPS concentration in plasma, and subsequently increased the secretion of adipokines. In a recent study, it was shown that *Lactobacilli* positively associated with human BMI and blood glucose values [50]. In addition, it was reported that *Lactobacilli* could reduce the LPS level, decrease blood glucose levels, and inflammation in HFD mice. Besides, *Lactobacilli sakei* OK67 could restore the expression of colonic tight junction protein expression and ameliorate HFD-induced hyperglycemia [51].

Moreover, in previous studies, it was demonstrated that nanoparticle loaded with berberine could protect tight junction against inflammation induced by LPS. And berberine-loaded nanoparticles turned out to be useful in the restoration of tight junctions in intestinal epithelial cells (IEC) [52]. Li *et al.* and Gu *et al.* reported that berberine could inhibit intestinal epithelial tight junction damage caused by proinflammation cytokines [53]. Pretreatment with berberine could reduce the intestinal permeability and improve LPS-induced redistribution of tight junction-related protein claudin-1 and claudin-4 [54]. Combined, these results indicated that berberine improved bacterial endotoxin induced intestinal barrier disruption and play a significant role in the maintenance of the intestinal epithelial tight junction.

Besides berberine, other natural products also showed powerful functions to protect the intestine from LPS-induced

gut microbiota. In a previous study the effects of curcumin were tested on Caco-2 cells and HT-29 cells, and it was found that curcumin could attenuate the disruption of intestinal epithelial barrier functions. Curcumin reduced the release of IL-1b secreted from LPS, induced IEC and macrophages, and prevented the disintegration of tight junction proteins, such as ZO-1, claudin-1, claudin-7, and actin filaments [55]. Therefore, curcumin can be a potential compound for treating intestine barrier injury through increasing the expression of tight junction proteins.

Similarly, *Flos Lonicera*, one of the most well-known traditional Chinese medicines, could modulate tight junctions at the cell-based level. It not only restored the side effects induced by LPS but also increased several microbiota, which had beneficial effects on maintaining the integrity of the intestinal barrier [18]. For example, Chelakkot *et al*. demonstrated that *akkermansia-muciniphila* could activate tight junction-related signaling of AMPK, especially in obesity and T2D patients [56]. In another study, it was suggested that the polyphenolic compound resveratrol (Res), which is found in grape seeds, grape skin, and red wine, attenuated intestinal barrier impairment and bacterial translocation induced by deoxynivalenol (DON) [57, 58]. Ling *et al*. reported that Res mainly facilitated claudin-4 expression to build up the tight junction complex and to resist DON-induced barrier dysfunction [59].

Together, these findings demonstrated that natural products can exert positive effects on the intestinal barrier by upregulating tight junction proteins, reducing inflammation, and increasing the abundance of probiotics. Gut microbiota disorders increased the secretion of LPS, thereby leading to a series of metabolic diseases [60, 61]. However natural products can directly or indirectly act on microbes to alleviate the condition.

5. Effect of Natural Products on Intestinal Mucosal Immunity

The intestinal mucosal immunity system consists of gut-associated lymphoid tissue (GALT), lymphocytes, and various immune-related factors. At present, it is believed that digestive system diseases, autoimmune diseases, pediatric allergic diseases, and tumors are closely related to intestinal mucosal immunity [62, 63]. Natural products may provide an alternative treatment approach for these diseases.

Many metabolic diseases are related to intestinal inflammation and gut microbiota, and it is the intestinal mucosal immunity that is the connection between them. As previously reported, the induction of IL-22 in innate lymphoid cells and $CD4^+$T cells is impaired in obese mice, and IL-22 deficiency in mice has shown that mice are prone to developing metabolic disorders [64]. Intestinal mucosal immunity in obese mice contributed to obesity-related insulin resistance via preserving the gut barrier and remitting fat inflammation [65].

Gut microbiota regulates host innate and adaptive immunity. Dysbiosis of gut microbiota can cause severe intestinal diseases [66]. Segmented filamentous bacteria can activate $CD4^+$ T cells and produce IL-17A to promote inflammation in the intestine [67]. Microbiota such as *Clostridium clusters* promoted the development of intestinal regulatory T cells (T reg), which are significantly decreased in colonic germ-free mice [68, 69]. Moreover, in the small intestine, TH17 cells secrete cytokines, such as IL-17/IL-22 to regulate the inflammation status in colon. However, *Clostridium arthromitus* and metabolites from microbiota, such as luminal adenosine triphosphate and tryptophan, promoted the development of TH17 cells [70–72]. Commensal bacteria modulated the abundance and activation of $\gamma\delta$ T cells, which produced IL-17 to promote inflammation in the intestine [73]. Gut microbiota could also inhibit natural killer T cells (iNKT) [74, 75].

Innate lymphoid cells (ILCs) share functional characteristics with T cells in the lamina propria. Gut microbiota may regulate the ILC either through direct recognition or by indirect induction of cytokine secretion by other cells [76]. On the contrary, microbiota can also regulate the activation of ILCs via inducing the production of IL-25, which confirms the opinion that microbiota is important for homeostasis [77, 78].

IgA constitutes approximately 75% of the total antibody production in mammals and is the most abundant immunoglobulin in mucosal secretions [79]. Gut microbiota is a strong inducer of IgA production. For example, orally administered flagellin abrogated IgA secretion in the intestine [80].

Recent studies have shown that berberine had beneficial effects on intestinal immune cells and immune factors. Moreover, berberine also inhibited the expression of various immune factors and reduced the low-grade inflammation [81]. For example, berberine has been widely used in the treatment of UC via modulating T reg cells and TH cells in the colon [82]. Researchers in China revealed that berberine improved lipid metabolism in the liver by changing microbiota and by regulating bile acid metabolism and the FXR pathway in the intestine [83]. In addition, M. charantia improved insulin resistance via decreasing the F/B ratio in the intestines of diabetic rats [84]. Therefore, it improved the inflammation status in the intestine and diabetes mellitus [85]. Curcumin could improve pancreatic β cells and decrease glucose levels, as well as other metabolic profile in T2D or atherosclerosis through inhibition of iNOS and COX-2 [86, 87]. Furthermore, a curcumin-supplemented diet increased the richness of *lactobacillales* and improved the index of colon tumors [88]. Ginsenoside also protected cardiac function and decreased blood glucose levels [89].

Natural products modulate the immune status via changing the level of immune factors, such as IL-22, as well as activating T reg cells or inhibiting the development of Th17 cells. Natural products can also decrease systemic inflammation via improving insulin resistance as well as other metabolic profiles. Natural products have promising therapeutic effects on metabolic diseases by improving the immune status in the body.

6. Conclusion

In the past, numerous studies have demonstrated that natural products derived from traditional Chinese medicine implement their pharmacological properties through restoring gut

homeostasis, including alteration of microbiota composition, adjustment of microbiota metabolites, enhancement of the expression of tight junction proteins, and enhancing mucosal immunity. Therefore, we conclude that gut microbiota and its subsequent changes of intestinal environment play very important roles in mediating the pharmacological effects of natural products. Given the fact that various roles of gut microbiota were gradually elucidated in human diseases and health, we hypothesize that the important roles of gut microbiota will increase and will be more realized and illuminated. It is to be expected that an increased number of potential drug targets arising from gut microbiota will be discovered.

Conflicts of Interest

The authors declare that they have no conflicts of interest.

References

[1] R. E. Ley, P. J. Turnbaugh, S. Klein, and J. I. Gordon, "Microbial ecology: human gut microbes associated with obesity," *Nature*, vol. 444, no. 7122, pp. 1022-1023, 2006.

[2] C. L. Gentile and T. L. Weir, "The gut microbiota at the intersection of diet and human health," *Science*, vol. 362, no. 6416, pp. 776–780, 2018.

[3] G. Guglielmi, "How gut microbes are joining the fight against cancer," *Nature*, vol. 557, no. 7706, pp. 482–484, 2018.

[4] M. Sigal, C. Y. Logan, M. Kapalczynska et al., "Stromal R-spondin orchestrates gastric epithelial stem cells and gland homeostasis," *Nature*, vol. 548, no. 7668, pp. 451–455, 2017.

[5] B. S. Wostmann, C. Larkin, A. Moriarty, and E. Bruckner-Kardoss, "Dietary intake, energy metabolism, and excretory losses of adult male germfree wistar rats," *Laboratory Animals*, vol. 33, no. 1, pp. 46–50, 1983.

[6] F. Bäckhed, J. K. Manchester, C. F. Semenkovich, and J. I. Gordon, "Mechanisms underlying the resistance to diet-induced obesity in germ-free mice," *Proceedings of the National Acadamy of Sciences of the United States of America*, vol. 104, no. 3, pp. 979–984, 2007.

[7] R. E. Ley, F. Bäckhed, P. Turnbaugh, C. A. Lozupone, R. D. Knight, and J. I. Gordon, "Obesity alters gut microbial ecology," *Proceedings of the National Acadamy of Sciences of the United States of America*, vol. 102, no. 31, pp. 11070–11075, 2005.

[8] L. Zitvogel, R. Daillère, M. P. Roberti, B. Routy, and G. Kroemer, "Anticancer effects of the microbiome and its products," *Nature Reviews Microbiology*, vol. 15, no. 8, pp. 465–478, 2017.

[9] C. L. Sears and W. S. Garrett, "Microbes, microbiota, and colon cancer," *Cell Host & Microbe*, vol. 15, no. 3, pp. 317–328, 2014.

[10] M. Y. Song, B. S. Kim, and H. Kim, "Influence of *Panax ginseng* on obesity and gut microbiota in obese middle-aged Korean women," *Journal of Ginseng Research*, vol. 38, no. 2, pp. 106–115, 2014.

[11] J. Xu, F. Lian, L. Zhao et al., "Structural modulation of gut microbiota during alleviation of type 2 diabetes with a Chinese herbal formula," *The ISME Journal*, vol. 9, no. 3, pp. 552–562, 2015.

[12] L.-L. Shi, Y. Li, Y. Wang, and Y. Feng, "MDG-1, an Ophiopogon polysaccharide, regulate gut microbiota in high-fat diet-induced obese C57BL/6 mice," *International Journal of Biological Macromolecules*, vol. 81, pp. 576–583, 2015.

[13] L.-Y. Wang, S. Wang, Y. Wang, K.-F. Ruan, and Y. Feng, "Effect of MDG-1 on oral glucose tolerance and intestinal microecological balance in diabetic mice," *World Chinese Journal of Digestology*, vol. 19, no. 19, pp. 2058–2062, 2011.

[14] M. Taghizadeh, N. Farzin, S. Taheri et al., "The Effect of Dietary Supplements Containing Green Tea, Capsaicin and Ginger Extracts on Weight Loss and Metabolic Profiles in Overweight Women: A Randomized Double-Blind Placebo-Controlled Clinical Trial," *Annals of Nutrition and Metabolism*, vol. 70, no. 4, pp. 277–285, 2017.

[15] D.-B. Seo, H. W. Jeong, D. Cho et al., "Fermented green tea extract alleviates obesity and related complications and alters gut microbiota composition in diet-induced obese mice," *Journal of Medicinal Food*, vol. 18, no. 5, pp. 549–556, 2015.

[16] T. Unno, M. Sakuma, and S. Mitsuhashi, "Effect of dietary supplementation of (-)-epigallocatechin gallate on gut microbiota and biomarkers of colonic fermentation in rats," *Journal of Nutritional Science and Vitaminology*, vol. 60, no. 3, pp. 213–219, 2014.

[17] C. Chang, C. Lin, and C. Lu, "Ganoderma lucidum reduces obesity in mice by modulating the composition of the gut microbiota," *Nature Communications*, vol. 6, p. 7489, 2015.

[18] J.-H. Wang, S. Bose, G.-C. Kim et al., "Flos Lonicera ameliorates obesity and associated endotoxemia in rats through modulation of gut permeability and intestinal microbiota," *PLoS ONE*, vol. 9, no. 1, Article ID e86117, 2014.

[19] A. M. Neyrinck, V. F. Van Hée, L. B. Bindels, F. De Backer, P. D. Cani, and N. M. Delzenne, "Polyphenol-rich extract of pomegranate peel alleviates tissue inflammation and hypercholesterolaemia in high-fat diet-induced obese mice: potential implication of the gut microbiota," *British Journal of Nutrition*, vol. 109, no. 5, pp. 802–809, 2013.

[20] Y. S. Lee, W. S. Kim, K. H. Kim et al., "Berberine, a natural plant product, activates AMP-activated protein kinase with beneficial metabolic effects in diabetic and insulin-resistant states," *Diabetes*, vol. 55, no. 8, pp. 2256–2264, 2006.

[21] Y. F. Zhang, X. Y. Li, D. J. Zou et al., "Treatment of type 2 diabetes and dyslipidemia with the natural plant alkaloid berberine," *The Journal of Clinical Endocrinology & Metabolism*, vol. 93, no. 7, pp. 2559–2565, 2008.

[22] H. Sun, N. Wang, Z. Cang et al., "Modulation of Microbiota-Gut-Brain Axis by Berberine Resulting in Improved Metabolic Status in High-Fat Diet-Fed Rats," *Obesity Facts*, vol. 9, no. 6, pp. 365–378, 2017.

[23] X. Zhang, Y. Zhao, M. Zhang et al., "Structural changes of gut microbiota during berberine-mediated prevention of obesity and insulin resistance in high-fat diet-fed rats," *PLoS ONE*, vol. 7, no. 8, Article ID e42529, p. e42529, 2012.

[24] P. Wan, H. Chen, Y. Guo, and A.-P. Bai, "Advances in treatment of ulcerative colitis with herbs: From bench to bedside," *World Journal of Gastroenterology*, vol. 20, no. 39, pp. 14099–14104, 2014.

[25] M. Guo, S. Ding, C. Zhao et al., "Red Ginseng and Semen Coicis can improve the structure of gut microbiota and relieve the symptoms of ulcerative colitis," *Journal of Ethnopharmacology*, vol. 162, pp. 7–13, 2015.

[26] S. J. Ko et al., "Effect of korean herbal medicine combined with a probiotic mixture on diarrhea-dominant irritable bowel syndrome: a double-blind, randomized, placebo-controlled trial," *Evid Based Complement Alternat Med*, vol. 2013, p. 824605, 2013.

[27] S.-J. Ko, B. Ryu, J. Kim et al., "Effect of herbal extract granules combined with probiotic mixture on irritable bowel syndrome

with diarrhea: study protocol for a randomized controlled trial," *Trials*, vol. 12, p. 219, 2011.

[28] P. D. Cani, "Human gut microbiome: Hopes, threats and promises," *Gut*, vol. 67, no. 9, pp. 1716–1725, 2018.

[29] J. M. Brown and S. L. Hazen, "Microbial modulation of cardiovascular disease," *Nature Reviews Microbiology*, vol. 16, no. 3, pp. 171–181, 2018.

[30] C. McKenzie, J. Tan, L. Macia, and C. R. Mackay, "The nutrition-gut microbiome-physiology axis and allergic diseases," *Immunological Reviews*, vol. 278, no. 1, pp. 277–295, 2017.

[31] L. Zhao et al., "Gut bacteria selectively promoted by dietary fibers alleviate type 2 diabetes," *Science*, vol. 359, no. 6380, pp. 1151–1156, 2018.

[32] C. Ma, M. Han, and B. Heinrich, "Gut microbiome-mediated bile acid metabolism regulates liver cancer via NKT," *Cells*, vol. 360, no. 6391, 2018.

[33] H. Yan, J. Lu, Y. Wang, W. Gu, X. Yang, and J. Yu, "Intake of total saponins and polysaccharides from Polygonatum kingianum affects the gut microbiota in diabetic rats," *Phytomedicine*, vol. 26, pp. 45–54, 2017.

[34] L. Chen, M. S. Brar, F. C. C. Leung, and W. L. W. Hsiao, "Triterpenoid herbal saponins enhance beneficial bacteria, decrease sulfate-reducing bacteria, modulate inflammatory intestinal microenvironment and exert cancer preventive effects in ApcMin/+ mice," *Oncotarget*, vol. 7, no. 21, pp. 31226–31242, 2016.

[35] S. P. Claus et al., "Colonization-induced host-gut microbial metabolic interaction," *MBio*, vol. 2, no. 2, pp. e00271–e00210, 2011.

[36] F. P. Selwyn, J. Y. Cui, and C. D. Klaassen, "Special section on drug metabolism and the microbiome RNA-seq quantification of hepatic drug processing genes in germ-free mice," *Drug Metabolism and Disposition*, vol. 43, no. 10, pp. 1572–1580, 2015.

[37] J. Xu, H.-B. Chen, and S.-L. Li, "Understanding the Molecular Mechanisms of the Interplay Between Herbal Medicines and Gut Microbiota," *Medicinal Research Reviews*, vol. 37, no. 5, pp. 1140–1185, 2017.

[38] K. Noh, Y. Kang, M. Nepal et al., "Role of intestinal microbiota in baicalin-induced drug interaction and its pharmacokinetics," *Molecules*, vol. 21, no. 3, p. 337, 2016.

[39] R. Feng, J. Shou, Z. Zhao et al., "Transforming berberine into its intestine-absorbable form by the gut microbiota," *Scientific Reports*, vol. 5, no. 1, p. 12155, 2015.

[40] M. Zhang, C. S. Peng, and X. B. Li, "In vivo and in vitro metabolites from the main diester and monoester diterpenoid alkaloids in a traditional chinese herb, the aconitum species," *Evid Based Complement Alternat Med*, vol. 2015, 23 pages, 2015.

[41] X.-W. Chen, E. S. Serag, K. B. Sneed, and S.-F. Zhou, "Herbal bioactivation, molecular targets and the toxicity relevance," *Chemico-Biological Interactions*, vol. 192, no. 3, pp. 161–176, 2011.

[42] J. Li, L. Zhang, Z. Jiang et al., "Toxicities of aristolochic acid I and aristololactam I in cultured renal epithelial cells," *Toxicology in Vitro*, vol. 24, no. 4, pp. 1092–1097, 2010.

[43] M. Liu, J. Yuan, W. Hu et al., "Pretreatment with broad-spectrum antibiotics alters the pharmacokinetics of major constituents of Shaoyao-Gancao decoction in rats after oral administration," *Acta Pharmacologica Sinica*, vol. 40, no. 2, pp. 288–296, 2019.

[44] H. Shen, X.-J. Gao, T. Li et al., "Ginseng polysaccharides enhanced ginsenoside Rb1 and microbial metabolites exposure through enhancing intestinal absorption and affecting gut microbial metabolism," *Journal of Ethnopharmacology*, vol. 216, pp. 47–56, 2018.

[45] E. K. Mallory, A. Acharya, S. E. Rensi, P. J. Turnbaugh, R. A. Bright, and R. B. Altman, "Chemical reaction vector embeddings: towards predicting drug metabolism in the human gut microbiome," in *Proceedings of the Pacific Symposium*, pp. 56–67, Kohala Coast, Hawaii, USA, 2018.

[46] J. Lindenbaum, D. G. Rund, V. P. Butler, D. Tse-Eng, and J. R. Saha, "Inactivation of Digoxin by the Gut Flora: Reversal by Antibiotic Therapy," *The New England Journal of Medicine*, vol. 305, no. 14, pp. 789–794, 1981.

[47] R. Feng, Z. Zhao, S. Ma, F. Guo, Y. Wang, and J. Jiang, "Gut microbiota-regulated pharmacokinetics of berberine and active metabolites in beagle dogs after oral administration," *Frontiers in Pharmacology*, vol. 9, p. 214, 2018.

[48] S. Guo, R. Al-Sadi, H. M. Said, and T. Y. Ma, "Lipopolysaccharide causes an increase in intestinal tight junction permeability in vitro and in vivo by inducing enterocyte membrane expression and localization of TLR-4 and CD14," *The American Journal of Pathology*, vol. 182, no. 2, pp. 375–387, 2013.

[49] P. D. Cani, R. Bibiloni, C. Knauf et al., "Changes in gut microbiota control metabolic endotoxemia-induced inflammation in high-fat diet-induced obesity and diabetes in mice," *Diabetes*, vol. 57, no. 6, pp. 1470–1481, 2008.

[50] J. ŠtŠepetova, E. Sepp, H. Kolk, K. Lõivukene, E. Songisepp, and M. Mikelsaar, "Diversity and metabolic impact of intestinal Lactobacillus species in healthy adults and the elderly," *British Journal of Nutrition*, vol. 105, no. 8, pp. 1235–1244, 2011.

[51] S.-M. Lim, J.-J. Jeong, K. H. Woo, M. J. Han, and D.-H. Kim, "Lactobacillus sakei OK67 ameliorates high-fat diet-induced blood glucose intolerance and obesity in mice by inhibiting gut microbiota lipopolysaccharide production and inducing colon tight junction protein expression," *Nutrition Research*, vol. 36, no. 4, pp. 337–348, 2016.

[52] S.-J. Wu, T.-M. Don, C.-W. Lin, and F.-L. Mi, "Delivery of berberine using chitosan/fucoidan-taurine conjugate nanoparticles for treatment of defective intestinal epithelial tight junction barrier," *Marine Drugs*, vol. 12, no. 11, pp. 5677–5697, 2014.

[53] C.-H. Chang, W.-Y. Huang, C.-H. Lai et al., "Development of novel nanoparticles shelled with heparin for berberine delivery to treat *Helicobacter pylori*," *Acta Biomaterialia*, vol. 7, no. 2, pp. 593–603, 2011.

[54] L. Gu, N. Li, J. Gong, Q. Li, W. Zhu, and J. Li, "Berberine ameliorates intestinal epithelial tight-junction damage and down-regulates myosin light chain kinase pathways in a mouse model of endotoxinemia," *The Journal of Infectious Diseases*, vol. 203, no. 11, pp. 1602–1612, 2011.

[55] J. Wang, S. S. Ghosh, and S. Ghosh, "Curcumin improves intestinal barrier function: Modulation of intracellular signaling, and organization of tight junctions," *American Journal of Physiology-Cell Physiology*, vol. 312, no. 4, pp. C438–C445, 2017.

[56] C. Chelakkot, Y. Choi, D. Kim et al., "Akkermansia muciniphila-derived extracellular vesicles influence gut permeability through the regulation of tight junctions," *Experimental & Molecular Medicine*, vol. 50, no. 2, p. e450, 2018.

[57] P. Pinton, C. Braicu, J. Nougayrede, J. Laffitte, I. Taranu, and I. P. Oswald, "Deoxynivalenol impairs porcine intestinal barrier function and decreases the protein expression of claudin-4 through a mitogen-activated protein kinase-dependent mechanism," *Journal of Nutrition*, vol. 140, no. 11, pp. 1956–1962, 2010.

[58] P. Raj, S. Zieroth, and T. Netticadan, "An overview of the efficacy of resveratrol in the management of ischemic heart disease,"

Annals of the New York Academy of Sciences, vol. 1348, no. 1, pp. 55–67, 2015.

[59] E. Chong, S.-L. Chang, Y.-W. Hsiao et al., "Resveratrol, a red wine antioxidant, reduces atrial fibrillation susceptibility in the failing heart by PI3K/AKT/eNOS signaling pathway activation," *Heart Rhythm*, vol. 12, no. 5, pp. 1046–1056, 2015.

[60] P. D. Cani et al., "Metabolic endotoxemia initiates obesity and insulin resistance," *Diabetes*, vol. 56, no. 7, pp. 1761–1772, 2007.

[61] C. L. Boulange et al., "Impact of the gut microbiota on inflammation, obesity, and metabolic disease," *Genome Medicine*, vol. 8, no. 1, p. 42, 2016.

[62] Y. Merga, B. J. Campbell, and J. M. Rhodes, "Mucosal barrier, bacteria and inflammatory bowel disease: possibilities for therapy," *Digestive Diseases*, vol. 32, no. 4, pp. 475–483, 2014.

[63] P. Rawla, S. S. Bandaru, and A. R. Vellipuram, "Review of infectious etiology of acute pancreatitis," *Gastroenterology Research*, vol. 10, no. 3, pp. 153–158, 2017.

[64] X. Wang, N. Ota, P. Manzanillo et al., "Interleukin-22 alleviates metabolic disorders and restores mucosal immunity in diabetes," *Nature*, vol. 514, no. 7521, pp. 237–241, 2014.

[65] H. Luck, S. Tsai, J. Chung et al., "Regulation of obesity-related insulin resistance with gut anti-inflammatory agents," *Cell Metabolism*, vol. 21, no. 4, pp. 527–542, 2015.

[66] H. Chung and D. L. Kasper, "Microbiota-stimulated immune mechanisms to maintain gut homeostasis," *Current Opinion in Immunology*, vol. 22, no. 4, pp. 455–460, 2010.

[67] D. A. Hill and D. Artis, "Intestinal bacteria and the regulation of immune cell homeostasis," *Annual Review of Immunology*, vol. 28, pp. 623–667, 2010.

[68] M. B. Geuking, J. Cahenzli, M. A. E. Lawson et al., "Intestinal bacterial colonization induces mutualistic regulatory T cell responses," *Immunity*, vol. 34, no. 5, pp. 794–806, 2011.

[69] K. Atarashi, T. Tanoue, T. Shima et al., "Induction of colonic regulatory T cells by indigenous *Clostridium* species," *Science*, vol. 331, no. 6015, pp. 337–341, 2011.

[70] K. Atarashi, J. Nishimura, T. Shima et al., "ATP drives lamina propria TH17 cell differentiation," *Nature*, vol. 455, no. 7214, pp. 808–812, 2008.

[71] I. I. Ivanov, K. Atarashi, N. Manel et al., "Induction of intestinal Th17 cells by segmented filamentous bacteria," *Cell*, vol. 139, no. 3, pp. 485–498, 2009.

[72] T. Zelante, R. Iannitti, C. Cunha et al., "Tryptophan catabolites from microbiota engage aryl hydrocarbon receptor and balance mucosal reactivity via interleukin-22," *Immunity*, vol. 39, no. 2, pp. 372–385, 2013.

[73] J. Duan, H. Chung, E. Troy, and D. L. Kasper, "Microbial colonization drives expansion of IL-1 receptor 1-expressing and IL-17-producing γ/δ T cells," *Cell Host & Microbe*, vol. 7, no. 2, pp. 140–150, 2010.

[74] T. Olszak, D. An, S. Zeissig et al., "Microbial exposure during early life has persistent effects on natural killer T cell function," *Science*, vol. 336, no. 6080, pp. 489–493, 2012.

[75] D. An et al., "Sphingolipids from a symbiotic microbe regulate homeostasis of host intestinal natural killer T cells," *Cell*, vol. 165, no. 1-2, pp. 123–133, 2014.

[76] N. Satoh-Takayama, C. A. J. Vosshenrich, S. Lesjean-Pottier et al., "Microbial flora drives interleukin 22 production in intestinal NKp46+ cells that provide innate mucosal immune defense," *Immunity*, vol. 29, no. 6, pp. 958–970, 2008.

[77] S. Sawa et al., "RORgammat+ innate lymphoid cells regulate intestinal homeostasis by integrating negative signals from the symbiotic microbiota," *Nat Immunol*, vol. 12, no. 4, p. 320, 2011.

[78] A. Mortha, A. Chudnovskiy, D. Hashimoto et al., "Microbiota-dependent crosstalk between macrophages and ILC3 promotes intestinal homeostasis," *Science*, vol. 343, no. 6178, Article ID 1249288, p. 1249288, 2014.

[79] A. J. Macpherson, M. B. Geuking, E. Slack, S. Hapfelmeier, and K. D. McCoy, "The habitat, double life, citizenship, and forgetfulness of IgA," *Immunological Reviews*, vol. 245, no. 1, pp. 132–146, 2012.

[80] Y. Cong, T. Feng, K. Fujihashi, T. R. Schoeb, and C. O. Elson, "A dominant, coordinated T regulatory cell-IgA response to the intestinal microbiota," *Proceedings of the National Acadamy of Sciences of the United States of America*, vol. 106, no. 46, pp. 19256–19261, 2009.

[81] J. Gong, M. Hu, Z. Huang et al., "Berberine attenuates intestinal mucosal barrier dysfunction in type 2 diabetic rats," *Frontiers in Pharmacology*, vol. 8, p. 42, 2017.

[82] H. Cui, Y. Cai, and L. Wang, "Berberine regulates Treg/Th17 balance to treat ulcerative colitis through modulating the gut microbiota in the colon," *Frontiers in Pharmacology*, vol. 9, p. 571, 2018.

[83] R. Sun, N. Yang, B. Kong et al., "Orally administered berberine modulates hepatic lipid metabolism by altering microbial bile acid metabolism and the intestinal FXR signaling pathway," *Molecular Pharmacology*, vol. 91, no. 2, pp. 110–122, 2017.

[84] J. Bai, Y. Zhu, and Y. Dong, "Response of gut microbiota and inflammatory status to bitter melon (Momordica charantia L.) in high fat diet induced obese rats," *Journal of Ethnopharmacology*, vol. 194, pp. 717–726, 2016.

[85] B. Bao, Y.-G. Chen, L. Zhang et al., "Momordica charantia (Bitter Melon) reduces obesity-associated macrophage and mast cell infiltration as well as inflammatory cytokine expression in adipose tissues," *PLoS ONE*, vol. 8, no. 12, Article ID e84075, p. e84075, 2013.

[86] S. Chuengsamarn, S. Rattanamongkolgul, B. Phonrat, R. Tungtrongchitr, and S. Jirawatnotai, "Reduction of atherogenic risk in patients with type 2 diabetes by curcuminoid extract: a randomized controlled trial," *The Journal of Nutritional Biochemistry*, vol. 25, no. 2, pp. 144–150, 2014.

[87] Y. Pan, Y. Wang, L. Cai et al., "Inhibition of high glucose-induced inflammatory response and macrophage infiltration by a novel curcumin derivative prevents renal injury in diabetic rats," *British Journal of Pharmacology*, vol. 166, no. 3, pp. 1169–1182, 2012.

[88] R.-M. T. Mcfadden, C. B. Larmonier, K. W. Shehab et al., "The role of curcumin in modulating colonic microbiota during colitis and colon cancer prevention," *Inflammatory Bowel Diseases*, vol. 21, no. 11, pp. 2483–2494, 2015.

[89] D. Dai, C.-F. Zhang, S. Williams, C.-S. Yuan, and C.-Z. Wang, "Ginseng on cancer: potential role in modulating inflammation-mediated angiogenesis," *American Journal of Chinese Medicine*, vol. 45, no. 1, pp. 13–22, 2017.